β-Lactam-Mediated Enhancement of Daptomycin Antibacterial Activity in Methicillin-Resistant *Staphylococcus aureus*

By

Cassandra Irene Lew

A dissertation submitted in partial fulfillment of

the requirements for the degree of

Doctor of Philosophy

(Pharmaceutical Sciences)

at the

UNIVERSITY OF WISCONSIN- MADISON

2022

Date of final oral examination: 5/18/2022

This dissertation is approved by the following members of the Final Oral Committee:

Warren E. Rose, Associate Professor, Pharmacy and Medicine

John- Demian (JD) Sauer, Associate Professor, Medical Microbiology and Immunology

Tim S. Bugni, Professor, Pharmaceutical Sciences

Jennifer Golden, Assistant Professor, Pharmaceutical Sciences

Charles T. Lauhon, Associate Professor, Pharmaceutical Sciences

Acknowledgements

First, I would like to thank my advisor Dr Warren Rose for giving me the opportunity to contribute to this project and for your continued guidance and support as I have grown and developed as a researcher. Also, to my other committee members- thank you for your continued feedback and helping me navigate graduate school these past five years. Also, thank you to Dr Jess Kelliher and Dr George Neuhaus for editing and providing feedback on portions of this dissertation.

I would like to acknowledge collaborators at UCLA, Dr Arnold Bayer and Dr Nagendra Mishra, who I've been fortunate to work closely with on several projects. Several individuals at UW Madison have helped me along the way: Dr Richard Proctor, Evan Rees, Lance Rodenkirch at the Optical Imaging Core, Ben August at the Electron Microscope Facility, and Molly Pellitteri Hahn and Dr Cameron Scarlett at the Analytical Instrumentation Center in the School of Pharmacy - thank you for your patience in teaching me and for your contribution to the work presented in this dissertation.

I would also like to acknowledge the individuals in my cohort. Thank you for being my accomplices on this wild ride, misery loves company. And a special thank you to Dr Michelle Boyd, who was my partner in crime on the 4th floor and was always there for a good rant or a coffee run. And especially to her dog Loki- who was my emotional support animal throughout grad school. Also, to Sue McCrone- thank you for the beers, for teaching me how to water ski (or at least trying), and for always being around to chat or bounce ideas off.

I am extremely grateful to Dr JD Sauer for accommodating me through a tough situation and for giving me a space to finish my work. To everyone in the Sauer lab- thank you for adopting me into the lab and for teaching me (perhaps more than I ever cared to know) about *Listeria*. Thank you all for providing a safe, fun, and always entertaining environment to work in. Especially Kim, who kept me constantly

laughing and made the writing process much more bearable. I have learned so much from each one of you, and I am smarter, wiser, and (perhaps) sassier for having been part of the lab.

Finally, to my friends and family. To all my friends- thank you for sticking with me through the messiness of the past couple years. I am so grateful to have a community of people who are so supportive, fun, and always down for whatever poorly thought-out adventure we cook up. Despite the distance, I cannot overstate the value of my friendships. I am incredibly grateful to my family for the continued support and love throughout this process. Especially my parents and my two brothers- you guys are so important and have made me the person and I am today. I would not be here without you. Also, to my cousin Tia, who was my de-facto older sister and brought so much light to my life- thank you for all the love, laughter, and joy. This one is for you. And finally, to my chosen family in Oregon. Thank you for always being in my corner and showing up for the good, the bad, and the ugly. Our trips, whether into the wilderness or all over the world, have sustained me throughout these past five years. Thank you for always giving me somewhere to run away to- I could not have done this without you guys.

Abstract

Methicillin-resistant *Staphylococcus aureus* (MRSA) is a serious clinical threat due to innate virulence properties, high infection rates, and the ability to develop resistance to multiple antibiotics, including the lipopeptide daptomycin (DAP). The occurrence of DAP resistant (DAP-R) MRSA isolates has been reported in the literature, often associated with gain-of-function mutations in multiple peptide resistance factor *mprF* and modification of the cell envelope. Standard β-lactams, although relatively inactive against MRSA, prevent the emergence of *mprF* mutations and DAP-R. **Chapter 2** describes the ability of β-lactams to revert DAP-R isolates to a DAP susceptible (DAP-S) phenotype. Following 28-day serial passage in subinhibitory concentrations of β-lactams, DAP minimum inhibitory concentrations (MICs) were significantly decreased. Whole genome sequencing (WGS) of passage isolates identified subsequent *mprF* mutations in addition to the initial *mprF* SNP. The causal role of secondary *mprF* mutations in mediating DAP resensitization was validated by allelic exchange. The data in **Chapter 3** show preconditioning with β-lactams, followed by DAP exposure [sequential dosing] significantly increased *in vitro* activity compared to simultaneous dosing of DAP and β-lactams. Proteomic analyses comparing β-lactam pre-treatments to untreated controls identified differential modulation of several well-known metabolic, cellular, and biosynthetic processes, i.e., the autolytic and riboflavin biosynthetic pathways. The data presented in **Chapter 4** describes the β-lactam induced cell response, with particular attention to cell envelope phenotypes. In general, exposure to β-lactams led to: i) decreased positive surface charge; ii) decreased membrane fluidity; iii) increased content and delocalization of cardiolipin; and iv) increased DAP binding in DAP-S (but not DAP-R) strains. To identify the differences in synergy of DAP combinations with β-lactams, **Chapter 5** screened nine DAP-R MRSA strains with a panel of six DAP- β-lactam combinations. In five of the study strains, all combinations had bactericidal activity [>3 $\log_{10}$ CFU/mL reduction]. The other four strains were unresponsive to at least one of the DAP- β-lactam combination.

WGS identified single nucleotide polymorphisms (SNPs) in innate immune evasion genes *sbi*, *sdrC*, and *sdrD* in multiple strains, along with several strain specific SNPs. In conclusion, β-lactam preconditioning improves synergy with DAP by genetic and phenotypic alteration of cells in a β-lactam specific manner.

Table of Contents

List of Tables

List of Figures

Abbreviations

CA-MRSA	community acquired methicillin-resistant *Staphylococcus aureus*
CC	clonal complex
CDC	Centers for Disease Control
CEC	cefaclor
CFU	colony forming units
CL	cardiolipin
CLSI	Clinical and Laboratory Standards Institute
CPT	ceftaroline
CRO	ceftriaxone
CytC	cytochrome C
DAP	daptomycin
DAP-NS	daptomycin non-susceptible
DAP-R	daptomycin resistant (denotes DAP-NS phenotype)
DAP-S	daptomycin susceptible
DM	double mutant
DPH	1,6-diphenyl-1,3,5-hexatriene
fCavg	free average concentration in human serum
FDA	Food and Drug Administration
FOS	fosfomycin
FOX	cefoxitin
HA- MRSA	hospital acquired methicillin-resistant *Staphylococcus aureus*
HDP	host defense peptide
HMM	high-molecular mass
IDSA	Infectious Disease Society of America
LB	lysogeny broth
LC-MS/MS	liquid chromatography- with tandem mass spectrometry
L-PG	lysyl-phosphatidylglycerol
LMM	low-molecular mass

LOX	cloxacillin
MEM	meropenem
MHA	Mueller-Hinton Agar
MHB	Mueller-Hinton Broth II
MIC	minimum inhibitory concentration
MRSA	methicillin-resistant *Staphylococcus aureus*
NAF	nafcillin
NAO	N-acrylamide orange
OXA	oxacillin
PBP	penicillin-binding protein
PG	phosphatidylglycerol
PGN	peptidoglycan
PGT	peptidoglycan glycosyltransferases
PI	polarization index
PL	phospholipid
PSM	phenol soluble modulin
S. aureus	*Staphylococcus aureus*
SCC*mec*	staphylococcal cassette chromosome *mec*
SNP	single nucleotide polymorphism
STED	stimulated emission depletion
STRING	Search Tool for the Retrieval of Interacting Genes/ Proteins
TCS	two-component system
TEM	transmission electron microscopy
UDP	undecaprenyl
VAN	vancomycin
VISA	vancomycin-intermediate *Staphylococcus aureus*
WGS	whole genome sequencing
WTA	wall teichoic acid

Chapter 1. Daptomycin Combinations with β-Lactams in Daptomycin-Non-susceptible *Staphylococcus aureus*

1.1. Antibiotic Resistance in *Staphylococcus aureus*

Antibiotic resistance continues to be a serious global threat that still lacks a viable solution. The 2019 report *Antibiotic Resistance Threats in the United States* released by the Centers for Disease Control (CDC) highlights that over 2.8 million antibiotic resistant infections occur each year, with over 35,000 deaths annually a result of antibiotic resistance. The so-called "ESKAPE" pathogens (*Enterococcus faecium, Staphylococcus aureus*, *Klebsiella pneumoniae*, *Acinetobacter baumannii*, *Pseudomonas aeruginosa*, and *Enterobacter* species) have high levels of drug resistance and are the leading cause of nosocomial (healthcare associated) infections (1). The treatment of these infections alone in the United States cost an estimated $4.6 billion annually (2). A key finding of the CDC is that addressing the ongoing crisis of antibiotic resistance will require a multifactorial approach including not only discovery of new antibiotics, but also alternative approaches including the use of synergistic antibiotic combinations or improving treatment strategies to hinder the development of resistance (3).

Staphylococcus aureus (*S. aureus*) is a Gram-positive bacterial pathogen that is dangerous due to its commonality and high mortality rate in bacteremic infection (4, 5). Increasingly the incidence of methicillin-resistant *S. aureus* (MRSA) has become prevalent in both healthcare and community acquired settings (6). Infections caused by MRSA alone contribute ~ $1.7 billion in healthcare costs and ~10,600 deaths annually (7). As MRSA has developed at least some level of resistance to nearly all relevant antibiotics, there is an urgent need to uncover for alternatives for treatment (8).

1.2 Biosynthesis of Peptidoglycan as the Target of β-Lactam Antibiotics

Most antibiotics used for treatment of Gram-positive bacterial infections inhibit key steps in cell wall biosynthesis pathways, which leads to osmotic rupture (**Figure 1.2.1**). In the case of β-lactam antibiotics and the glycopeptide vancomycin (VAN), this is accomplished by targeting keys steps in the biosynthesis of the cell wall structural component peptidoglycan (PGN) and its precursors (9, 10). Initiated by biosynthesis and translocation of precursor lipid II [the target of VAN], the glycan is polymerized by peptidoglycan glycosyltransferases (PGT) and crosslinked by transpeptidase enzymes (11, 12). Polymerization and cross-linking functions often take place in distinct domains on a single protein, such as the penicillin binding proteins (PBPs). The mechanism of action of β-lactam antibiotics involves covalently binding and inactivating these PBPs (13). There are two distinct categories of PBPs: high-molecular mass (HMM) PBPs and low-molecular mass (LMM) PBPs. HMM PBPs contain transpeptidase domains that cross-link glycan strands, while LMM PBPs function as D,D-carboxypeptidases that hydrolyze the terminal D-Ala of the peptide (14, 15).

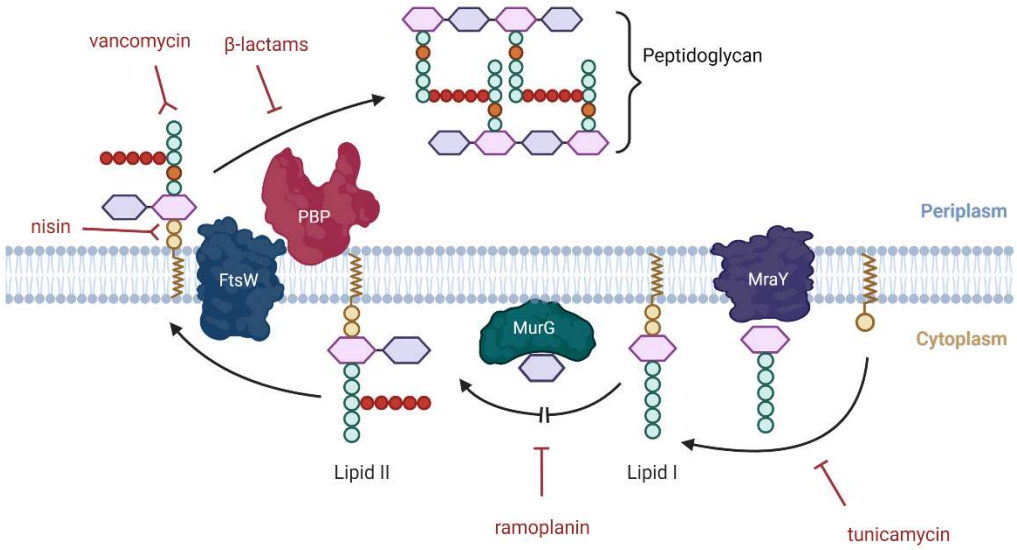

Figure 1.2.1 Several of the most effective antibiotics (in red) against Gram-positive pathogens target key steps in the peptidoglycan biosynthesis pathway.

There are four PBPs in methicillin-susceptible *S. aureus*, three of which are HMM PBPs (PBP 1-3) and the other is a LMM PBP (PBP 4) (15-20). The HMM PBPs can further be separated into two categories: class A and class B. Both categories contain the peptidoglycan transpeptidase domain, however they differ in the function of their N-terminal domain. The N-terminal domain in class A HMM PBPs (PBP 2 in *S. aureus*) is a PGT responsible for glycan polymerization, while in class B HMM PBPs (PBP 1 and PBP 3 in *S. aureus*) the function of this domain remains unknown (21). Genetic deletion experiments have shown that only PBP 1 and PBP 2 are required for normal shape and growth of *S. aureus* (22).

Methicillin-resistance in *S. aureus* occurs via acquisition of the mobile genetic element staphylococcal cassette chromosome *mec* (SCC*mec*) (23). Within SCC*mec* lies the gene *mecA* that encodes an additional PBP, known as PBP 2A (24). This additional class A HMM PBP has a low affinity for the β-lactams, which allows retention of cross-linking functionality when the others are bound and inactivated (25). Importantly, assembly of PGN by PBP 2A in the presence of β-lactams requires PBP 2-mediated transglycosylation as PBP 2A lacks this functionality alone (26). PBP 2A expression is induced following acylation of the transmembrane MecR sensor protein by a β-lactam antibiotic. In 2013, Otero et al. discovered that the PBP 2A active site is under allosteric control and opens in response to PGN substrate (27, 28). This discovery made way for the development of newer β-lactams, such as ceftaroline, that bind the allosteric site and are therefore active against MRSA (29). However there have been documented cases of clinical and microbiologic resistance to ceftaroline, amplifying the importance of not only understanding resistance mechanisms but also finding a way to curb the initial development of resistance (30, 31).

1.3 Daptomycin Mechanism of Action

As β-lactams have become increasingly ineffective against *S. aureus*, alternative antibiotic treatments have become more widely used for MRSA infections. VAN is typically the first line treatment option for suspected MRSA infections; however, reduced VAN antistaphylococcal activity ("MIC creep") has been widely reported as the number of VAN intermediate (VISA) or even VAN resistant (VRSA) infections is on the rise (32-35). Daptomycin (DAP) is a cyclic lipopeptide natural product that has potent bactericidal activity in multi-drug resistant Gram-positive pathogens, including MRSA (36, 37). DAP is an effective treatment for invasive MRSA infections, including those that are refractory to VAN (38, 39). Further highlighting its importance, DAP remains the only rapidly bactericidal anti-MRSA antibiotic with consistent efficacy in bacteremia and infective endocarditis (32, 40, 41).

The antibacterial activity of DAP is known to involve disruption of the cell envelope and is dependent on the presence of the anionic phospholipid phosphatidylglycerol (PG) and Ca^{+2} ions (42, 43). The mechanism depicted in **Figure 1.3.1** shows DAP and Ca^{+2} oligomerization in a tripartite complex with PG and undecaprenyl (UDP)-coupled cell wall precursors (44, 45). Initial binding of DAP to the cell membrane occurs in fluid microdomains at regions of active PGN synthesis, often at the cell septum (45, 46). This delocalizes membrane bound proteins by sequestering fluid phospholipids to the site of insertion and leads to delocalization of PGN biosynthetic machinery (45). In the membrane itself, DAP oligomerizes and distorts the membrane to induce localized patches of increased curvature (47). At high concentrations the cell is unable to compensate for these alterations, leading to loss of membrane potential, ion leakage, and eventual cell death (48-50).

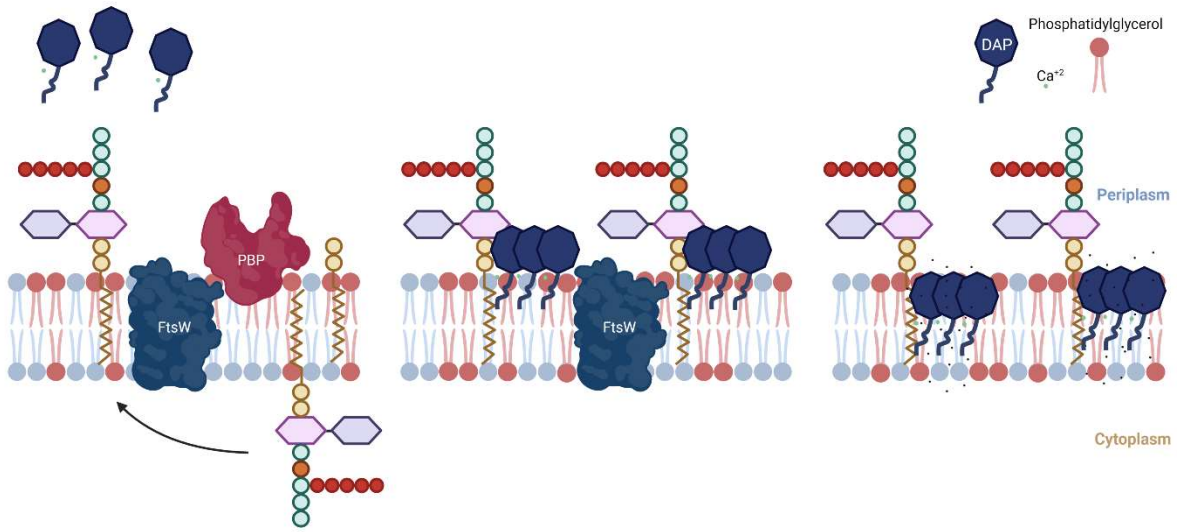

Figure 1.3.1 DAP complexes with Ca^{+2} and oligomerizes in a tripartite complex with PG and undecaprenyl-coupled cell wall precursors [such as lipid II] in the cell membrane. DAP molecules subsequently insert into these fluid membrane regions, leading to membrane curvature, ion leakage, and cell death.

1.4 Daptomycin Non-Susceptibility

Based on the limited clinical data delineating the MIC at which DAP is ineffective for treatment, susceptible-only breakpoints are defined for DAP. This translates to isolates being defined as either DAP susceptible (DAP-S) or DAP non-susceptible (DAP-NS), without having a DAP resistant (DAP-R) classification. The DAP minimum inhibitory concentration (MIC) susceptibility breakpoint for *S. aureus* is ≤1 mg/L as defined by Clinical and Laboratory Standards Institute (CLSI) (51). DAP-NS isolates often emerge during unsuccessful DAP treatment and are often recalcitrant, deep-seated infections and those with high bacterial burdens (52-54). DAP-NS MRSA infections, although still relatively uncommon, are associated with high morbidity and mortality (53, 55). The mechanism behind development of the DAP-NS phenotype is multifactorial, strain-dependent, and involves alteration of the cell envelope (56). For ease of understanding, DAP-R will be used to denote the clinical designation DAP-NS in the remaining text.

1.4.1 Characteristics of the Cell Membrane in DAP-R Isolates

Single nucleotide polymorphisms (SNPs) in the gene encoding multiple peptide resistant factor (*mprF*) are common in DAP-R isolates (57-60). The mechanism of the MprF protein along with a detailed annotation of DAP-R associated SNPs is illustrated in **Figure 1.4.1**. MprF is a bifunctional membrane protein that catalyzes the lysinylation and translocation of the positively charged phospholipid lysyl-phosphatidylglycerol (L-PG) (61, 62). The N-terminal domain of the protein is involved in flippase activity, while the C-terminal domain controls lysinylation activity (63-65). Between these two domains lies a 'bifunctional' domain that plays a role in both the lysinylation and translocation functions. Deletion of *mprF* leads to increased susceptibility to DAP, as well as host defense peptides (HDPs) (66, 67). HDPs are cationic antimicrobial peptides that are a first line of defense in the innate immune system. The fact cross-resistance between HDPs and DAP are linked to *mprF* mutations suggest that endogenous HDP exposure could lead to resistance even without previous DAP exposure (67, 68). DAP-R in isolates without prior DAP treatment occasionally occurs, however it remains relatively rare. The *mprF* polymorphisms associated with DAP-R are exclusively gain-of-function mutations, resulting in partial neutralization of the anionic bacterial cell surface via increased incorporation of positively charged L-PG (64).

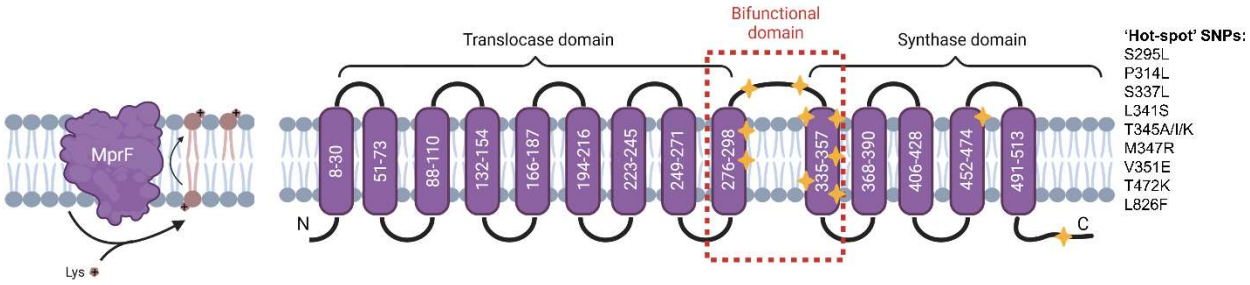

Figure 1.4.1 MprF is the protein responsible for the lysinylation and translocation of lysyl-phosphatidylglycerol (L-PG) in the cell membrane. The synthase domain adds the lysyl group to PG and the translocase domain flips the L-PG from the inner to the outer leaflet. The so called "bifunctional" domain is involved in both activities. Several key "hot-spot" mutations have been repeatedly identified in DAP-R isolates, many of which are in the bifunctional domain of the protein.

Initial studies investigating the evolution of DAP-R suggested that this neutralization of surface charge would cause a decrease in the amount of DAP binding to the cell (69-71). Several reports support this hypothesis, showing decreased DAP binding in DAP-R isolates compared to their DAP-S counterparts (58, 70, 72). Despite these findings, surface charge does not strictly correlate to the magnitude of DAP resistance, implying additional outside mechanisms at play (68, 73). An additional mechanism by which these SNPs may enhance DAP-R is by decreasing the amount of PG in the membrane. As PG is the precursor for L-PG, the increased biosynthesis resulting from *mprF* SNPs would result in decreased PG abundance, and therefore fewer binding sites for DAP on the membrane (74).

In support of this hypothesis, SNPs in two other phospholipid biosynthesis proteins (*cls2* and *pgsA*) are also common in DAP-R isolates (75, 76). Cardiolipin synthase 2 (*cls2*) encodes the primary protein responsible for the biosynthesis of cardiolipin (CL) in the cell membrane. CL plays a major role in modulating the negative surface charge of the membrane and localization of membrane-associated proteins. In enterococci, CL redistribution is a major source of DAP resistance (77, 78) and several novel SNPs in *cls2* have been identified in DAP-R MRSA isolates (79). Phenotypes associated with these SNPs remain largely undefined, although CL has been shown to prevent membrane translocation and permeabilization by DAP (80). In addition, CDP-DG-glycerol-3-phosphate 3-phosphatidyltransferase A (*pgsA*) encodes the protein responsible for PG biosynthesis (81-83). Mutations in *pgsA* block the biosynthesis of PG, further removing this potential docking site for DAP (76).

Aside from altering the composition of phospholipids in the cell membrane, *S. aureus* has also been shown to release membrane phospholipids that bind DAP (84, 85). DAP binding to these released phospholipids sequesters the antibiotic and thereby reduces DAP binding to the cell membrane (85). Wild-type MRSA also sheds phospholipids in response to DAP; however, the *agr* quorum-sensing system triggers release of lytic phenol soluble modulins (PMSs) that bind the phospholipids. As such, this mechanism of DAP inactivation is particularly effective in isolates with defective *agr* quorum-sensing

systems, as often occurs in VISA isolates and patients with persistent bacteremia (86-89). Notably, the rate of this lipid shedding was reduced in the presence of the β-lactam antibiotic oxacillin (OXA) (84).

1.4.2 Characteristics of the Cell Wall in DAP-R Isolates

DAP-R isolates have structural changes in the cell wall that are highly associated with three *S. aureus* two-component systems (TCSs): GraRS, WalRK, and VraRS (57, 72, 90). TCSs consist of a transmembrane histidine kinase and a cytosolic response regulator that control gene expression profiles in response to environmental stimuli (91). The TCS GraSR is involved in regulation of virulence, cell wall homeostasis, and specifically the response to HDP exposure (92). WalKR and VraSR are both involved in the regulation of cell envelope homeostasis.

The GraRS TCS promotes the development of antibacterial peptide (VAN/HDP) resistance. GraRS senses the presence of antibiotic peptides and responds by upregulating the expression of cell wall and cell membrane biosynthesis genes (e.g. *mprF* and the *dlt* operon) (93, 94). Proteins encoded in the *dlt* operon are responsible for incorporation of D-alanine (D-ALA) into lipoteichoic acids (LTA) and wall teichoic acids (WTA) (95). DAP-R isolates of have SNPs in the *dltABCD* operon that enhance its expression (56, 96, 97). The addition of the D-ALA group to LTA and WTA increases the surface charge of the cell wall; thus, these data support the hypothesis of resistance defined by alteration of cell surface charge (96, 98). The DAP-R phenotype is based on the enhanced capacity of these isolates to synthesize D-ALA-LTA and D-ALA-WTA. Increased expression of both the *dlt* operon and *tag* operon (responsible for WTA production) correlate with DAP-R phenotypes including a thickened cell wall, increased LTA and WTA and D-alanylation, and enhanced net surface positive charge (98, 99).

SNPs and insertions in the essential two-component regulator WalKR have been widely reported in DAP-R MRSA and VAN-intermediate *S. aureus* (VISA) (100, 101). These mutations significantly reduce the autolytic activity of cells and increase cell wall thickness, driven by blocking WalR-mediated activation

of *S. aureus* autolysins (100, 102, 103). DAP-R isolates with SNPs in WalKR often present with thickened cell wall phenotype (103-106).

The TCS VraSR is involved in the coordinating the cellular response to cell wall stress, signaled by damage to PGN (107-109). DAP-R strains often have increased expression of *vraSR* compared to their respective DAP-S parent strains (72, 110). The primary phenotype associated with overexpression was an increase in cell wall thickness mediated by genes under control of VraSR, including *murZ*, *mgt*, and *pbp2* (111). The enzymes MurA and MurZ catalyze the first committed step of PGN biosynthesis (112, 113). MurA is the primary enzyme during normal growth; however, in the presence of PGN biosynthesis inhibitors (such as β-lactams) the expression of *murZ* is highly induced (114). Mgt is a monofunctional nonessential transglycosylase that, like PBP2, plays a role in cross-linking of the PGN (115). The activity of these proteins, and therefore increased PGN biosynthesis, is induced upon overexpression of the regulator VraSR.

Comprehensively, DAP-R strains have an increased positive cell surface charge, mediated by higher levels of positively charged L-PG. The cell wall of DAP-R strains have an increased thickness and also an increase in D-alanylation of LTA and WTA (56). The phenotypic differences between the cell envelopes of DAP-S and DAP-R MRSA isolates are illustrated in **Figure 1.4.2**.

1.4.3 DAP-R Adaptations Outside the Cell Envelope

SNPs in the genes encoding RNA polymerase β and β' subunits, *rpoB* and *rpoC* respectively, have been repeatedly identified in MRSA isolates with reduced DAP susceptibility (116-118). The *rpoB*- and *rpoC*-mediated resistance was accompanied by a reduced negative cell surface charge, increased cell wall thickness, reduced expression of virulence factors, and slow growth (119). In addition to reduced DAP and VAN susceptibility, mutations in *rpoB* and *rpoC* are linked to reduced rifampicin resistance and have been shown to promote *S. aureus* survival in human blood (120, 121).

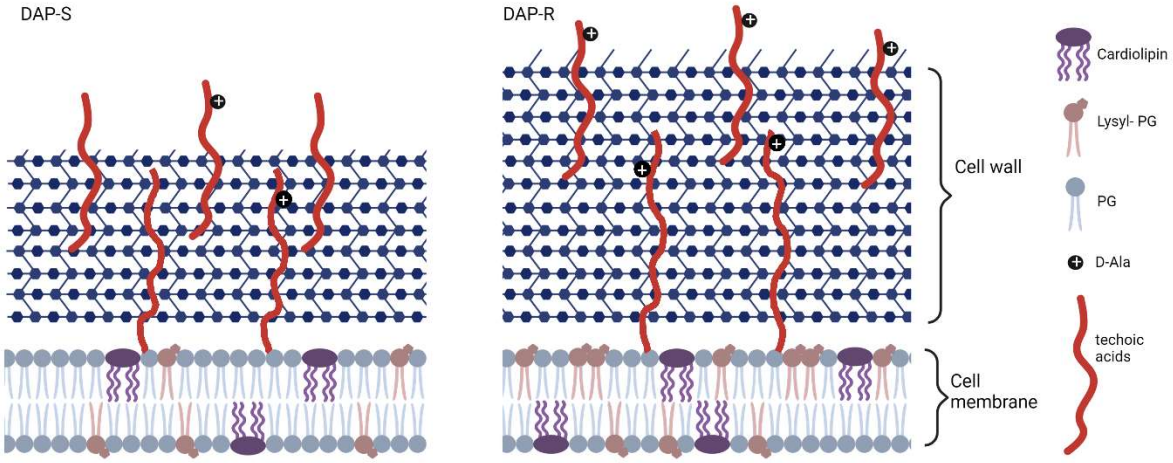

Figure 1.4.2 Phenotypic changes associated with DAP-R commonly include alteration of the cell envelope, including increased L-PG and decreased PG in the cell membrane, increased cell wall thickness, and an increase in D-alanylation of teichoic acids in the cell wall.

1.5 Daptomycin Combinations with β-Lactams

As DAP is the "last- line" treatment for MRSA bacteremia and endocarditis, when isolates develop DAP-R there is virtually no individual antibiotic that is effective for treatment. In cases of DAP-R MRSA, treatment involves DAP supplemented with other antibiotics, often a β-lactam (122-125). The emerging clinical evidence highlighting the usefulness of this combination agrees with extensive in vitro data supporting adjunctive β-lactam treatment to enhance the activity of DAP in DAP-R MRSA (126-128). While the benefits of adding a β-lactam to DAP treatment have been thoroughly described in the literature, the mechanism(s) underlying the improved activity remain largely undefined (127, 129-131).

1.5.1 "See-Saw" Effect

Decrease in susceptibility to DAP in MRSA often coincides with an increase in susceptibility to β-lactams, termed the "see-saw" effect (132-134). While this effect has been well documented, the driving force behind the phenotype remains unclear. Current evidence suggests the postranslocational

chaperone lipoprotein PrsA plays a primary role. Among other functions, PrsA is important for the proper maturation of the *mecA* encoded protein PBP 2A (135, 136). Improper localization and altered function of PrsA is associated with decreased amounts of functional membrane-bound PBP2A, characteristic of DAP-R MRSA strains sensitized to β-lactams (137, 138). In addition, PrsA plays a role in maintenance of cardiolipin-enriched fluid membrane microdomains, which are important sites for DAP membrane insertion (137).

The cause of misfolding by PrsA remains undefined, although there are two main hypotheses. The first is that dysregulation of the TCS VraSR impairs either the function or structure of PrsA maturation (139-141). In support of this hypothesis, overexpression of VraSR has been linked to decreased DAP susceptibility and increased susceptibility to β-lactams (72, 135). The second hypothesis is based on DAP-induced *mprF* mutation leading to reorganization of the membrane that displaces proteins required for PrsA maturation. The protein Lgt, which controls the lipidation of lipoproteins, uses PG as a substrate (142). The "gain-of-function" *mprF* mutations in DAP-R MRSA limit the amount of PG available for Lgt-mediated anchoring of lipoproteins, such as PrsA, to the membrane (143). Inhibiting PrsA lipidation would impair PrsA-mediated maturation of PBP 2A, leading to increased β-lactam susceptibility. Further, DAP-R-associated *mprF* mutations independently alter the localization and function of membrane bound proteins, including PrsA (135, 144). While these mechanisms are not exclusive, the extent of influence each system has on the see-saw effect mediated by PrsA is not completely understood.

1.5.2 DAP Synergy with β-Lactams

Combination therapies of DAP with a supplemental β-lactam have been effective in treating *S. aureus*, notably in isolates that are phenotypically non-susceptible to both antibiotics (i.e., DAP-R MRSA) (123, 145-148). Initial studies investigating potential combinations of DAP with adjunctive antibiotics found that combinations with gentamycin, rifampin, β-lactams, trimethoprim/ sulfamethoxazole (TMP-

SMX), or clarithromycin were effective, and often superior to, DAP monotherapy (149-151). Combinations of the β-lactam OXA with DAP led to bacterial killing in clinical DAP-R MRSA isolates, even at sub-MIC concentrations of both antibiotics (127, 132). The ability of the β-lactam to improve DAP activity was hypothesized to be based solely on the increase in DAP binding observed in the presence of β-lactams (152, 153). However follow up studies showed that the extent of DAP binding did not necessarily correlate with the level of synergy, suggesting a more complex mechanism (154).

The synergy between DAP and β-lactams has since been widely reported in DAP-R MRSA strains. While the synergistic effect has been shown with a variety of β-lactams, the extent of activity is highly variable depending on the β-lactam and specific MRSA isolate (155, 156). There has been no correlation found between β-lactam class and extent of synergy with DAP; however, the literature suggests PBP binding selectivity may play a role. At high concentrations β-lactams will bind non-selectively to PBPs, but as the concentration decreases some β-lactams bind preferentially to specific PBPs (157-159). Although β-lactams that preferentially bind PBP 1, PBP 2, or those that are non-selective have increased synergistic activity compared to those selective for other PBPs, the concentrations at which PBP specific binding occurs remains undefined (154, 160, 161). This makes correlating PBP specific inhibition with DAP synergy difficult.

Cationic antimicrobial peptides, such as the HDP LL-37, also synergize with β-lactam antibiotics (162-164). Although both DAP and LL-37 disrupt the cell membrane, their mechanisms of action are distinct. LL-37 forms discrete pores in the bacterial cell membrane and further exerts its antimicrobial activity by separately modulating the innate immune response, leading to eradication of MRSA (165-167). While combinations of DAP or LL-37 with β-lactams are both synergistic, the relationship between their respective activities remains a question. Preliminary activity data suggests β-lactam and strain specificity both play a role in activity between DAP + β-lactam combinations and LL-37 + β-lactam combinations.

1.5.3 β-lactams Hinder Development of DAP-R

In addition to the effectiveness of DAP + β-lactam combinations against highly DAP-resistant isolates, this combination has also been shown to hinder development of DAP-R in DAP naïve strains (168-170). Based on the finding that adjunctive antibiotics can enhance the activity of DAP in DAP-R strains, Berti et al evaluated the effect that DAP combinations have on the development of DAP resistance. Antibiotics have differing impacts on the development of DAP-R, ranging from significantly increasing the rate of resistance development (linezolid) to the cell sustaining a DAP-S phenotype (OXA) (124). In particular, the addition of a β-lactam was the only condition where the strain retained the DAP-S phenotype after four weeks of passage (124). Further, the combination of DAP with a β-lactam prevents the selection of DAP-R variants (124).

This *in vitro* evidence is further supported by a recent retrospective clinical study that compared the efficacy of DAP alone vs DAP + β-lactam combination therapy for treatment of MRSA (126). Use of the combination has been proven effective in treatment of multi-drug resistant MRSA, and patients are less likely to have recurrent infections (145, 156, 171). Unlike other potential β-lactam combinations (such as VAN + β-lactams), DAP + β-lactam combinations do not lead to an increase in toxicity (172, 173).

1.6 Conclusions

As the efficacy of β-lactams continues to be unmatched by any new classes of antibiotics, there has been substantial interest in finding a way to repurpose them in resistant isolates (174). A common method to counteract resistance is combination therapy with adjunctive antibiotics, such as DAP or VAN. Supplemental β-lactams have been highly effective in potentiating the activity of peptide-based antibiotics, even at sub-inhibitory levels. In addition to improving the antibacterial activity of these

agents, there is no danger of further resistance due to the "see-saw" effect. In fact, supplementing with β-lactams can even prevent initial development of resistance to last-line agents.

Despite the promise and clinical evidence supporting the use of DAP combinations with β-lactams in multi-drug resistant MRSA, there is limited information on the mechanisms underlying the effectiveness of the combination. A fundamental understanding of how these antibiotics interact is important both in order to optimize their use and to find other potential combinations. Translationally, the top priority is determining which isolates can be effectively treated by DAP combinations with β-lactams and which will require alternative treatment methods. Ideally, clinicians would have the ability to predict outcomes of DAP combinations with β-lactams as treatment based on isolate lineage, genotype, or other characteristics; and they would know which β-lactam would be most effective. The potential of DAP combinations with β-lactams to not only treat DAP-R infections, but also prevent initial development of DAP resistance make further investigation of this combination critical to combat the overarching challenge of antibiotic resistance.

To address the gaps in our understanding of DAP combinations with β-lactams we focused on the potential of β-lactams to improve DAP activity. In **Chapter 2**, we describe the mechanism of DAP resensitization driven by subsequent mutations in *mprF* induced through β-lactam passaging. The data in **Chapter 3** shows pre-conditioning with β-lactams improves DAP activity (compared to treating with both antibiotics simultaneously). Additional experiments in **Chapter** 3 and **Chapter 4** clarify the role of β-lactam-induced cellular response on improving DAP activity on cells. Finally, we found that diverse DAP-R MRSA clinical isolates have unique activity profiles with different DAP-β-lactam combinations in **Chapter 5**. We further identified several potential genotypic markers that may be useful in identifying strains where DAP-β-lactam combinations are less effective in bacterial killing. Overall, the data presented in this dissertation suggests that DAP-β-lactam synergy is strain specific and further mediated by β-lactam induced alteration of cells.

Chapter 2. Reestablishment of Daptomycin Susceptibility Mediated by β-Lactam-Induced Adaptations

Authors and their contributions:

Rachel E Jensen: Planned and conducted passaging experiments, wrote and edited manuscript

Sarah L Baines: Planned and conducted sequencing experiments, wrote and edited manuscript

Benjamin P Howden: Supervised research and contributed to design of experiments

Nagendra N Mishra: Supervised research and contributed to design of experiments

Sabrina Farah: Planned and conducted time kill experiments

Cassandra Lew: Planned and conducted confocal imaging experiments, wrote and edited manuscript

Andrew D Berti: Planned and conducted passaging experiments

Sanjay K Shukla: Supervised research and contributed to design of experiments

Arnold S Bayer: Supervised research and contributed to design of experiments

Warren E Rose: Supervised research and contributed to design of experiments

Ashleigh S Hayes: Planned and conducted allelic exchange experiments

Christian K Lapitan: Planned and conducted phospholipid composition, surface charge, and membrane fluidity experiments

Portions of this chapter have been previously published as:

Jenson, RE, Baines SL, Howden BP, Mishra NN, Farah S, Lew C, Berti AD, Shukla SK, Bayer AS, Rose WE. 2020. Prolonged Exposure to β-lactam Antibiotics Reestablished Susceptibility of Daptomycin-Nonsusceptible *Staphylococcus aureus* to Daptomycin. Antimicrob Agents Chemother. 64(9):e00890-20.

Mishra NN, Bayer AS, Baines SL, Hayes AS, Howden BP, Lapitan CK, Lew C, Rose WE. 2021. Cell Membrane Adaptations Mediate β-Lactam-Induced Resensitization of Daptomycin-Resistant (DAP-R) *Staphylococcus aureus* In Vitro. Microorganisms. 9(5):1028

2.1 Introduction

Staphylococcus aureus has developed at least some level of resistance to virtually every class of antimicrobials (175, 176). DAP is an effective treatment against MRSA with consistent efficacy in bacteremia and infective endocarditis (32, 40). Despite the effectiveness of DAP in treatment of MRSA infections, several published clinical reports document the *in vivo* development of DAP-R during treatment (116, 152). Since DAP has been considered a last resort antibiotic treatment option for severe MRSA infections, evolution of DAP-R can be highly problematic for patients. In addition, newer anti-MRSA antibiotics either have no proven efficacy in severe bacteremic syndromes (telavancin, tedizolid), have evoked documented clinical and microbiologic resistance (ceftaroline), and/or have issues regarding optimal dosing regimens in systemic MRSA infections (dalbavancin, oritavancin) (30, 31, 177-179). Therefore, it is important to design strategies that can both salvage the bactericidal activity of DAP, as well as prevent the development of DAP-R during treatment.

Characterization of several DAP-R MRSA isolates demonstrate that mutations within cell envelope associated, and global regulatory genes contribute to the DAP-R phenotype (56, 71, 180). The most frequently cited mutations in MRSA associated with DAP-R are perturbations in conserved "hot spots" within the multipeptide resistance factor (*mprF*) gene (56, 71, 180). These SNPs result in an enhancement of net positive surface charge and putative formation of a more charge-repulsive milieu against Ca^{+2}-DAP oligomeric aggregates, which reduces DAP insertion into the target membrane (64, 67-69, 73, 97, 181-183). Interestingly, DAP-R isolates with these hot spot *mprF* mutations can become "resensitized" *in vitro* to DAP when additional *mprF* point mutations are gained. Isolates with such genotypes are associated with a loss of *mprF* functionality in terms of reduced lysinylation of PG and/or its outer membrane translocation (74, 181). Of note, DAP-R MRSA strains often undergo several other phenotypic

modifications in cell membrane properties including in membrane order (fluidity/rigidity), carotenoid content, and fatty acid composition (69, 73, 97, 182, 183).

Currently, the Infectious Diseases Society of America (IDSA) recommends DAP plus β-lactam therapy as a principal option for treatment of such persistent MRSA infections (175). This recommendation reflects previous findings suggesting oxacillin (or nafcillin) can enhance the antimicrobial effects of DAP and prevent or delay the emergence of the DAP-R (71, 180). One novel finding that has frequently accompanied the evolution of DAP-R in *S. aureus* is the "see-saw" effect, where increasing DAP MICs are associated with a concomitant and significant enhancement in β-lactam susceptibility, despite retention of *mecA* encoding for β-lactam resistance (132, 184-186). These findings underscore both the likely complex adaptations that underlie the DAP-R phenotype and the possibility of modifying the DAP-R to a DAP-S phenotype pharmacologically (187). Although the see-saw mechanism has not been fully elucidated, it appears to involve at least two genes which impact either cell wall homeostasis (*vraSR*) and/or PBP2A chaperoning, folding and membrane localization (*prsA*) (135, 188).

β-lactam antibiotics enhance the activity of DAP *in vitro* and *in vivo* against both DAP-S and DAP-R MRSA (154). The mechanisms associated with this combinatorial interaction are incompletely understood but have been suggested to include: **i**) β-lactam-induced enhancement of DAP binding to the target bacterial surface (154); or **ii**) more targeted binding to those cell membrane regions where DAP is most effective (i.e., the cell divisome) (45, 78, 189). The synergistic interaction has been shown to be most potent with β-lactams that inhibit PBP-1. This monofunctional transpeptidase is responsible for cell division and separation, and it locates at the divisome of *S. aureus* (190). The cell divisome is also where DAP exerts its most potent cell membrane depolarization and cell division protein mislocalization activities (46). Given these elegantly linked mechanisms of DAP + β-lactam combined activity, we hypothesized that exposure to β-lactams might potentially resensitize DAP-R *S. aureus* to DAP.

In this study, DAP-R isolates were passaged in β-lactams with either selective or non-selective PBP-binding profiles, and then evaluated for their resulting phenotypic and genotypic characteristics. Based on these results, allelic exchange was performed based on passage strains from three of the DAP-R/DAP-S strain pairs and relevant membrane phenotypic modifications were assessed.

2.2 Materials and Methods

Bacterial strains. This study used a well-characterized collection of 50 clinical MRSA isolates that represent DAP-S and DAP-R (MICs ≥ 2 mg/L) pairs derived from bacteremic patients. Previous publications with targeted or whole genome sequence data have described these isolates in detail (100, 117, 180). This collection includes 22 DAP-S/DAP-R pairs of clinical bloodstream isolates from the Cubist Pharmaceuticals Isolate Collection, two DAP-S/DAP-R MRSA pairs from patients successfully treated with DAP plus nafcillin following DAP-NS emergence, and one DAP-S/DAP-R MRSA pair isolated after vancomycin (VAN) treatment (these latter three isolates were kindly supplied by George Sakoulas and Benjamin Howden).

The three isogenic DAP-S parental (WT) / DAP-R MRSA strain pairs (J01/J03, D592/D712, and C24/C25) were selected for the second part of this study: (**i**) clinically derived DAP-S isolates and their respective DAP-R variants emerging during DAP therapy; and (**ii**) the most common clonal complex (CC) types causing clinical infections in the United States (USA100 and USA300, CC5 and CC8 respectively) (181).

Growth conditions. The antibiotics used in this study and their PBP binding profile include: nafcillin (NAF), PBP-nonselective; cloxacillin (LOX) PBP-1 selective; meropenem: (MEM) PBP-1 selective; ceftriaxone (CRO), PBP-2-selective; and cefoxitin (FOX) PBP-4- selective; The β-lactams were purchased from Sigma-Aldrich (Sigma, St. Louis, MO, USA). DAP was commercially purchased, and its activity

confirmed by quality control susceptibility testing against ATCC 29231 per CLSI guidelines, version M100 ED28:2018 (51). Mueller-Hinton Broth II (MHB) (BD, Sparks, MD, USA) supplemented with 25 mg/L calcium (as $CaCl_2$), 12.5 mg/L magnesium (as $MgCl_2$), and 2% sodium chloride was used to grow *S. aureus* in liquid culture with β-lactams. All DAP assays used MHB with 50 mg/L calcium as recommended (51).

Antibiotic susceptibility testing. The MICs of all isolates (n=25 pairs, 50 isolates) to DAP and β-lactams were determined in triplicate by broth microdilution according to the CLSI guidelines (51). DAP MICs were also confirmed by Etest. The passaged isolates were evaluated for DAP MIC in triplicate following 7, 14, 21, and 28 days of passage in each β-lactam. Visual inspection for MIC determination occurred following 18-24 hours of incubation at 37°C. Isolate pairs with a positive see-saw effect was defined by ≥ 4-fold decrease in β-lactam MIC in the DAP-R isolate as compared to its respective parental DAP-S strain.

Serial passage. Four DAP-R isolates were passaged in triplicate daily for 28 days in exposure arms of no antibiotic, NAF, LOX, CRO, or FOX The free average concentration in human serum (fC_{avg}) after standard dosing was used for β-lactam daily passage (NAF 2.6 mg/L; LOX 1.4 mg/L; MEM 24 mg/L; CRO 19 mg/L). If these concentrations were above the β-lactam MIC, then 0.5x MIC concentrations were used to allow for bacterial growth as previously described (161). On day zero, bacterial colonies from overnight growth on Mueller-Hinton agar were suspended in normal saline and turbidity adjusted to equivalent of 0.5 McFarland standard. Each culture was diluted 1:100 into three replicates with fresh MHB25+2% salt to a total volume of 1 mL and containing each β-lactam. Each sample was grown overnight at 37°C with shaking at 160 rpm. Following incubation, 10 µl of each culture was transferred into fresh media and placed back on the shaker to grow as previously described (117). This process continued for 28 consecutive days with subsequent DAP susceptibility testing on samples obtained on days 7, 14, 21, and 28 of passage.

Whole genome sequencing of serial passage isolates. Genomic changes in all isolates and replicates pre- and post-passage were analyzed by whole genome sequencing. Genomic DNA was extracted with the JANUS Automated Workstation, using the Chemagic DNA/RNA kit (Perkin Elmer). Unique dual index libraries were prepared using the Nextera XT DNA preparation kit (Illumina), and libraries were sequenced on a NextSeq (Illumina) with 2 x 150 bp chemistry, as per the manufacturer's instructions. The short-read sequence data for all isolates was mapped to reference *S. aureus* J01 (RefSeq accession NZ_CP040619.1), D712 (NZ_CP040665.1), or JKD6004 (NZ_CP040622.1), using Snippy v4.4.3 (https://github.com/tseemann/snippy). Variants were called using a minimum mapped read depth of five, and base-call stringency of 90%. Allelic frequencies were calculated from the mapped alignment without application of the listed thresholds, displayed as the proportion of mapped reads containing the alternative allele compared to those containing the reference allele. Predicted protein consequences of variants were identified using snpEff v4.4 (191), with custom databases constructed from the above listed RefSeq genomes and configured to use the "Bacterial and Plastid" codon table.

Construction of mprF -mutants by allelic exchange. Introduction of a secondary *mprF* mutation into the three DAP-R backgrounds (which contain a single *mprF* mutation) was conducted using the allelic exchange protocol developed by Monk & Stinear (192) with modification. Oligonucleotides tailed with sequence complementary to pIMAY-Z were designed to amplify a ~1.2kb region surrounding the secondary *mprF* mutation (**Supplementary Table 2.1**) (193) the LOX passaged DAP-resensitized strains serving as a donor for the sequence. *E. coli* strain IM08B was used for electrocompetent transformation (194).

Suspected *mprF* double mutant (DM) colonies and cultures of the parent DAP-R strains used for allelic exchange underwent whole genome sequencing (WGS) to confirm their genotype (NextSeq; Illumina). Both the primary (from the DAP-R parent) and secondary (introduced) *mprF* mutations were

confirmed in all three backgrounds. Only one off-target missense mutation was identified; a A308V amino acid change in predicted gene FFX42_RS09315 in the D712 *mprF* DM (reference D592, CC5 background).

*BODIPY-DAP fluorescence microscopy***.** DAP binding was performed using confocal microscopy with BODIPY-labeled DAP. Cells were incubated with BODIPY-labeled DAP as previously described (152). The cells were concentrated 20-fold, and 3 µL was placed on a glass slide. Slides were set with prolonged diamond antifade mountant and a #1.5 glass coverslip. Images were collected using a Leica SP8 3X STED Super-Resolution Confocal Microscope using a 489 nm laser line and 510-579 nm emission with 660 nm depletion. ImageJ was utilized to measure integrated fluorescence density of 30 cells and corrected cell total fluorescence was calculated.

Cell membrane phospholipid (PL) composition and amino-PL (L-PG) asymmetry. The lipid extraction methodology has been described before (69, 97, 182, 183). *S. aureus'* major PLs (lysyl-phosphatidylglycerol [L-PG]; phosphatidylglycerol [PG]; and cardiolipin [CL]) were separated using two-dimensional thin-layer chromatography (2D-TLC), using a unique solvent system as previously described (69, 97, 182, 183). The isolated PL spots on TLC plates were scraped, digested at 180^0C for 3 h with 0.3 mL 70% perchloric acid to convert into inorganic form of phosphate and quantified spectrophotometrically at OD_{660} by phosphate estimation assay. The identification of all spots on the TLC plate were carried out by exposure to iodine vapors and by spraying with $CuSO_4$ (100 mg/ml) containing 8% phosphoric acid (v/v) and heated at 180°C.

Fluorescamine labeling (a membrane-impermeant UV fluorophore which binds to amino PLs, such as L-PG, in the outer membrane leaflet and is a measure of L-PG translocation), was performed, using the same 2-D TLC plates (69, 97, 182, 183). The percentage of fluorescamine-labeled L-PG was calculated from the phosphorus data relative to total PLs. In general, L-PG resides predominantly in the inner leaflet of the *S. aureus* cell membrane; however, variable amounts of LPG can be translocated from the inner-to-outer

membrane leaflet to maintain lipid homeostasis. Fluorescamine labelling of outer membrane (O)-L-PG was detected by using a UV detector (365 nm). Fluorescamine-labelled L-PG alters its mobility characteristics, and its ability to be detected by ninhydrin staining is attenuated. Unlabeled L-PPG (inner cell memnrabe [I]-L-PG), was visualized by ninhydrin staining. The identity of each of the major TLC spots was made in relation to known positive control PLs. Data were presented as the mean (±SD) percentages of the three major PLs (Total L-PG + PG + CL = 100%).

*Surface charge***.** The relative positive cell surface charge of the three DAP-S/DAP-R/LOX-DAP-resensitized strain-sets was assayed using the standard polycationic cytochrome C (CytC) binding assay as described elsewhere (97, 182, 183). Briefly, *S. aureus* strains were grown in BHI broth to stationary phase, washed with MOPS (3-morpholinopropane-1-sulfonic acid) buffer (pH 7.0), resuspended in the same buffer at OD_{578} ~1.0, and then incubated with 0.5 mg/ml of CytC for 10 min. The residual quantity of CytC remaining in the bacterial supernatant was then measured spectrophotometrically at OD_{530} nm as described previously (97, 182, 183). A decrease in the quantity of CytC binding (i.e., more cation in the supernatant) reflects a greater positively charged bacterial surface (97, 182, 183). The data are presented as mean (± SD) of bound CytC. A minimum of three independent experiments were performed on separate days.

Cell membrane order (fluidity/rigidity). Membrane order profoundly impacts the interactions of DAP with the *S. aureus* cell membrane. MRSA strain-sets were grown overnight in BHI broth at 37°C, harvested by centrifugation, then washed with PBS. A whole-cell suspension of the MRSA strains was prepared at an OD_{600} = 1.0 (~10^8 CFU ml^{-1}). Membrane fluidity was measured by polarizing spectrofluorometry utilizing the fluorescent probe, 1,6-diphenyl-1,3,5-hexatriene (DPH) [excitation and emission wavelengths of 360 and 426 nm]. The detailed methods for quantifying DPH incorporation into membranes and the calculations of the degree of fluorescence polarization [polarization index (PI)] are described elsewhere (184, 185). An inverse relationship occurs between PI values and membrane fluidity

(i.e., lower PI equates to a greater extent of membrane fluidity) (69, 73, 97, 182, 183). These experiments were carried out a minimum of four times for each strain-set on different days.

Statistical analysis. DAP MIC results were evaluated using Wilcoxon rank sum test. Two-tailed Student *t*-test was used for statistical analysis of all other quantitative data. Spearman r was used to determine antibiotic susceptibility correlations. *P* values of ≤0.05 defined significance.

2.3 Results

Antibiotic susceptibilities. The susceptibilities to tested antibiotics of 25 DAP-S and DAP-R isolate pairs and their previously identified *mprF* mutations are provided in **Supplemental Table 2.2** (104, 117, 161, 195). Overall, baseline DAP MICs ranged from 0.19–0.75 mg/L in the DAP-S isolates, and 2-4 mg/L for DAP-R isolates derived *in vivo* following DAP treatment. Isolate JKD6005 displayed a DAP MIC of 1 mg/L by both broth dilution and 2 mg/L by Etest, which is similar to the reported value (100). However, this isolate was derived *in vivo* from a patient receiving VAN treatment only, and lacks an *mprF* mutation, so this discordance is not unexpected.

The see-saw effect between elevated DAP MICs and lower β-lactam MICs was apparent among many β-lactams tested (**Figure 2.3.1**). A ≥4-fold decrease in the MICs for at least one β-lactam in the DAP-NS vs DAP-S isolates occurred in 48% of pairs, most notably with the PBP-1 specific LOX (44% of pairs). Analysis of the correlation between DAP-R and β-lactam susceptibilities revealed a significant negative association between DAP and LOX MICs (P = 0.032), while NAF, MEM, and CRO susceptibilities demonstrated similar trends toward negative association, but lacked statistical significance ($P \geq 0.118$) (**Figure 2.3.1**).

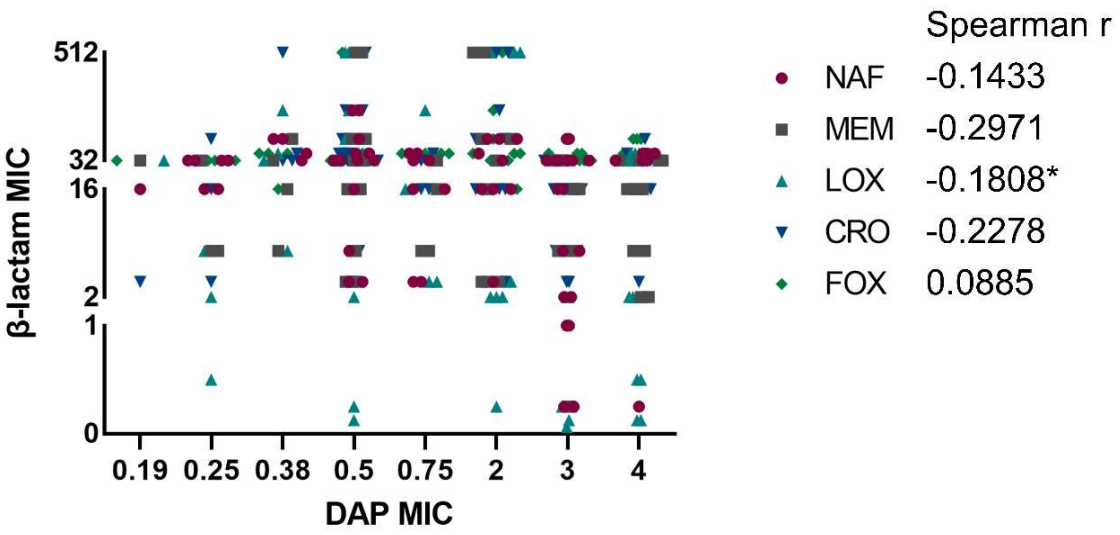

Figure 2.3.1 Correlation of DAP and β-lactam MIC in all 50 isolates. ***p=0.032**

*Serial passage***.** DAP-R isolates, J03, D712, C25, and JKD6005, were passaged in triplicate daily for 28 d in exposure arms of: no antibiotic (media alone); NAF; LOX; CRO; or FOX. Selection of these isolates for passage was based on their containing common, but distinct, "hot spot" mutations within the bifunctional domain of MprF for J03 (T345I), D712 (L341S), and C25 (S295L) (71). Isolate JKD6005 was selected as a "negative" control to interrogate the importance of pre-existing *mprF* mutations, as it contained a wildtype *mprF* sequence.

Figure 2.3.2. displays the DAP MIC fold-change over the 28 d exposures with or without different β-lactams. Of note, in isolates with pre-existing *mprF* mutations, passage in β-lactams was often able to resensitize the isolate to DAP. This occurred as early as day 7 of passage and continued throughout the 28 day exposure. Overall, LOX was most effective at resensitizing isolates to DAP, followed by NAF. In isolate C25, CRO was also highly effective in DAP resensitization, but a limited resensitizing effect of this agent was noted in other isolates. Enhanced DAP susceptibility with β-lactam passage did not occur in JKD6005 lacking a pre-existing *mprF* polymorphism. This strain does contain a mutation in WalR (YycF/VicR), an

essential response regulator implicated in both DAP-R and the seesaw effect, so this may play a role in preventing re-sensitization (100). The DAP-β-lactam seesaw effect accompanied DAP resensitization, with at least a 2-fold MIC increase in the respective β-lactam used in passage (**Table 2.3.1**).

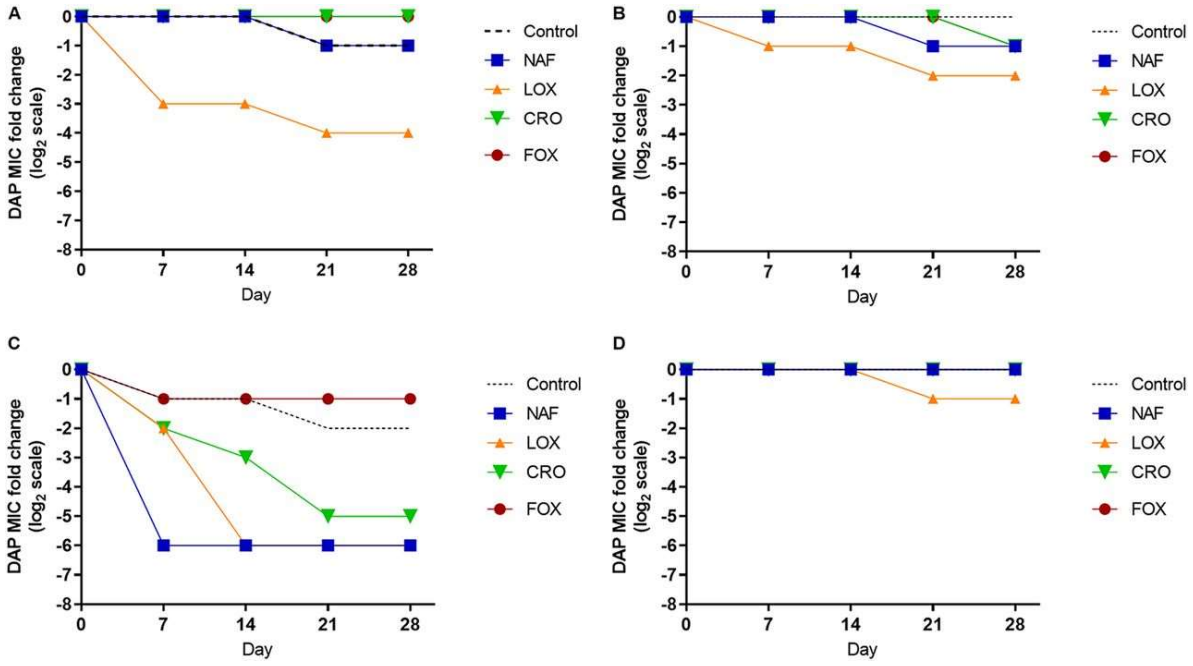

Figure 2.3.2. Serial passage in isolates J03 (A), D712 (B), C25 (C), and JKD6005 (D) with no antibiotic or β-lactams. Data represent median DAP MIC changes over 28 days with different exposures.

Whole genome sequencing. The isolates selected for serial passage were sequenced at day zero prior to β-lactam passage and then at end of treatment (day 28). Passage isolates maintained the pre-existing *mprF* mutations identified in the J03, D712, and C25 backgrounds, and gained additional mutations in *mprF*, a cell division gene (*div1b*), the beta- and beta'- subunits of the RNA polymerase (*rpoBC*), and several genes associated with metabolic function (**Table 2.3.1**; **Supplemental Table 2.3**). Of particular interest were the accumulation of additional *mprF* mutations. This was observed in all three isolate backgrounds with LOX passage; the passage isolates with these genotypes also demonstrated

increased sensitivity to DAP, with up to 32-fold difference in susceptibility (e.g., MIC changes from 3-4 mg/L to 0.125 mg/L). The largest shifts in DAP susceptibility were also associated with gain of *div1b* mutations. Mutations in *mprF* were not identified in the JKD6005 background with any β-lactam passage, indicating that a pre-existing *mprF* mutation may be necessary for β-lactams to induce this latter effect.

Table 2.3.1 Daptomycin susceptibility and *mprF* polymorphisms with β-lactam passage after 28 days.

ISOLATE	PASSAGE		DAP MIC (mg/L)	β-lactam MIC (mg/L)	*mprF* SNP	*mprF* DOMAIN	*div1b* SNP	*rpoB/C* SNP
J01	None		0.5		-	-		
J03	None		2		$T_{345}I$	Bifunctional		*rpoB* $S_{464}P$
	Media[a]	ii	1		$Y_{325}H$	Bifunctional		
	Media[a]	iii	1		$R_{437}P$	Synthase		
	CRO[a]	ii	0.75	512	$V_{152}G$	Translocase		
	LOX[a]	ii	0.125	32	$R_{788}L$	Synthase	Q_{425}*	
	LOX[a]	iii	0.125	32	$R_{788}L$	Synthase	Q_{415}*	
D592	None		0.5		-	-		
D712	None		2		$L_{341}S$	Bifunctional		
	NAF[b]	iii	1	256	$S_{337}P$	Bifunctional		
	CRO[b]	i	2	2048	$M_{609}T$	Synthase		*rpoC* $A_{567}V$
	CRO[b]	iii	0.5	2048	$G_{389}A$	Synthase		*rpoB* $G_{767}C$
	FOX[b]	ii	0.5	512	$F_{657}L$	Synthase		
	LOX[b]	i	0.5	1024	$S_{136}L$	Translocase		
	LOX[b]	ii	0.5	1024	$S_{136}L$	Translocase		
C24	None		0.5		-	-		
C25	None		3-4		$S_{295}L$	Bifunctional		
	Media[c]	i	1		S_{825}*	Synthase		
	Media[c]	ii	1		S_{825}*	Synthase		
	FOX[c]	iii	1	64	$A_{315}S$	Bifunctional		
	LOX[c]	i	0.125	8	L_{84}*	Translocase	$A_{420}E$	
	LOX[c]	ii	0.125	8	L_{84}*	Translocase		
	LOX[c]	iii	0.125	8	L_{84}*	Translocase	E_{416}*	

[a]passage isolates maintained MprF $T_{345}I$ and RpoB $S_{464}P$
[b]passage isolates maintained MprF $L_{341}S$
[c]passage isolates maintained MprF $S_{295}L$
*nonsense stop-gain mutation resulting in premature end of translation

To determine the temporal relationship between these identified mutations and phenotype, interim-passaged strains at days 7, 14, and 21 were also whole genome sequenced. This identified, first,

that no new mutations occurred in any passaged strains during this 7-21 day period compared to those identified at day 28 of passage (**Table 2.3.1** and **Supplemental Table 2.3**). Second, this also determined the approximate time of appearance and sustainability of these mutations throughout continued passage. With *mprF*, *div1b*, and *rpoB/C* mutations, this interim sequencing identified that *mprF* SNPs were present at day 7, while *div1b* were first detected at day 21, and *rpoB*/C only at day 28.

Resensitization to DAP-S phenotype. The DAP-R strains J03, D712, and C25 were resensitized to DAP after serial passage for 28 days *in vitro*. The secondary *mprF* mutations derived from LOX passage strains were reintroduced (*mprF* DM) into each respective DAP-R parental strains. The allelic replacement resulted in reduction of DAP MICs to levels similar to the post- LOX passage strains (**Table 2.3.2**).

Table 2.3.2 List of study strains including DAP-S parental strain, DAP-R strain, DAP resensitized strain from LOX passage, and DAP resensitized strain generated by allelic exchange of passage strain *mprF* into DAP-R strain (double mutant, DM). [*nonsense mutation]

ISOLATE	DAP MIC (mg/L)	LOX MIC (mg/L)	*mprF* SNPS	*mprF* DOMAIN(S)
J01	0.5	8	-	-
J03	2	4	$T_{345}I$	Bifunctional
J03- LOX (ii)	0.125	8	$T_{345}I + R_{788}L$	Bifunctional + Synthase
J03- *mprF* DM	0.125	16	$T_{345}I + R_{788}L$	Bifunctional + Synthase
D592	0.5	512	-	-
D712	2	512	$L_{341}S$	Bifunctional
D712- LOX (ii)	0.5	1024	$L_{341}S + S_{136}L$	Bifunctional + Translocase
D712- *mprF* DM	0.5	1024	$L_{341}S + S_{136}L$	Bifunctional + Translocase
C24	0.5	16	-	-
C25	3-4	2	$S_{295}L$	Bifunctional
C25- LOX (ii)	0.125	32	$S_{295}L + L_{84}*$	Bifunctional + Translocase
C25- *mprF* DM	0.125	16	$S_{295}L + L_{84}*$	Bifunctional + Translocase

DAP binding. Binding of BODIPY-DAP to the DAP-R parent strains, LOX passage strains, and DM strains was quantified by confocal microscopy (**Figure 2.3.3A**). Both the LOX passage strains and the DM bound significantly more DAP than their respective wild-type DAP-R strain. Representative images of the

D712 isolates show enhanced DAP- resensitization correlated with increased BODIPY- DAP binding (**Figure 2.3.3B**).

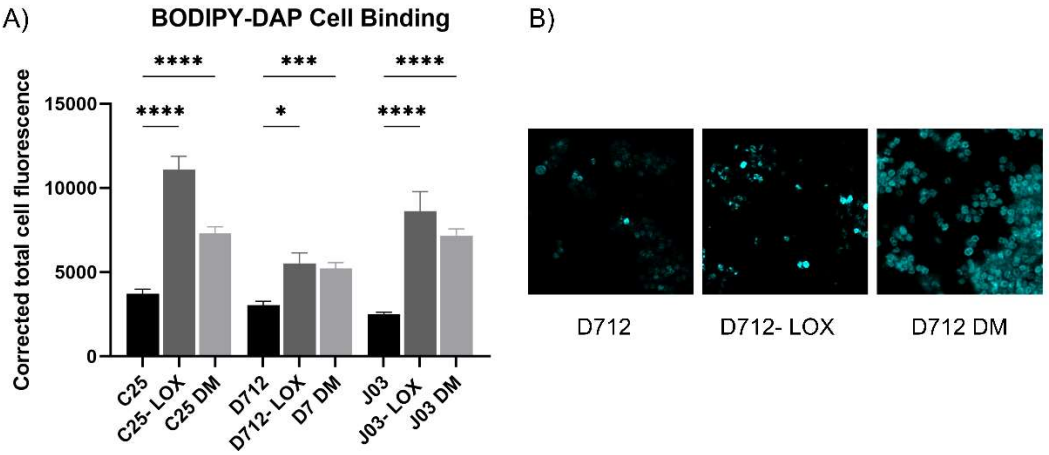

Figure 2.3.3 Binding of BODIPY-DAP to *S. aureus* study strains. (A) Corrected total cell fluorescence of BODIPY-DAP bindings and (B) representative confocal microscopy images of BODIPY-DAP binding to D series strains. ***p<0.01, ***p<0.001, ****p<0.0001**

Cell membrane phospholipid (PL) content. As expected, the DAP-R variants showed membrane PL profiles featuring increased total L-PG content vs the respective DAP-S parental strains consistent with other previously described DAP-R strains, reflecting gain-of-function impacts typical of single *mprF* mutations (161). Of interest, the increased total L-PG content in the DAP-R strains were associated with enhanced synthesis, but not increased outer cell membrane translocation (*data not shown*). In contrast, the DAP-resensitized variants, either derived post-LOX passage or via allelic replacement, demonstrated reductions in overall synthesis of L-PG, to levels comparable with the DAP-S parental strain (**Table 2.3.3**). This membrane PL profile in the DAP-resensitized strains is consistent with the documented accumulation of an additional *mprF* mutation in these strains, resulting in a phenotype of decreased function.

Table 2.3.3 Phospholipid composition (%) of LOX passage strains and *mprF* DM vs DAP-S/ DAP-R.

ISOLATE	L-PPG	PPG	CL
J01	22 ± 2	70 ± 2	8 ± 2
J03	31 ± 7[a]	66 ± 6[a]	3 ± 1[a]
J03- LOX (ii)	20 ± 1[b]	78 ± 3[b]	3 ± 2[b]
J03- *mprF* DM	16 ± 3[c]	78 ± 4[c]	6 ± 1[c]
D592	20 ± 3	77 ± 3	2 ± 3
D712	23 ± 2[a]	74 ± 4[a]	3 ± 2
D712- LOX (ii)	16 ± 4[b]	81 ± 5[b]	3 ± 2
D712- *mprF* DM	21 ± 2	75 ± 2	4 ± 1
C24	12 ± 3	80 ± 6	8 ± 5
C25	25 ± 5[a]	70 ± 5[a]	6 ± 3
C25- LOX (ii)	5 ± 1[b]	94 ± 1[b]	2 ± 1[b]
C25- *mprF* DM	11 ± 2[c]	83 ± 4[c]	6 ± 6

[a]p-value < 0.05 DAP-R vs DAP-S, [b]p-value < 0.05 LOX passage vs DAP-R, [c]p-value < 0.05 *mprF* DM vs DAP-R

Cell surface charge. As shown in **Table 2.3.4.**, more unbound cytochrome c (reflecting a more positive cell surface charge) was observed vs their respective DAP-S parent strains in 2 of the 3 DAP-R strains. In strains with secondary *mprF* mutations derived post-LOX passage as well as in the allelic reintroduction strains (*mprF* DM), a more negative surface charge was observed as compared to respective DAP-R strains (p≤0.05) and similar to the DAP-S parent strain.

Table 2.3.4 Surface charge and membrane fluidity of LOX passage strains and *mprF* DM vs DAP-S/DAP-R.

ISOLATE	% CYTOCHROME C UNBOUND	MEMBRANE FLUIDITY (PI VALUE)
J01	58 ± 0	0.381 ± 0.01
J03	48 ± 0[a]	0.359 ± 0.01
J03- LOX (ii)	55 ± 0[b]	0.395 ± 0.01[b]
J03- *mprF* DM	44 ± 0[c]	0.430 ± 0.03[c]
D592	56 ± 0	0.480 ± 0.01
D712	85 ± 3[a]	0.372 ± 0.01[a]
D712- LOX (ii)	46 ± 1[b]	0.389 ± 0.00[b]
D712- *mprF* DM	57 ± 1	0.395 ± 0.00[c]
C24	53 ± 1	0.389 ± 0.01
C25	62 ± 0[a]	0.370 ± 0.01[a]
C25- LOX (ii)	54 ± 0[b]	0.413 ± 0.00[b]
C25- *mprF* DM	45 ± 0[c]	0.368 ± 0.00

[a]p-value < 0.05 DAP-R vs DAP-S, [b]p-value < 0.05 LOX passage vs DAP-R, [c]p-value < 0.05 *mprF* DM vs DAP-R

Cell membrane order (fluidity/rigidity). There appears to be an optimal degree of membrane order for the interaction of most membrane-targeting cationic peptides, including calcium-complexed DAP (69, 182, 196). As seen with other DAP-R mutants of MRSA (104), the three DAP-R mutants in our study displayed more fluid membranes vs each respective parental DAP-S strain. The DAP-resensitized strains had an overall shift in membrane order toward a less fluid (more rigid) cell membrane, like that pattern of their respective DAP-S parental strains (**Table 2.3.4**).

2.4 Discussion

Several studies have described the synergistic relationship between β-lactam antibiotics and both DAP and cationic HDPs (152, 162). This synergy with HDPs is thought to be advantageous in enhancing β-lactam treatment, and it may contribute to the unambiguously superior clinical outcomes with β-lactams compared to VAN in MSSA bacteremic syndromes (40, 197). Although prior studies have shown that β-lactams can suppress the evolution of DAP or VAN resistance *in vitro* (198-200), few studies have determined the impact of β-lactams to prevent emergence of resistance to these agents *in vivo*. In the case of DAP-R, this impact has been linked to the ability of β-lactams to prevent emergence of *mprF* mutations (198, 199). However, to our knowledge, no report has conclusively documented the ability of β-lactams to resensitize clinically derived DAP-R isolates to DAP. The results of our current investigation indicate that β-lactam passage can, indeed, resensitize DAP-R isolates to DAP; this event appears to be mediated, at least in part, through the accumulations of additional point mutations in *mprF*.

Based on our data and others, the PBP-binding profile of those β-lactams that seem to be associated with DAP synergy in MRSA are likely selective, not global (135, 188). We previously found that β-lactams that target PBP-1 either as part of promiscuous PBP binding (PBPs 1-4, 2a) or via PBP-1 specifically result in highly synergistic interactions with DAP vs DAP-R MRSA. This synergy does not appear

to occur exclusively through enhanced DAP binding to the cell membrane, but rather through a dual mechanistic effect at distinct β-lactam and DAP cell wall divisome targets (154).

In the current study, using a large collection of well-characterized DAP-S/DAP-R isolate- pairs derived from patients, we evaluated the ability of β-lactams with a range of PBP-binding specificity profiles to resensitize DAP-NS strains. The most profound synergistic effects with DAP occurred with LOX, a PBP-1-specific antibiotic, although similar trends were observed with NAF, MEM, and CRO (Table 1, Figure 1). We were somewhat surprised to find a substantial see-saw effect with CRO, a PBP-2 specific antibiotic (8/25 pairs [32%]); Of note, the see-saw effect among specific DAP-S/DAP-R isolate-pairs was generally harmonious for LOX vs CRO. CRO MICs were the highest among all the β-lactams tested in the 25 DAP-S isolates (MIC_{50}= 64), perhaps allowing for a greater "window" for disclosing a see-saw relationship. By contrast, The DAP-S isolates were more susceptible to LOX and MEM (MIC_{50}= 16).

This work has potentially important clinical translational implications. As previously described, DAP-R isolates derived from patients treated with DAP who failed DAP therapy quite frequently exhibited point mutations in *mprF* (20/25 isolates [80%] in this investigation) (60, 180, 181). Although DAP-R can evolve without DAP treatment, this has been shown to occur primarily in VAN treatment in which cross-resistance to both VAN and DAP develops, most likely via a combination of a cell wall thickening phenotype, as well as distinct metabolic adaptations (202-205). In this study, we identified that prolonged β-lactams passage can reverse the elevated DAP MICs of DAP-R isolates, resulting in some passaged isolates that were up to 16-fold more DAP-susceptible than their respective DAP-R isolates, and 4-fold lower than the original DAP-S parental isolate. This effect was noted in all LOX-passaged isolates from backgrounds with pre-existing *mprF* polymorphisms*,* while no significant resensitization occurred with prolonged β-lactam passage in JKD6005, possessing the wild-type *mprF* sequence. Although the β-lactam passage was done without DAP in culture, there may be benefits to adding β-lactams to DAP treatment

during prolonged courses of therapy to either prevent DAP-NS development or revert emerging DAP-R subpopulations toward a more DAP-S phenotype (117).

In a recent study by Yang and colleagues (181), introduction of dual point-mutations in *mprF* via genetic complementation substantially lowered DAP MICs as compared to the DAP-NS host isolate, as well as the DAP-S parental isolate. These investigators incorporated combinations of two common "hot spot" *mprF* mutations in DAP-R isolates, S295L+L826F and T345A+L826F, resulting in: i) enhanced DAP susceptibility; and ii) evidence of reduced MprF functionality (i.e., significant reductions in outer membrane L-PG flipping). In our current passage experiments, these same hot spot mutations were present in J03 (T345X) and C25 (S295L), while another common hot spot *mprF* mutation was present in isolate D712 (L341S). Similar to the findings of the Yang group (181) we found additional *mprF* mutations lead to DAP resensitization in these isolates induced by β-lactam passaging, however the additional mutations in our passage isolates were not in "hot spot" locations.

Isolates exposed to LOX with the same pre-existing *mprF* mutations as studied by Yang et al resulted in exquisite susceptibility to DAP (MIC=0.125 mg/L) in these dual-point *mprF* mutation, post-passage isolates. These additional point mutations occurred in either the synthase or translocase domain, while none were mapped to the bifunctional domain (Table 2). However, the present study presents an interesting association, but does not indicate causality of these dual point *mprF* SNPs. The changes associated with membrane phospholipid composition and order with these dual-point *mprF* mutations and their causality for DAP-R reversal are a focus of future studies.

As noted above, prolonged LOX passage induces the accumulation of secondary mutations in *mprF*; however, the causal nature of this event for daptomycin resensitization was unclear, since other genetic mutations were also observed, most notably in *div1b* and *rpoC.* In this present study, we confirmed that these secondary *mprF* mutations (either via LOX passage or allelic exchange) are, indeed,

sufficient to restore parental level daptomycin MICs, as well as induce prototypical modifications in cell membrane phenotypes. Studies are in-progress to understand the mechanism(s) by which β-lactams can trigger the accumulation of secondary *mprF* mutations.

All three DAP-resensitized strains demonstrated substantially decreased membrane fluidity as compared to their respective DAP-R strains, and like their respective DAP-S parental strains. There are optimal biophysical metrics within the cell membrane microenvironment that appear to maximize interactions of cationic peptides with the mambrane of MRSA (132, 184, 185, 187). Therefore, MRSA membranes containing extremes of rigidity/fluidity are comparatively resistant to interactions with such peptides (69, 104, 182). The similar patterns of membrane order of DAP-S parental and DAP-resensitized strains, on the one hand, vs the distinctly different patterns of membrane order in their respective DAP-R variants, underscored the likelihood that this phenotype is playing a relevant role in the overall differences in ultimate DAP-induced killing.

We recognize that the current investigation has several key limitations: **i**) although a large well-characterized MRSA strain collection was used for susceptibility screening, only three DAP-S/DAP-R/DAP-resensitized strain-sets were studied for phenotypic characterization; **ii**) only a relatively focused cadre of phenotypic characteristics were interrogated in comparing the strain-sets; **iii**) only a single β-lactam antibiotic was used for prolonged passage, leaving unresolved whether other PBP-specific or PBP-promicsuous β-lactams can elicit the same adaptations; **iv**) the linkage of our cell membrane perturbations with specific metabolic modifications was not explored (207) and; **vi**) additional mutations documented previously in prolonged LOX-passaged strains (182) were not systematically investigated (e.g., via allelic exchange) to determine their impacts on the above cell membrane parameters. It should be noted that DAP-resensitization did not occur post-LOX passage in DAP-R strains lacking a primary *mprF* mutation; thus, it is highly likely that *mprF* and its associated cell membrane changes play a critical role in the DAP-resensitization phenomenon.

In summary, this study provides novel insights on the activity of β-lactam antibiotics in DAP-R MRSA. It points towards an important role of PBP-1-targeting antibiotics to induce mutations that may potentially reverse or prevent the DAP-R phenotype. These findings support the previous notion of β-lactam prevention of DAP-R through inhibiting *mprF* mutation development (117). However, it also introduces the exciting notion that β-lactams can reverse DAP-R by inducing additional mutations in signature genes related to DAP-R, such as *mprF*.

Chapter 3. Proteomic Correlates of Enhanced Daptomycin Activity with β-Lactam Pre-Conditioning

Authors and their contributions:

Cassandra Lew: Planned and conducted experiments, wrote and edited manuscript

Molly Pellitteri Hahn: Planned and conducted proteomics experiments

Cameron Scarlett: Contributed to design of proteomics experiments

Aaron Rottier: Contributed to design of activity experiments

Andrew D Berti: Contributed to design of activity experiments

Richard A Proctor: Contributed intellectual input

Arnold S Bayer: Supervised research and contributed to design of experiments

Warren E Rose: Supervised research and contributed to design of experiments

Portions of this chapter have been previously published as:

Lew C, Pellitteri Hahn M, Scarlett C, Rottier A, Berti AD, Proctor RA, Bayer AS, Rose WE. 2022. Proteomic Correlates of Enhanced Daptomycin Activity Following β-Lactam Pre-Conditioning in Daptomycin-Resistant Methicillin-Resistant *Staphylococcus aureus.* Antimicrob Agents Chemother. 66(3)

3.1 Introduction

MRSA is a problematic invasive clinical pathogen with high associated patient mortality rates, as well as an alarming ability to evolve resistance to multiple antibiotics (208). The development of resistance to DAP in clinical MRSA is not rare, and results in DAP treatment failures (40, 56, 209, 210). DAP has a complex mechanism of action that involves inhibition of cell wall synthesis, as well as targeting and perturbation of the cell membrane (211-213). Accordingly, SNPs in components related to multiple cell envelope homeostatic pathways have been associated with acquisition of the DAP-R phenotype (71, 75, 213). These SNPs are often located in genes responsible for membrane lipid biosynthesis, membrane polarization, surface charge maintenance, and divisome organization (e.g., *mprF*, *cls2*, and *yycF*) (75, 214).

Clinical studies have validated certain combinations of DAP + selected β-lactams are effective in the treatment of DAP-R MRSA infections, particularly DAP in combination with ceftaroline (79, 215). Such approaches are supported by extensive studies showing *in vitro* synergistic activity of these combinations against DAP-R MRSA (216, 217). In addition, such combinations have been shown to inhibit the emergence of DAP-R in MRSA by forestalling the development of SNPs in the multiple peptide resistance factor gene, *mprF* (218). Further, as described in **Chapter 2**, serial passaging with selected β-lactams has been shown to re-sensitize DAP-R strains to a DAP-S phenotype, associated with acquisition of multiple *mprF* mutations. Despite the substantial data on salutary clinical outcomes using these combinations, the mechanism(s) behind DAP/β-lactam combination efficacy in DAP-R MRSA appear to be multifactorial and remain incompletely understood (73, 79, 104, 154).

The impacts of β-lactams upon specific cellular proteomic pathways of MRSA have not been well characterized. Given that β-lactams also synergize with innate host defense cationic peptides (162, 219), understanding their more fundamental effects upon MRSA may improve future therapeutic strategies against this pathogen. The objective of the present study was to validate the role of β-lactam-induced

cellular responses on DAP activity by characterization of the proteomic profiles of a clinically derived DAP-S/ DAP-R MRSA strain pair, with or without pre-conditioning to a range of β-lactam antibiotics that vary in their PBP-targeting specificities.

3.2 Materials and Methods

Bacterial strains and culture conditions. The DAP-S/ DAP-R MRSA strains D592/ D712 were utilized in this study. These strains have been used in other delineations of the DAP-R phenotype, and their clinical isolation and microbiologic characterizations have been previously published (152). There is a gain-of-function SNP in the *mprF* gene (161) within one of the prototypical "hot spots" related to the DAP-R phenotype, L341S (71). The DAP MIC of the DAP-S/ DAP-R strains are 0.5 mg/L and 2-4 mg/L, respectively, as determined by broth microdilution assay.

The following β-lactams with wide-ranging penicillin-binding protein (PBP) selectivity were employed: LOX [PBP-1], MEM [PBP-1], NAF [PBP 1-4; non-selective], CRO [PBP-2], CEC [PBP-3], and FOX [PBP-4]. The free average unbound concentrations (*f*Cavg) of these β-lactams selected for use in this study were calculated based on the reported maximum and minimum unbound concentrations in a typical dosing interval (161). These test concentrations were selected to approximate clinically relevant, human-equivalent blood levels. Six biological replicates for each condition were performed. All β-lactam exposure concentrations for pre-conditioning were confirmed to be sub-inhibitory and did not differentially affect growth kinetics for the study MRSA strain in pilot studies (**Supplementary Figure 3.1**).

β-lactam exposure conditions. For all β-lactam exposures, 2.5 mL of an overnight culture was added to 250 mL of cation-adjusted MHB with the following *f*Cavg concentrations of the various β-lactams: NAF (2.6 mg/L), MEM (24 mg/L), LOX (1.35 mg/L), CRO (19 mg/L), CEC (3.25 mg/L), or FOX (22 mg/L). Such

preconditioned cells were incubated for ~ 4 hr shaking at 220 rpm and 37°C to an OD_{600} of 0.1 at which point cultures were harvested for further study.

Antibacterial activity by spectrophotometry. Overnight cultures of D712 were diluted 1:100 in fresh cation-adjusted MHB in the presence or absence of *f*Cavg of the β-lactams as listed above. Cultures were incubated for ~4 hr at 37° to achieve an OD_{600} nm of 0.1 (defined as t = 0hr) to mimic proteomic analysis conditions. DAP was added to such β-lactam-"*pre-conditioned*" cultures, at a concentration equivalent to its approximate *f*Cmax in humans following a standard 6 mg/kg iv dose (6.9 mg/L) (220). In cultures grown without antibiotic, the same β-lactam and DAP concentrations above were added *simultaneously* (i.e., no β-lactam preconditioning) for comparison to the respective preconditioned exposures. Cells were grown in 2.5 mL cultures and absorbance was then determined spectrophotometrically at OD_{600} nm after 1, 2, and 4 hr to assess antibacterial activity over time during log-phase growth (maximal phase of β-lactam activity).

Bactericidal activity. Culture growth conditions mimicked the pre-conditioned and simultaneous exposure dosing methods used in the assay above, except cells were grown to an OD_{600} nm of 0.3. Cells were grown in 1 mL cultures and 100 µL aliquots were collected immediately following DAP dosing and after 4 hr. Samples were plated on MHA plates and the colony-forming units (CFU)/mL were quantified after 24 hr incubation. Data were expressed as mean $\log_{10}$ CFU/mL (+/- SD), and preconditioning groups compared by the change in such counts at 4 hr growth relative to the starting number of cells ($\Delta \log_{10}$ CFU/mL [+/- SD]).

TEM sample preparation and imaging. Overnight cultures of D712 were diluted 1:100 in fresh cation-adjusted MHB in the presence or absence of 2.5 mg/L of the β-lactams as listed above. Cultures were incubated for ~16 hr at 37° to achieve an OD_{600} nm of 0.5 (defined as t = 0hr). DAP was then added to β-lactam-"pre-conditioned" cultures. In parallel, the same β-lactam and DAP concentrations above

were added simultaneously (i.e., no β-lactam preconditioning) for comparison to the respective preconditioned treatment. After 24 hr, cultures were rinsed in PBS and pelleted for processing. Transmission electron microscopy (TEM) was performed following previously described techniques (221) except for acetone being used in place of ethanol for dehydration. Samples were processed yielding an immersion-fixed pellet, dehydrated, embedded, and sectioned for imaging using a Philips CM120 electron microscope and MegaView III side-mounted digital camera. TEM samples were viewed at 15000X magnification, concentrating on major impacts on cell wall integrity.

Preparation of cell lysate for proteomics analysis. Cell pellets from the treatment conditions described above were isolated in parallel by centrifugation at 4000 rpm for 10 min at 4°C, washed twice with cold PBS, and then resuspended in 500 µL lysis buffer (6 M urea, 100 mM ammonia bicarbonate, and 5 mM fresh dithiothreitol [DTT]) (Thermo Fisher Scientific, IL). Cells were lysed using a bead beater for 60 s at speed 50- 5 times. Insoluble debris was pelleted, and the supernatant was precipitated with 1:1 volume cold Optima grade acetone (Thermo Fisher Scientific, IL) and incubated on ice for 1 hr. The protein was pelleted by centrifugation at 10,000 G for 20 minutes at 4°C (Eppendorf, MA). Protein pellets were air-dried on ice for 10 min and then resuspended in 100 µL 100 mM ammonia bicarbonate with 1M urea in preparation for digestion. Protein concentrations were measured using MicroBCA assay (Thermo Fisher Scientific, IL). Samples were reduced with 10 mM DTT for 30 min, followed by alkylation with 45 mM Iodoacetimide to break disulfide bonds. For each sample, 20 µg of total protein was digested with 2 µg sequencing grade trypsin, adding 1 µg twice during digestion (Promega Corp., WI). Samples were incubated overnight at 30°C, dried in a speed vac, and prepared for LCMS/MS by C18 Zip-Tip purification according to the manufacturers protocol (Millipore Inc. Billerica, MA). Peptide samples were resuspended in 20 µL water with 0.1% formic acid (v/v) and analyzed by nano-LC-MS/MS.

LC-MS/MS protein identification and quantification. For label-free relative quantitative analysis, six replicates of each sample were analyzed by nano-LC/MS/MS. For each run, 1 µg of the peptide digest

was separated using a trap-elute strategy with a Waters NanoAcquity system equipped with a Symmetry C18 180 µm x 20 mm trap column, and a Waters M-class peptide BEH C18, 75 µm x 150 mm analytical column (Waters Corp., MA). Trapping was done at a rate of 5 µL/min for a total of 5 min before the valve switched and the flow was reduced to 0.35 µL/min. Peptides were eluted from the analytical column with a linear, 140-minute gradient. Optima grade liquid chromatography solvents were water / 0.1% formic acid (A) and acetonitrile / 0.1% formic acid (B). The gradient went from 3% to 35% B in 110 min. At 115 minutes the gradient increased to 95% B and held there for 10 minutes. At 130 minutes the gradient returned to 3% for 10 mins to re-equilibrate the column for the next injection. A short 50-minute linear gradient blank was run between samples to prevent sample carryover. Peptides eluting from the column were analyzed by data-dependent MS/MS on a Q-Exactive Orbitrap mass spectrometer (Thermo Fisher Scientific, MA). A top 15 method was used to acquire data. The instrument settings were as follows: resolution was set to 70,000 for MS scans and 17,500 for the data dependent MS/MS scans to increase speed. The MS automatic gain control (AGC) target was set to 10^6 counts, while MS/MS AGC target was set to 10^5. The MS scan range was from 300-2000 m/z. MS scans were recorded in profile mode, while the MS/MS was recorded in centroid mode, to reduce data file size. Dynamic exclusion was set to a repeat count of 1 with a 5 second duration.

Data processing. Data was searched using the Sequest HT Proteome Discoverer 2.4 search engine (Thermo Fisher Scientific), against Uniprot MRSA strain Mu50 at a false discovery cut off ≤ 1%. Following protein identification, LC-MS/MS data was aligned, and quantitation of peptides was performed on processed data using the Proteome Discoverer 2.4 label-free method pipeline. Peak intensities from all LC-MS/MS runs were normalized by the total ion chromatogram intensity, and MS intensities from raw LC-MS data was used to find statistical proteomic differences between samples. Proteins were filtered for abundance ratio adjusted p-value of ≤ 0.05 and at least 2 peptides identified per protein. Heat map and PCA plots based on protein abundances in β-lactam treated samples were exported.

Biochemical pathway analysis. To determine which biochemical pathways were affected by the distinct β-lactam exposures, lists of significantly up- or down-regulated ($p \leq 0.05$) proteins were analyzed using the Search Tool for the Retrieval of Interacting Genes / Proteins (STRING) database (222). Initially, proteins abundances between the DAP-S and DAP-R strains either with or without β-lactam exposures were compared. The second analysis focused on proteins altered in the DAP-R strain with β-lactam pre-conditioning strategies as compared to untreated controls. The final analysis identified differences between distinct β-lactam pre-exposures using Proteome Discoverer 2.4 and Uniprot retrieve / ID mapping to classify gene ontology.

Statistical analysis. Differences in DAP-R MRSA killing in the activity assay was determined by one-way ANOVA with Tukey's post-hoc test with $p \leq 0.05$ considered significant. Filtering in Proteome Discoverer software calculated p-value from t-tests based on background populations of proteins. Enrichment of biological processes in the comprehensive β-lactam analysis was performed using the Benjamini-Hochberg procedure to calculate p-values corrected for multiple testing, with $p \leq 0.05$ considered significant.

3.3 Results

DAP + β-lactam activity. The bactericidal activity of DAP + selected β-lactams in the DAP-R strain D712 was assessed following either overnight growth in distinct β-lactams followed by DAP (PRE-TREATMENT) or exposure to both antibiotics simultaneously at t = 0 hr (SHOCK). Control strains with no antibiotic exposure grew to OD_{600} of 1.8. Both SHOCK and PRE-TREATMENT cultures had increased MRSA clearances (lower OD_{600}) as compared to DAP exposure only. The PRE-TREATMENT samples had significantly more bacterial killing compared to SHOCK samples at both 2 and 4 hr time points in all combinations (**Figure 3.3.1A**). Notably, NAF, CRO, and LOX pre-conditioning led to the most impressive

impacts on killing as compared to SHOCK treatments. The significant trends identified in the antibacterial assay above were verified by the bactericidal assay at the 4 hr time point (**Figure 3.3.1B**). All β-lactam PRE-TREATMENT samples (except CEC) had significantly more bacterial killing as compared to their respective SHOCK treatments after 4 hr.

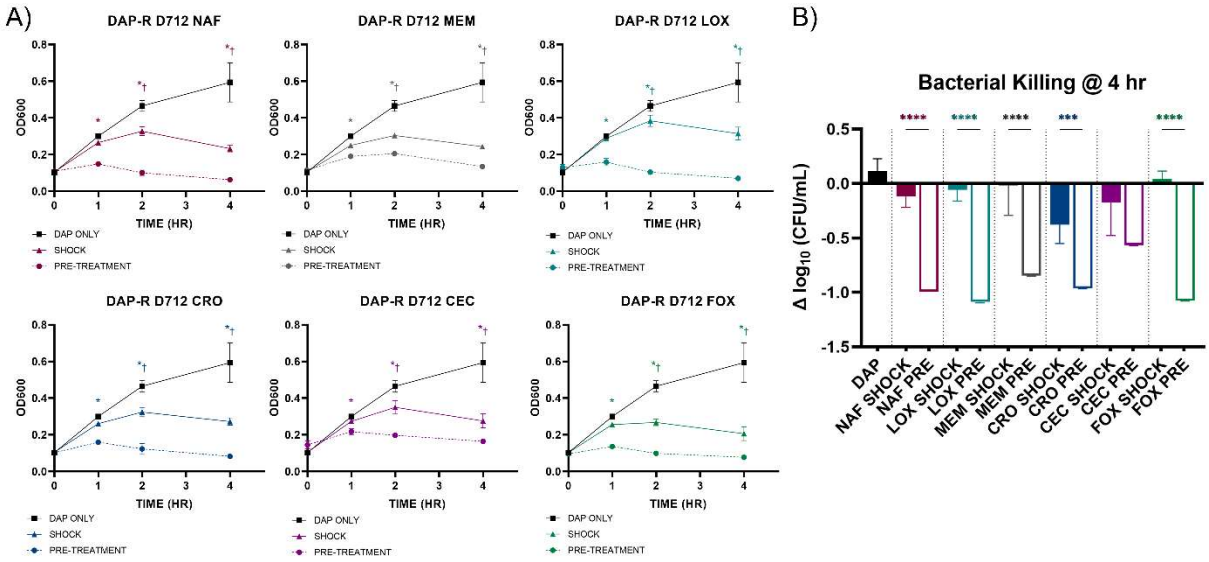

Figure 3.3.1 Activity of DAP + β-lactam combinations against DAP-R MRSA strain D712 following either sequential (PRE-TREATMENT) or simultaneous (SHOCK) dosing. (A) OD_{600} growth curve. *indicates PRE-TREATMENT significantly improved MRSA killing compared to DAP only. ‡indicates PRE-TREATMENT significantly improved MRSA killing compared to SHOCK treatment ($p \leq 0.05$ considered significant). (B) Quantification of D712 bacterial killing by change in CFRU/mL after 4 hr. *****p<0.001, ****p<0.0001**

Representative TEMs of cells following either DAP, SHOCK, or PRE-TREATMENT conditions are depicted in **Figure 3.3.2**. As apparent in the enlarged images, cells from the DAP and SHOCK conditions had largely deformed cell walls with moderate cell death. Strikingly, in the PRE-TREATMENT condition, there were few intact cells with most cell walls being broken down or undergoing degradation. As is clear by analysis of the images, TEMs from the PRE-TREAMENT group showed evidence of more bacterial death, as well as notable cell lysis as compared to SHOCK and DAP-only treatment.

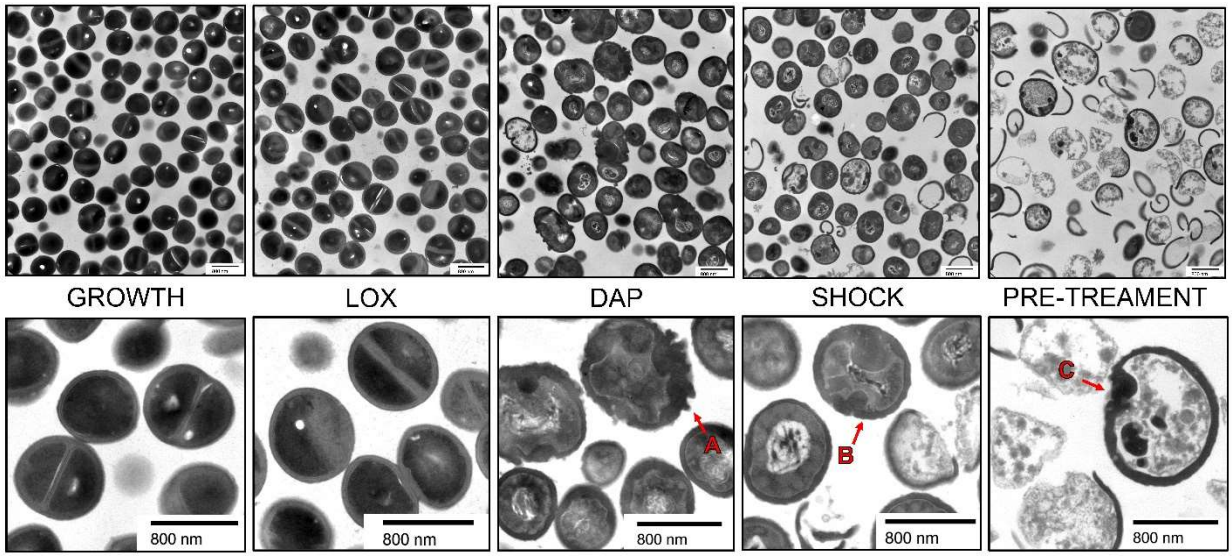

Figure 3.3.2 Representative TEM images of D712 growth without antibiotic, in the presence of LOX, in the presence of DAP, DAP + LOX SHOCK, and DAP + LOX PRE-TREATMENT conditions. In the DAP and SHOCK conditions, there is apparent cell death and in live cells abnormalities of the cell wall (A,B). In the PRE-TREATMENT images there are few intact cells with the majority having free cell contents (C).

*Proteins with altered abundance in the DAP-S verses DAP-R strain (**Supplementary Table 3.2**).* Analysis of the proteomes comparing the DAP-S and DAP-R strain with no antibiotic and with each β-lactam condition identified 10 proteins that were changed in most of the comparisons. The phosphatidylglycerol lysyltransferase MprF and the chaperone PrsA, both previously associated with DAP resistance, were found in increased abundance in D712 compared to D592 (**Table 3.3.1**). Other proteins of interest identified include both members of the two-component regulator VraSR, which were both increased in the DAP-R strain. Proteins involved in techoic acid biosynthesis and modification, LtaS and DltB/D respectively, were also increased in the DAP-R strain. Of interest, staphylococcal protein a (Spa) was decreased in the DAP-R strain compared to it's DAP-S parent.

Table 3.3.1 Proteins with differential abundance in D592 compared to D712 in the same treatment conditions. Ratios <1 indicates increased abundance in the DAP-R (vs DAP-S) strain; blank spots indicate no significant differences.

Protein	Gene	NO ABX	NAF	MEM	LOX	CRO	CEC	FOX
SA1701	*vraS*	0.681		0.405			0.723	
SA1700	*vraR*		0.680			0.601		
SA1659	*prsA*	0.439	0.611	0.512	0.564	0.506	0.668	0.856
SA0674	*ltaS*			0.550		0.573		0.569
SA1549	*htrA1*		0.692	0.590		0.521		0.815
SA1059	*fmt*					0.474	0.747	0.726
SA1193	*mprF*		0.666		0.547	0.440	0.748	0.564
SA0796	*dltD*		0.687			0.597		0.750
SA0794	*dltB*					0.434		0.691
SA0107	*spa*	2.579	3.127					
SA2113			0.702				0.686	0.753

*Protein expression with β-lactam pre-treatments (**Supplementary Tables 3.3 and 3.4**).* Proteomic changes in response to β-lactam stress were assessed to better understand mechanistically how pre-conditioning with β-lactams improves DAP-mediated bacterial killing. The relative proteomic quantitation data were filtered for proteins with significantly altered abundance following β-lactam pre-conditioning compared to untreated controls. After filtering proteins for data quality, we compared the results for all β-lactam treatments to identify proteins that were consistently altered. There were nine proteins in D712 with significant abundance ratios for differential expression with all β-lactam pre-treatments: MecA, InfA, AtpB, SA2332, SA0954, RpmF, SceD, and BacA (**Table 3.3.2**). The protein PBP 2A (encoded by MecA) was increased consistently following β-lactam exposure. Abundances of SceD and AtpB, a peptidoglycan lytic transglycosylase and F0F1 ATP synthase subunit A, respectively, were decreased with β-lactam pre-treatment (vs untreated controls). Three uncharacterized proteins SA2332 and SA0954 were similarly found to be consistently decreased following β-lactam exposure. RpmF is the 50S ribosomal protein L32. Pre-treatment with CRO led to increased amounts of this protein, while in MEM, CEC, and FOX conditions, RpmF exhibited decreased levels.

Table 3.3.2 Proteins with differential abundance following β-lactam conditioning compared to untreated control in D712. Ratios <1 indicates decreased abundance with β-lactam pre-treatment; Ratios >1 (bold) indicates increased abundance with β-lactam pre-treatment; blank spots indicate no significant differences.

Protein	Gene	DAP-R D712					
		NAF	MEM	LOX	CRO	CEC	FOX
SA0038	*mecA*	**7.844**	**6.503**	**7.290**	**4.840**	**3.941**	**5.040**
SA2026	*infA*		**2.508**		**1.829**	**1.800**	**1.914**
SA1911	*atpB*	0.072	0.125	0.025	0.033		0.165
SA2332		0.308	0.053		0.275	0.080	0.062
SA0954			0.226	0.269	0.203	0.143	0.156
SAS033	*rpmF*		0.027		**1.779**	0.017	0.022
SA1891	*sceD*	0.167	0.083				0.040
SA0638	*bacA*	0.339	0.220		0.333		0.147

Five of these proteins, MecA, AtpB, SA2332, RpmF, and SceD, had similarly altered abundance across β-lactams in D592. In addition, RpoY, EssC, and membrane protein SA2221 also had increased abundance with β-lactam conditioning (**Table 3.3.3**). MecA was once again significantly increased with in all β-lactam treatments. Abundances of SceD, AtpB, and SA2332 were similarly decreased with β-lactam pre-treatment (vs untreated controls). Abundances of the ribosomal protein RpmF was altered differentially, similarly to the DAP-R strain, with it increasing in NAF, LOX, CRO and decreasing in the other three conditions. The DNA directed RNA polymerase subunit epsilon RpoY, the type VII secretion protein EssC, and the uncharacterized membrane protein were also consistently decreased.

Table 3.3.3 Proteins with differential abundance following β-lactam conditioning compared to untreated control in D592. Ratios <1 indicates decreased abundance with β-lactam pre-treatment; Ratios >1 (bold) indicates increased abundance with β-lactam pre-treatment; blank spots indicate no significant differences.

Protein	Gene	DAP-S D592					
		NAF	MEM	LOX	CRO	CEC	FOX
SA0038	*mecA*	**10.478**	**6.195**	**11.905**	**8.896**	**5.928**	**7.488**
SA1911	*atpB*	0.061	0.113	0.049	0.020		0.115
SA2332		0.207	0.039	0.469		0.092	0.064
SA0491	*rpoY*	0.248		0.447	0.194		0.371
SAS033	*rpmF*	**2.524**	0.064	**2.878**	**3.538**	0.032	0.033
SA1891	*sceD*	0.010	0.010	0.374	0.234	0.122	0.010
SA0276	*essC*	0.010		0.220	0.174		0.325
SA2221		0.220		0.458	0.141		0.537

A comprehensive list of the all proteins which were differentially expressed with β-lactam pre-treatments was compiled and analyzed using the STRING database. The gene ontology analysis for functional categorization revealed regulation of 15 enriched biological processes, with the 10 most significant represented in **Figure 3.3.3**. The three most highly enriched pathways were metabolic processes, cellular macromolecule biosynthetic processes, and cellular processes, with 62, 29, and 68 proteins respectively. Most of the other enriched pathways are either biosynthetic or metabolic processes.

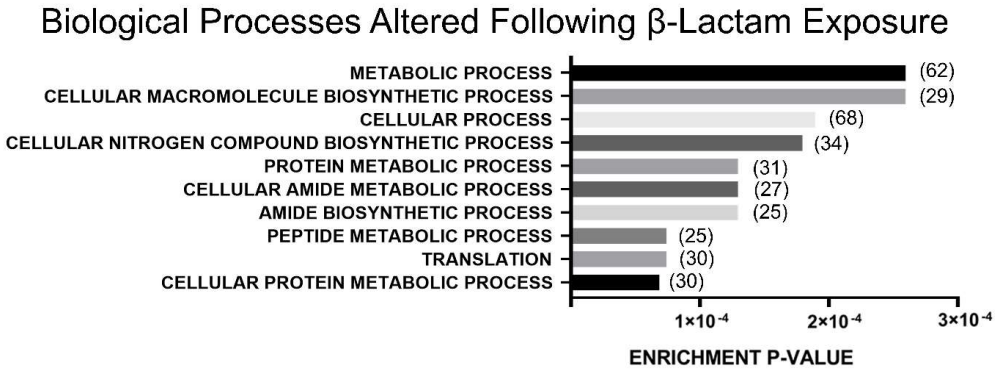

Figure 3.3.3 Enrichment of biological processes of proteins with altered abundance in β-lactam exposed strains compared to untreated control identified by STRING gene ontology. Values next to bars indicate number of proteins.

Comparison of distinct β-lactam induced response. The set of β-lactams in this study was selected for analysis based on clinical relevance and varying PBP specificities. For each β-lactam, abundance ratios of antibiotic-free (NO ABX) control samples vs. β-lactam pre-treated samples were evaluated. Comparing trends in protein abundance between β-lactam pre-treatments (**Figure 3.3.4A**), there was wide variation in abundance levels of proteins. In general, β-lactam treatments lead to similar responses in both the DAP-S and DAP-R isolates. PCA analysis in **Figure 3.3.4C** demonstrates the similarities in abundance between NAF, LOX, and CRO samples, with these treatments clustering together in both the susceptible and resistant strains.

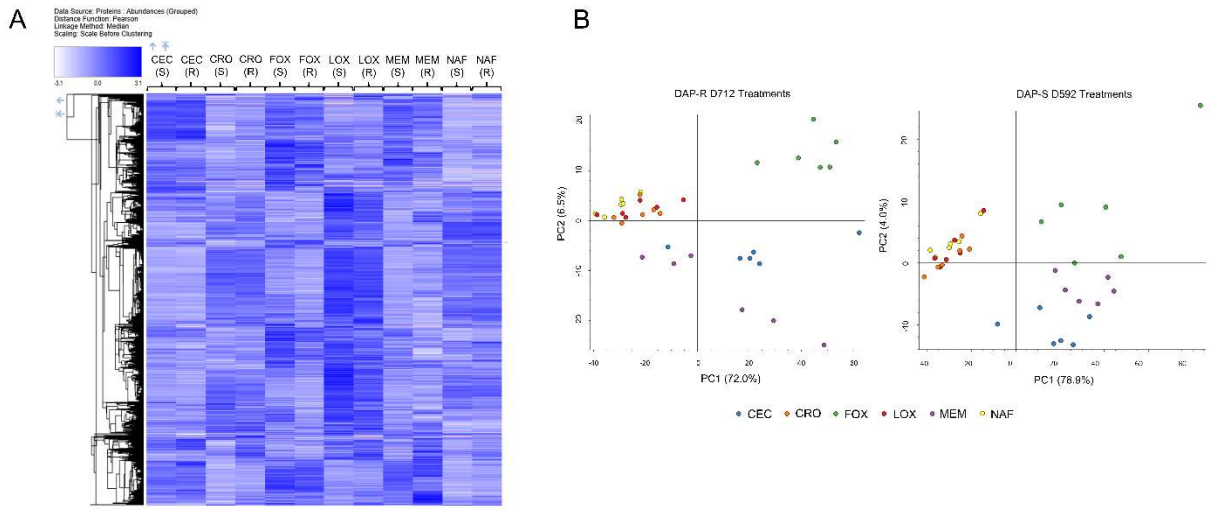

Figure 3.3.4 Comparison of proteomic response following β-lactam exposures. (A) Comprehensive heat map of protein abundances in each condition- darker blue represents higher abundance, white represents decreased abundance, and pin indicates undetected in sample. (B) PCA plot comparisons of distinct β-lactam conditions based on protein abundances.

Specific protein groups. Two distinct categories of proteins were repeatedly identified as having significantly altered abundance following β-lactam preconditioning: major *S. aureus* autolysins and proteins involved in riboflavin biosynthesis. Several proteins in the *rib* operon responsible for riboflavin biosynthesis were noted in the different analyses with particularly striking ratios. **Table 3.3.4** lists the

abundance ratios of each of the proteins comparing the β-lactam treatments vs untreated control. In the resistant strain LOX and FOX treatments the abundances of *ribHABD* proteins were decreased compared to the untreated control. With MEM treatment, RibB and RibD were significantly decreased vs the untreated control. Consistent with results in D712, LOX, MEM, and FOX lead to decreased protein abundance, although significant in fewer conditions for the latter two. Additionally, NAF exposure decreased the abundance of all proteins in the *rib* operon.

Table 3.3.4 Proteins in the *rib* operon and their associated ratios in different conditions. Ratios <1 indicate decreased abundance with β-lactam treatment, blank spots indicate no significant differences.

Condition		RibD	RibE	RibBA	RibH
D712 ABX / NO ABX	MEM	0.202	0.202		
	LOX	0.097	0.097	0.323	0.263
	FOX	0.087	0.087	0.219	0.084
D592 ABX / NO ABX	NAF	0.318	0.243	0.243	0.298
	MEM		0.669		
	LOX	0.161	0.033	0.118	0.156
	FOX	0.225			

The other set of proteins identified consistently as differentially expressed in our analysis were the major *S. aureus* autolysins AltA, IsaA, LytM, SceD, Sle1, and SsaA. The abundance ratios of these proteins comparing each β-lactam pre-treatment vs untreated controls are listed in **Table 3.3.5**. Treatment with MEM led to a significant decrease in all the autolysins in both strains. Similarly, FOX-pretreated samples had decreased amounts of 5 of the 6 autolysins in both D592 and D712. NAF-pre-treated strains had significantly decreased levels of IsaA, SceD, and LytM. In the DAP-S strain, all β-lactam conditions led to a decreased abundance of SceD. Interestingly, both LOX and CRO exposures lead to significant increases in the abundance of LytM (14 and 16-fold respectively).

Table 3.3.5 Identified autolysins with significant abundance ratios in different conditions. Ratios <1 indicates decreased abundance with β-lactam pre-treatment; Ratios >1 (bold) indicates increased abundance with β-lactam pre-treatment; blank spots indicate no significant differences.

Condition		AtlA	IsaA	LytM	SceD	Sle1	SsaA
D712 ABX / NO ABX	NAF		0.344	0.060*	0.167		
	MEM	0.224	0.138	0.010*	0.083	0.140	0.211
	FOX	0.222	0.133	0.010*	0.040		0.178
D592 ABX / NO ABX	NAF		0.249	0.010*	0.010*		
	MEM	0.178	0.080	0.010*	0.010*	0.164	0.108
	LOX			**14.007**	0.374		0.247
	CRO			**16.892**	0.234		
	CEC			0.093	0.112		
	FOX	0.133	0.119	-	0.010*	0.284	0.122

*indicates ABX abundance below detection limit

3.4 Discussion

Synergy between DAP and β-lactams has been widely reported, although the exact mechanism(s) of the interplay between these two antibiotic classes remains elusive. As shown in **Chapter 2**, *in vitro* passage of DAP-R MRSA in distinct β-lactams can resensitize cells to a DAP-S phenotype, in part related to accumulation of multiple *mprF* SNPs. These results prompted the theory that enhanced DAP bactericidal activity induced by β-lactam cellular "stress" response might underlie β-lactam + DAP synergy. Based on this data, we hypothesized that pre-conditioning with β-lactams would provide more of an opportunity for β-lactam-induced adaptations, improving the synergistic activity with DAP.

In the present study, we assessed bacterial killing with β-lactam + DAP combinations, comparing either sequential or concomitant exposures of a prototype DAP-R strain. Killing of the DAP-R strains was most extensive following pre-conditioning with the entire range of β-lactams, followed by DAP exposure (as compared with simultaneous exposure to both antibiotics). This stark contrast in bacterial killing is especially apparent in the TEM images, featured by differences in the extent of cell lysis comparing the different treatments. Of note, the concentrations of β-lactams associated with the above enhanced DAP-

killing readouts were far below the MIC values for each of the β-lactams (**Supplementary Table 3.1**). It is thus conceivable that the use of sequential dosing strategies (i.e., β-lactams followed by DAP) could lead to improved activity at lower concentrations than would be required for concurrent treatment of DAP-R MRSA with such combinations. Clinically, these results suggest that even in patients with MRSA, initial β-lactam treatment could be beneficial to enhance the activity of subsequent antibiotics such as DAP. We are in the process of studying such strategies in relevant *ex vivo* and *in vivo* models.

Based on our findings of enhanced DAP activity following β-lactam preconditioning, we hypothesized that β-lactams, as a group, likely induce important proteomic changes in MRSA that may well "prime the cell" for subsequent DAP synergy. There were nine proteins with significantly different abundance in the DAP-R strain compared to the DAP-S strain. MprF, one of the primary proteins involved in the development of DAP-R in MRSA, was significantly increased in D712 (223). As gain-of-function SNPs lead to DAP-R, it is unsurprising to find that the abundance of MprF was increased in the DAP-R strain. PrsA is a chaperone is important for the proper maturation of several proteins, including PBP 2A (136). In relation to DAP, PrsA is hypothesized to play a key role in the 'see-saw' effect, wherein an increase in β-lactam susceptibility occurs in conjunction with resistant to DAP (134, 137, 188). VraSR is important for regulation of a number of proteins, including PrsA and members of the cell wall biosynthesis machinery (109). LtaS is involved in the biosynthesis of lipoteichoic acid, a key component of the MRSA cell wall (224). Lipoteichoic acid is the precursor for wall teichoic acids (WTA), which play an important role in DAP-R (225). Specifically, an increase in the amount of D-alanylation of WTA (mediated by DltD and DltB) increases the surface charge of the cell repelling the cationic DAP-Ca^{+1} complex (226). Staphylococcal protein A is a key player in evasion of the innate immunity by binding and inactivating IgG proteins (227). The decreased abundance of this protein suggests that DAP-R isolates may be more susceptible to natural innate antibacterial activity.

As expected with β-lactam challenge, the abundance of PBP 2A was consistently increased. The protein SA 2332 is similar to secretory antigen precursor (SsaA) autolysin, and like the other autolysins the abundance of SA 2332 was decreased with β-lactam treatment (228). The 50S ribosomal protein L32 (RpmF) was increased in NAF, LOX, and CRO samples, but decreased in MEM, CEC, and FOX samples. The discrepancy in abundance likely stems from the extent of β-lactam stress on the cells in each treatment condition. AtpB; the F0F1 ATP synthase subunit A, was also frequently decreased in the β-lactam treated strains. Previous studies have linked inactivation of this latter protein to increased susceptibility of gentamicin and polymyxin; however, this protein has not previously been associated with β-lactam activity and/or hyper-susceptibility (229, 230). The decrease in AtpB abundance is consistent with activation of the cell wall stress regulon, as β-lactams stimulate ATP synthesis (231).

The protein YycF is an important regulator that is activated by lipid II-Gly3, a precursor for peptidoglycan synthesis (232). One of the proteins decreased in the presence of β-lactams, BacA, plays a role in the biosynthesis of lipid II-Gly3. Thus, β-lactam pre-treatment (leading to decreased BacA) reduces YycF-mediated positive regulation of the peptidoglycan lytic transglycosylase SceD and the autolysins SsaA, LytM, and AltA, as supported by the data presented in **Table 3.3.5** (233).

To analyze the gene ontology of the proteins that were altered, we assessed differentially expressed proteins through the STRING database to quantitatively identify specific biological process regulation related to β-lactam pre-exposures. We noted key differences in 15 biological pathways, 13 of which were either metabolic, cellular, or biosynthetic processes. These results are consistent with a previous study analyzing the MRSA proteome following exposure to only a single β-lactam, oxacillin (234). The alterations in proteins associated with energy generation and metabolism are likely a method of cellular adaptation to β-lactam-induced stress.

The final analysis of the proteomic data focused on comparing exposure of each β-lactam to one another. The difference in efficacy of β-lactams in DAP-R MRSA has been well documented with prior studies suggesting this may be due to selective differences in PBP-targeting (154). The data from the current study (in a single strain) shows no distinct correlation between individual β-lactam PBP preferences and key proteomic responses at clinically relevant concentrations. This may imply that the sensitizing effect of β-lactams on subsequent DAP-mediated killing is more of an antibiotic "class impact".

Comparing the response of different β-lactams, there was no consistent pattern in protein abundance metrics. PCA analysis revealed similarities in the protein abundances of NAF, LOX, and CRO samples, while CEC, FOX, and MEM had more distinct proteomic profiles. As this clustering was apparent in both the DAP-S and DAP-R strains, it is likely that at these β-lactams elicit a similar response at these clinically relevant concentrations. Understanding the characteristics that lead to similarities or differences in proteomic outcome has the potential to inform future studies assessing variation between β-lactams.

Aside from these large-scale analyses, we consistently identified two specific protein groups that appeared in several of our runs, namely riboflavin biosynthesis proteins and autolysins. The *rib* operon includes four genes (*ribHABD*) that are responsible for the biosynthesis of riboflavin (235). Riboflavin or vitamin B2, is an important antioxidant that plays a role in response to oxidative stress. A 2013 transposon screen identified that enhanced expression of the *rib* operon led to reduced susceptibility to DAP (236). As our data shows, β-lactam pre-treatment led to decreased abundance of these proteins compared to untreated control. If the *rib* operon plays a role in development of DAP-R, suppression of this protein theoretically offers a novel mechanism of DAP re-sensitization and/or enhanced DAP activity when combined with a β-lactam.

Treatment with β-lactams has been shown to enhance autolytic activity, leading to cell lysis, although this event often follows cell death (237). Moreover, derepression of autolytic gene expression

by knockout of autolysin repressors (e.g., the *mgrA* locus (238)), yields enhanced susceptibility to β-lactams. Further, in the current study, β-lactam pre-conditioning yielded evidence of notable cell lysis, as compared to DAP-only treatment, with few intact cells on TEM and most cell walls being broken down or undergoing degradation. Unexpectedly, our proteomics analyses identified a significant reduction in many of the major staphylococcal autolysins following pre-conditioning with a variety of β-lactams, such as MEM, FOX and NAF. Of interest, cells with inactivated PBP1 transpeptidase domains had decreased transcription of the autolytic system compared to wild type (190). This apparent paradox between functional autolysis and protein-level autolytic content after β-lactam preconditioning is currently being studied in our laboratories. Further complicating the story, LOX and CRO condition in D592 led to significant increase in LytM compared to the untreated control. The lytic activity of LytM is lower than that of other autolysins which has brought into question whether there are alternative functions of this protein (239, 240). The striking increase in only LytM abundance compared to the other autolysins in the DAP-S strain supports the hypothesis of an alternative function for this protein.

The main limitation of this study includes the focus on only one prototypic DAP-S/ DAP-R MRSA strain pair; thus, future studies should determine whether these trends are consistently found among other MRSA isolates. In the current investigation, we highlighted several specific proteins apparently related to β-lactam induced DAP resensitization. Follow up studies, using strategic gene knockouts related to these proteins-of-interest are certainly warranted. This seems especially relevant for the cadre of differentially expressed autolysin proteins that emerged from our analyses. Finally, we recognize that these datasets are predominantly “hypothesis generating” but may well allow a future focus on specific biological pathways to further unravel the mechanisms and optimal treatment of DAP-R MRSA.

Chapter 4. β-Lactam-Induced Cell Envelope Adaptations Underlie Daptomycin-β-Lactam Synergy

Authors and their contributions:

Cassandra Lew: Planned and conducted surface charge, membrane fluidity, and confocal imaging experiments, wrote and edited manuscript

Nagendra N Mishra: Planned and conducted spectrofluoremetry experiments, wrote and edited manuscript

Arnold S Bayer: Supervised research and contributed to design of experiments

Warren E Rose: Supervised research and contributed to design of experiments

Portions of this chapter have been previously published as:

Lew C, Mishra NN, Bayer AS, Rose WE. 2021. β-Lactam-Induced Cell Envelope Adaptations, Not Solely Enhanced Daptomycin Binding, Underlies Daptomycin-β-Lactam Synergy in Methicillin-Resistant *Staphylococcus aureus*. Antimicrob Agents Chemother 65(8):e0035621.

4.1 Introduction

MRSA is a problematic pathogen with high associated mortality rates, principally related to its innate virulence properties, as well as an ability to evolve resistance to multiple antibiotics (208). The development of clinical MRSA resistance to "last-line" antibiotics, including DAP, has been well-detailed, resulting in treatment failures (40, 56, 209). DAP's mechanism of action is multifactorial, involving both cell wall synthesis inhibition (46, 214, 241) and cell membrane targeting (46). DAP associates with Ca^{+2} to form its active amphipathic structure (44). This structure then forms a tripartite complex with PG in the membrane and undecaprenyl-coupled intermediates (45). Aggregated DAP molecules then insert in the membrane leading to ion leakage and eventual cell death (211-213). Accordingly, alterations in genetic pathways responsible for cell envelope homeostasis have been linked to the acquisition of the DAP-R phenotype (46, 56, 78, 96, 242).

Emerging clinical studies favor the utilization of DAP + β-lactam combination therapy for treatment of MRSA infections (126, 147, 206). Combination treatments specifically reduce the rates of bacteremia relapse and persistence (126, 156). The use of combination therapy is supported by extensive in-vitro studies showing *in vitro* synergistic activity in MRSA strains, including those resistant to either antibiotic alone (127, 129, 243).

Moreover, such combinations may also prevent the development of DAP-R in MRSA strains through forestalling emergence of SNPs in the multiple peptide resistance factor gene, *mprF*, which is involved in maintenance of positive surface charge (199). Further, β-lactams can reduce relative positive surface charge and enhance DAP cell membrane binding in some MRSA strains (69, 104); however, these latter events do not appear to be essential for DAP-β-lactam synergy *in vitro*, suggesting other mechanisms are in-play (154). In addition, as MRSA strains become progressively more resistant to DAP *in vitro* and *in vivo*, they tend to become more β-lactam-susceptible (the 'see-saw effect') (188). Despite

the above observations, the precise mechanism(s) responsible for DAP-β-lactam synergy remains incompletely understood (117, 152, 154, 206).

As discussed in **Chapter 2**, passaging in β-lactam can revert DAP-R strains to a DAP-S phenotype, including reversion of cell membrane phenotypes to those common in DAP naïve strains. Further, the data presented in **Chapter 3** shows that even short-term β-lactam conditioning can improve the activity of combination therapy, compared to treating with both antibiotics simultaneously. The proteomic response following β-lactam conditioning included changes in the abundance of cell wall autolysins, however there were few membrane proteins that were altered. The proteomic results instigated the question of whether a single β-lactam exposure could induce cell envelope changes to improve the activity of DAP, whether different β-lactams would lead to similar or distinct phenotypic alterations, and whether these changes were consistent among diverse MRSA isolates.

With these hypotheses in mind, several key cell envelope phenotypes were delineated in a well-defined set of isogenic DAP-S / DAP-R MRSA strain-pairs (n = 9) following exposure to sub-inhibitory concentrations of selected β-lactams with diverse PBP-targeting profiles. We focused on those envelope metrics previously associated with DAP-R in MRSA (70, 97), including cell membrane order and surface charge, quantified with and without β-lactam exposure. Moreover, we assessed the role of anionic membrane phospholipid content (predominantly CL) and its distribution under the same conditions. Finally, the degree of overall DAP binding was quantified following distinct β-lactam exposures.

4.2 Materials and Methods

Bacterial strains and growth conditions. This study focused on analysis of nine previously characterized clinical bloodstream DAP-S/DAP-R isogenic MRSA strain-pairs (40, 104). These strain-pairs

were prioritized to include DAP-R strains with or without particular *mprF* mutations and have been previously characterized for certain phenotypic and genotypic characteristics (104).

The following β-lactams with wide-ranging PBP selectivity were employed: LOX [PBP-1], MEM [PBP-1], NAF [PBP 1-4; non-selective], CRO [PBP-2], CEC [PBP-3], and FOX [PBP-4] (99). Exposure concentrations of these β-lactams were chosen based on extensive pilot experiments to determine drug levels for each single antibiotic that exerted a sub-lethal (bacteriostatic) impact in vitro, defined as < 2-log10 CFU/mL reduction in growth over a 24-hour period (**Supplementary Table 4.1**). Bacteriostatic concentrations were selected to compile an overarching analysis of all β-lactam-induced adaptations (rather than using fixed β-lactam concentrations for all strains based on human-achievable serum levels).

Surface charge. The relative net positive cell surface charge was quantified using the spectrophotometric-based CytC binding assay (a highly cationic molecule) as previously described (67). Study strain-pairs were grown overnight in the presence or absence of sublethal concentrations of the individual β-lactams listed above. Bacterial suspensions were then centrifuged at 5,000 rpm for 5 minutes, supernatant then removed (containing the β-lactam-of-interest) and cells resuspended in fresh medium. Cells were then washed twice with MOPS (morpholinepropanesulfonic acid) buffer (20 mM, pH 7.0), adjusted to an optical density at 600 nm (OD600) of 1.0, and collected from 1-ml aliquots via centrifugation. Cell pellets were resuspended in 200 µl MOPS buffer and combined with 50 µl of CytC (2.5 mg/ml solution). Samples were incubated for 10 min at room temperature and separated by centrifugation. OD530 was determined in the supernatant, and the magnitude of CytC binding was then determined using a standard curve. The more CytC remaining in the supernatant is a measure of a relative increase in the relative bacterial positive surface charge.

Quantification of anionic phospholipids. DAP-S/DAP-R MRSA pairs were grown overnight to stationary phase in the presence or absence of bacteriostatic concentrations of the aforementioned β-

lactams. CL is the principal anionic phospholipid species in the MRSA cell membrane; we utilized an anionic phospholipid-specific dye (N-acrylamide orange [NAO])-based spectrofluorometric assay as a surrogate for membrane CL content. As negative controls for this NAO binding assay, we employed cardiolipin synthase knockout mutants N315 Δ*cls1* and N315 Δ*cls2* (244) (**Supplementary Figure 4.1**). For this assay, 1.0 x 107 CFU/mL of each MRSA strain were exposed to 20 µM NAO, and then incubated at 4°C for 20 minutes. NAO fluorescence intensity was measured using spectrofluorometry (excitation = 525 nm; emission = 640 nm).

Anionic phospholipid localization. Anionic phospholipid localization was visualized using stimulated emission depletion (STED) fluorescence microscopy. Cells were grown to exponential phase while shaking at 37°C in LB medium overnight in the presence or absence of bacteriostatic concentrations of each distinct β-lactam. NAO was then added at 20 µM for 1 h at room temperature. Cells were washed and resuspend in PBS. For nuclei staining, 1 µL of NucSpot Live 650 Nuclear Stain was added to 1 mL suspension and incubated for 10 minutes at room temperature. The cells were concentrated 20-fold at the last step, and 3 µL were placed on a glass slide. Slides were set with prolonged diamond anti-fade mountant and a #1.5 glass coverslip. Images were collected using a Leica SP8 3X STED Super-Resolution Confocal Microscope using standard filter sets for either: GFP (495 nm excitation and 510-579 nm emission, with 592 nm depletion) to visualize NAO; or Cy 5 (633 nm excitation and 667-742 nm emission with 775 nm depletion) to visualize NucSpot as per manufacturer's instructions. Images were processed with Huygens software deconvolution wizard. In addition to CL visualization to identify effect on its membrane localization, overall average CL quantification within individual cells was determined by measurement of integrated fluorescence density in ImageJ for 30 cells total in the NAO channel, and corrected cell total NAO fluorescence was then calculated.

Cell membrane order (fluidity/rigidity). Strains were grown at 37°C for 72 h in TSB, replacing the media and β-lactam antibiotic every 24 h, with or without exposure to the average unbound concentration

of each selected β-lactam. Membrane fluidity/rigidity was then measured using the fluorescent probe DPH. Methods for DPH incorporation into the membrane, measurement of fluorescence polarization, and calculation of the polarization index have been previously described in detail (153). A BioTek Synergy H1 Hybrid Multi-Mode Reader with excitation of 360 nm and emission of 426 nm was used.

BODIPY-DAP fluorescence microscopy. To quantify DAP binding (in the presence of absence of each β-lactam), cells were harvested at exponential phase from LB cultures supplemented with 50 μg/mL Ca^{+2}. Cells were incubated with 16 ug/mL BODIPY-labeled DAP as previously described (152). The cells were concentrated 20-fold, and 3 μL were placed on a glass slide. Slides were set with prolonged diamond antifade mountant and a #1.5 glass coverslip. Images were collected using a Leica SP8 3X STED Super-Resolution Confocal Microscope using a 489 nm laser line and 510-579 nm emission with 660 nm depletion. ImageJ was utilized to measure integrated fluorescence density of 30 cells and corrected cell total fluorescence was calculated.

Statistical Analysis. The two-tailed Student T-test was used for statistical analysis of β-lactams compared to untreated strains. One-way ANOVA was used for β-lactam comparisons.

4.3 Results

Surface charge. In line with previous literature, DAP-R strains exhibited significantly less CytC binding (i.e., elevated cell surface positive charge) (32) as compared to DAP-S strains overall ($p < 0.05$). The surface charge of cells following β-lactam exposures was significantly decreased compared to cells without antibiotic exposure (with the exception of CEC) evidenced by an increase in binding to CytC (**Figure 4.3.1A**). Consistent in both the DAP-R and DAP-S strains, LOX conditioning led to a significant decrease in surface charge compared to the other tested β-lactams ($p<0.05$). Cells following NAF, MEM, or FOX

exposures bound roughly 50% and 60% in DAP-S and DAP-R strains respectively. Meanwhile, CRO and CEC exposures had modest but significant increased in CytC binding compared to untreated samples.

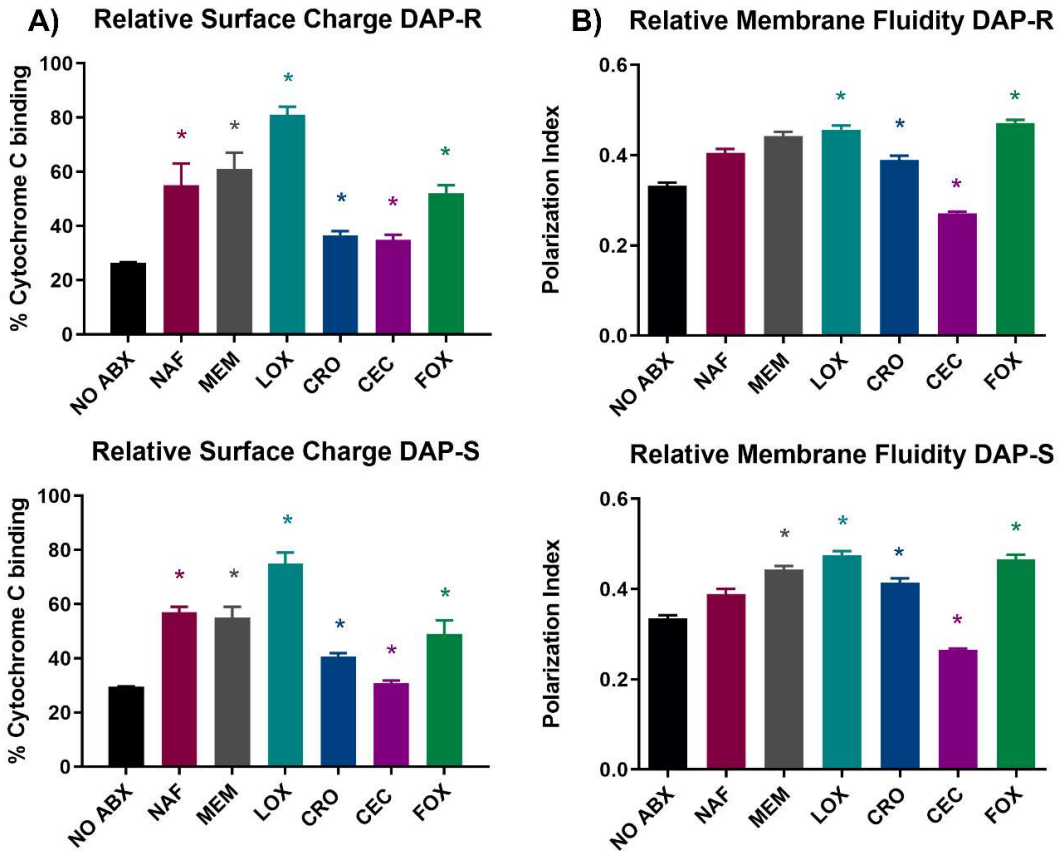

Figure 4.3.1 Membrane characteristics previously associated with DAP-R. (A) Relative surface charge of DAP-S and DAP-R strains with or without β-lactam conditioning via CytC binding assay. Higher percentage CytC binding indicates more negative surface charge. (B) Membrane fluidity of DAP-S and DAP-R strains with or without β-lactam conditioning via membrane polarizing spectrofluorometric assay. Polarization index is inversely correlated to membrane fluidity, i.e. higher polarization index equates with decreased membrane fluidity. ***p<0.05 vs NO ABX**

Cell membrane order. Collectively, there was no significant difference in membrane order (fluidity/rigidity) between the DAP-R and DAP-S strains. In the DAP-R isolates, exposure to four of the six β-lactams (MEM, LOX, CRO, and FOX) lead to significant decreases in membrane fluidity. Likewise, in the DAP-S isolates three of those same β-lactams (LOX, CRO, FOX) led to significant decreases (**Figure 4.3.1B**).

Interestingly, cells exposed to CEC had significantly increased membrane fluidity compared to untreated cells ($p<0.05$).

NAO content. Spectrofluorometry was utilized to quantify relative overall NAO content (as a principal measure of CL content) following β-lactam exposure. These data show a general, albeit modest, trend of increased CL content in both DAP-S and DAP-R strains exposed to this panel of β-lactams **Figure 4.3.2A**. Increases in fluorescence intensity were most impactful in MEM and LOX conditions.

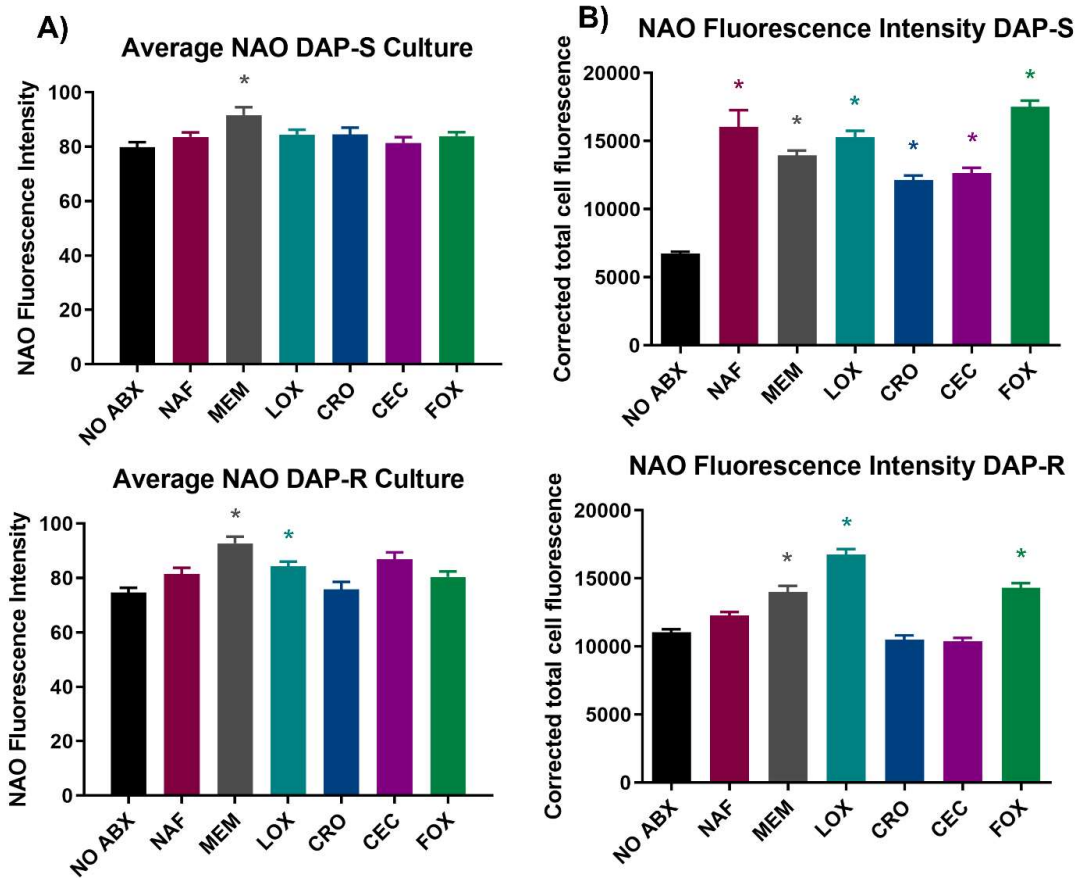

Figure 4.3.2 Average anionic PL content quantified by (A) NAO staining and (B) quantification of confocal images of DAP-S and DAP-R strains, with or without β-lactam treatment. ***p<0.05 vs NO ABX**

To visualize and quantify the differences in CL content on a cellular level, we performed confocal microscopy. Confocal images were acquired following growth to exponential phase, with or without

exposure to selected β-lactams. Fluorescence quantification of the confocal images further validated the apparent increase in anionic phospholipid content following β-lactam exposure **Figure 4.3.2B**. At baseline, DAP-R strains had more CL/cell than DAP-S strains. CL content/cell was significantly increased following all β-lactam exposures in the DAP-S strains, to a relatively consistent level ($p<0.05$). In DAP-R strains, only MEM, LOX, or FOX conditioning increased CL content compared to untreated samples.

Anionic phospholipid distribution. The confocal images allowed investigation of differences in the localization of CL around the cell. Images in **Figure 4.3.3** include one representative DAP-S/DAP-R strain-pair as similar trends were observed universal. Pre-antibiotic exposure, cells show concentrated CL clusters which tended to be at either the poles or in the cell septal division plane. In contrast, following β-lactam exposures, cells showed more global, non-septal distribution of CL around the membrane circumference. This perturbed CL distribution was more apparent and distinct in DAP-R compared to DAP-S strains.

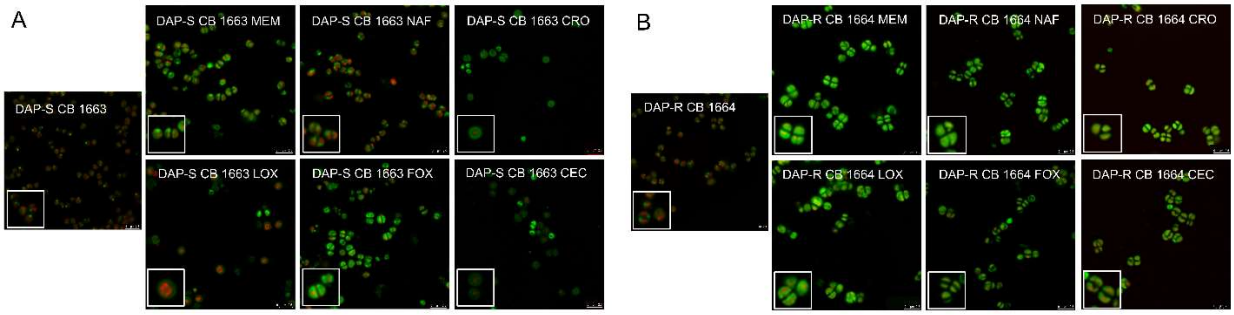

Figure 4.3.3 Confocal images of one representative DAP-S/DAP-R strain pair (CB1663/CB1664) with or without β-lactam conditioning. NAO is represented in green, and NucSpot isrepresented in red.

DAP binding. Binding of BODIPY-DAP was quantified via fluorescence intensity from confocal images, with or without β-lactam exposure. At baseline, DAP-R strains on average bound more DAP than

DAP-S counterparts. This was based primarily on two strains, CB 185 and CB 5082, which highly bound DAP compared to other study strains (*data not shown*). Among DAP-S strains, exposure to all β-lactams studied yielded significantly increased DAP binding (vs untreated strains; panel A - **Figure 4.3.4**) ($p<0.05$). In contrast, among DAP-R strains, the impact of β-lactam exposures tended to be more variable. NAF and CRO resulted in significantly decreased DAP binding, while CEC exposure caused significantly increased DAP binding ($p<0.05$).

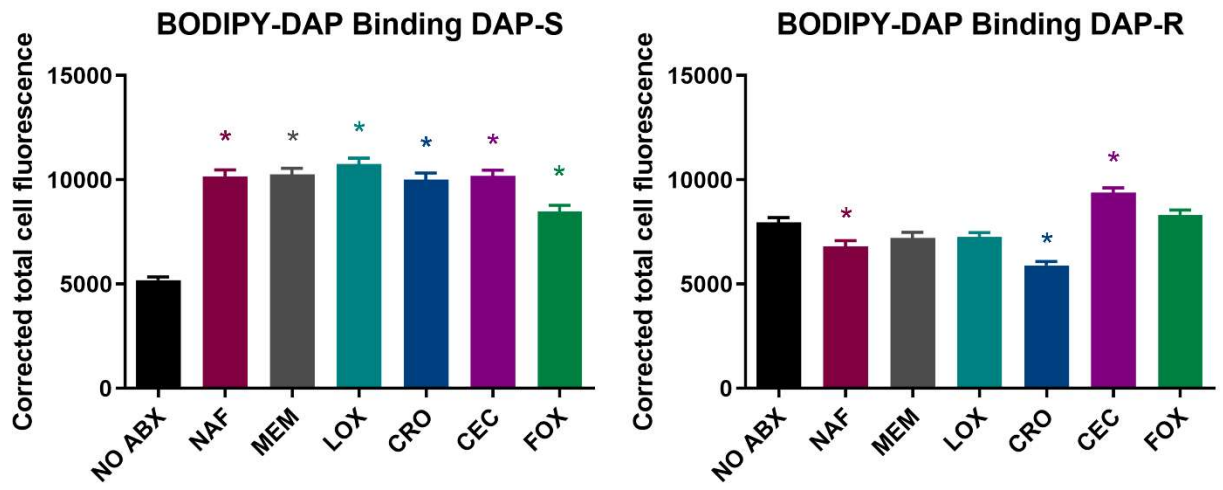

Figure 4.3.4 Quantification of fluorescence intensity of BODIPY-DAP confocal images of (A) DAP-S and (B) DAP-R strains with or without β-lactam treatment. Average binding (± standard deviation) for DAP-S/DAP-R strains. ***p<0.05 vs NO ABX**

Overview of cell envelope parameter impacts by β-lactam exposures. Since clinically, DAP-β-lactam combinations are geared to treat DAP-R MRSA strains, **Table 4.3.1** summarizes the overall cell envelope alterations identified among our 9 DAP-R strains following β-lactam exposures. The table indicates whether these phenotypes are significantly increased, decreased, or unchanged compared to untreated samples. In the last row of the table, the cell envelope changes predicted to improve DAP activity are listed based on the data presented.

Table 4.3.1 Overview of changes in cell envelope characteristics following β-lactam treatment of DAP-R strains compared to untreated strains and adaptations favorable for DAP activity.

Phenotype	NAF	MEM	LOX	CRO	CEC	FOX
Surface charge	-	-	-	-	+	-
Membrane fluidity	NC	-	-	-	+	-
CL content cultures	NC	+	+	NC	NC	NC
CL content cells	NC	+	+	NC	NC	+
DAP binding	-	NC	NC	-	+	NC
Potential mechanism of DAP potentiation	Decreased surface charge	Decreased surface charge	Decreased surface charge	Decreased surface charge	Increased DAP binding	Decreased surface charge
		Decreased membrane fluidity	Decreased membrane fluidity	Decreased membrane fluidity		Decreased membrane fluidity
		Increased CL content	Increased CL content			

4.4 Discussion

The exact mechanism underlying development of DAP-R in MRSA appear to be heterogeneous and multifactorial. Relevant to the current investigation, alterations in cell envelope phenotypes virtually always accompany development of DAP-R (46, 59, 68, 96, 196, 242). Clinically, the addition of different β-lactams (e.g., nafcillin, ceftaroline) to DAP treatment has proven effective in recalcitrant MRSA infections caused by DAP-R strains (78, 126, 243). Despite the promise of DAP + β-lactam treatments, mechanism(s) behind the salutary outcomes using these combinations is not well understood. As the results from **Chapter 2** and **Chapter 3** exemplify, β-lactam exposure improves the activity of DAP on MRSA isolates. Based on the integral role of the cell envelope in the activity of DAP, we hypothesized that β-lactam exposure may induce cell membrane and/or cell wall alterations that could enhance DAP's activity.

The first phenotype we investigated was relative cell surface charge by CytC binding assay. Uniformly, conditioning with a β-lactam significantly decreased the relative positive cell surface charge compared to untreated strains. In both the DAP-S and DAP-R isolates, LOX exposure lead to the greatest alteration. Several studies have linked the DAP-R phenotype with increased cell surface charge, mediated

by SNPs in *mprF* and/or dysregulation of the *dlt* operon (67, 96, 97, 180). Initially, this increase in relative positive surface charge was thought to repel the bio-active DAP-Ca^{+2} complex (245). However, consequent results have challenged this hypothesis as the major mechanism of DAP-R as change in surface charge is not universal among DAP-R isolates and the degree of charge does not correlate with the extent of resistance (97, 246). Alternatively, it has been suggested that the increased surface charge indicates a decrease in the available PG binding sites for DAP on the cell (56). Despite the uncertainty behind the exact role surface charge plays on DAP-R, there are clear correlations between resistance and relative cell surface charge. The decrease in surface charge following β-lactam exposure evidenced by our data would likely enhance the activity of DAP on the cell.

The role of membrane order (fluidity/rigidity) on DAP activity remains unexplained. Changes in membrane order often accompany development of DAP-R dependent on whether resistance occurs *in vivo* or *in vitro*. Isolates that develop DAP-R in patients upon treatment failure tend to have more fluid membranes compared to their respective DAP-S parents, while lab strains that are passaged to develop DAP-R tend to have more rigid membrane than their parent strains (59, 247). This paradox hints that there may be an optimal membrane order for DAP to exert its maximal activity on the cell, and perturbations in either direction decrease that activity. Further emphasizing the importance of membrane order on DAP activity, DAP has been shown to preferentially bind and disrupt fluid lipid microdomains (75, 78).

The strains utilized in the current study are all clinically derived bloodstream isolates (40, 104), and accordingly the DAP-R strains were slightly more fluid than the DAP-S strains, albeit not significantly. Following β-lactam exposures, both strains exhibited a decrease in fluidity comparted to non-treated strains. It seems reasonable to assume that this β-lactam induced effect would revert the membrane order of DAP-R clinical isolates to a state more conducive for DAP activity. Whether this alteration of membrane order impacts DAP binding and/or membrane insertion remains unexplored.

In enterococci, DAP-R is mediated by delocalization of CL from the divisome leading redistribution more globally throughout the cell membrane (248). Although SNPs in *cls2* have been linked with development of DAP-R in *S. aureus*, the phenotype resulting from these SNPs is not entirely defined (75). In our study, an overall increase in CL was observed with select β-lactam exposures. As CL carriers a -2 charge, it is possible that such increases could contribute to a decreased surface charge, however our analysis of membrane surface charge found universal decreases, while CL was only increased in certain conditions. Alternatively, an increase in CL would result in compensatory decrease in PG content, thus reducing the number of anchoring sites for DAP (71, 181, 249). From the point of bacterial cultures, MEM and LOX conditioning in the DAP-R strains (or MEM only in the DAP-S strain) lead to increased CL content compared to the untreated strains. Analysis on the cellular level revealed more universal increases in CL.

Yang et al documented specific point mutations in *cls2*, linked to the development of DAP-R, led to increased CL content accompanied by a compensatory decrease in PG levels; however this study focused on laboratory derived strains with only *cls2* point mutations (181). As the authors noted, other DAP-R associated mutations occur in the transmembrane region of *cls2* which could lead to delocalization of CL in the membrane (181). Considering the limitations of this study, and the absence of isolates with SNPs in other cell membrane biosynthesis genes (e.g., in *mprF* or *pgsA*), it is arduous to draw any overarching conclusions.

The confocal images collected following NAO staining implies β-lactam conditioning induces delocalization of CL from the divisome to a more generalized distribution. The outcome of this delocalization on DAP activity is complex. On one hand, CL-rich membrane regions are more susceptible to bending and stretching due to lateral interaction with other phospholipids (181). Therefore, redistribution of CL around the membrane would increase the prevalence of such regions. The increase in flexibility of the membrane could thus reduce the amount of energy required for DAP to insert in the

membrane. On the other hand, it is possible that delocalization of CL away from the divisome, a principal site of DAP activity, could impede DAP activity similar to what has been reported in enterococci (248).

Initial studies on DAP + β-lactam combinations in MRSA hypothesized that increased binding of DAP to the membrane explained the observed synergy (152, 250). Contradictory to this hypothesis, Berti et al demonstrated that the extent of DAP binding on the membrane did not uniformly correlate with DAP + β-lactam synergy (152, 154). In support of this latter notion, results from the current study do not show a consistent relationship between DAP binding and β-lactam exposure. In DAP-S strains, DAP binding was consistently enhanced with β-lactam exposures, but in DAP-R strains this trend was only seen in CEC conditioned samples. Not only was DAP binding not universally increased, in NAF and CRO samples, DAP binding decreased. The distinction between response in DAP-R and DAP-S strains underscores the difference in response to β-lactam stress in these two populations (104, 188).

Breaking down the data by strain, CB 185 and CB 5082 had 2-fold decreases in NAF and CRO conditioned strains compared to their respective untreated levels. In the other DAP-R strains, there was no significant difference in DAP binding between NAF and CRO treated and untreated strains (*data not shown*). Previous studies in other DAP-R MRSA strains have shown that NAF + DAP combinations increase DAP binding compared to treating with DAP only (152). The more comprehensive strain set analyzed in this study sheds light on important strain-to-strain variations, and, on average, lower DAP binding following β-lactam exposures. While the source of discontinuity between our data and others remains unclear, it is possible that the time of dosing is important. Here we focused on preconditioning cells with β-lactam, then subsequently adding the BODIPY-DAP tag, while the aforementioned study dosed both antibiotics simultaneously (152).

In conclusion, our evidence supports the model of discrete mechanisms of cellular response to specific β-lactams. These reported differences provide possible explanations to the inconsistent synergy

of DAP + β-lactam combinations in DAP-R MRSA. NAF conditioning led to a decrease in net positive surface charge, pointing to reversal of DAP-R induced increased in net positive surface charge as a mechanism of synergy. Comparatively, CRO and FOX treatments resulted in decreased surface charge and membrane fluidity compared to untreated strains, implying that such a cell membrane profile may favor DAP activity. MEM and LOX exposures similarly induced these membrane changes, in addition to an increased in CL content. As all of these phenotypes were altered with treatment, it is likely that these changes play a combinatorial role in synergy with DAP. Finally, CEC conditioning prompted a significant increase in DAP binding, hinting this as a primary mechanism of synergy. Collectively, these findings underscore the diversity in cellular response to exposure with distinct β-lactams. Furthermore, these data imply the mechanisms underlying DAP + β-lactam synergy are both strain and β-lactam specific.

Chapter 5. Variation in Daptomycin Synergy with β-Lactams is Both Strain and β-Lactam Dependent

Authors and their contributions:

Cassandra Lew: Planned and conducted experiments, wrote and edited manuscript

Evan R Rees: Conducted sequencing analysis

Evan Chrisler: Conducted time-kill experiments

Arnold S Bayer: Contributed intellectual input

Warren E Rose: Supervised research and contributed to design of experiments

5.1 Introduction

DAP-R MRSA infections have been reported in patients with high bacterial burden and often result in poor clinical outcomes and high mortality rates (116, 251). In such highly resistant infections, it is common to utilize the synergistic combination of DAP with a β-lactam antibiotic (128, 252). Despite numerous clinical studies reporting the use of DAP combinations with β-lactams for the treatment of MRSA, the effectiveness of this combination against specific isolates is variable (126, 145, 156).

A factor contributing to the prevalence of MRSA is its ability to develop resistance to most antibiotics. Most community acquired (CA)-MRSA infections can be treated with aminoglycosides, erythromycin, or clindamycin; however, hospital acquired (HA)-MRSA tends to be more resistant and is typically treated with VAN (175, 253). Upon VAN treatment failure or identification of a VISA isolate, clinicians will switch to DAP for treatment (39, 175). In isolates treated with multiple antibiotics, it is 71impossible to determine which cell phenotypes are caused by each individual antibiotic.

The synergy of DAP combinations with β-lactams has been explored using several β-lactams (127, 200, 254, 255), however there is limited information delineating responses to different β-lactams. In 2013, Berti et al. reported differences in the ability of certain β-lactams to enhance DAP in specific DAP-R isolates (161). Based on the discrepancy in activity, the authors hypothesized that PBP-binding selectivity played a role, further supported by their subsequent studies (154). However, as the study focused primarily on a single strain and the concentration at which each β-lactam binds selectively to certain PBPs is unknown, further investigation is required to examine the validity and prevalence of this phenomenon.

To better understand the inconsistency in synergy of DAP combinations with β-lactam, we utilized a diverse set of nine isogenic DAP-S/ DAP-R clinical bloodstream isolates. These isolates were collected from patients treated exclusively with DAP before developing a DAP-R phenotype (40). Time-kill assays were employed to assess the activity of six different DAP + β-lactam combinations in each strain. The

strain pairs were then whole genome sequenced and SNPs within each respective strain pair were annotated. Sequencing results were compared with genotypic data to identify characteristics of isolates where the activity of the combination was reduced.

5.2 Materials and Methods

Bacterial strains and antibiotics. This study utilized nine isogenic, clinically derived DAP-S/ DAP-R strain pairs that have been previously characterized (104). These strains were collected from patients treated exclusively with DAP and therefore encompass variation in development of DAP-R independent of prior antibiotic treatments (40). This set was prioritized to include DAP-R strains from a variety of genetic backgrounds and with varying SNPs in *mprF*. The lipopeptide DAP and six β-lactams with wide-ranging PBP binding selectivity were utilized in this study: LOX [PBP-1], MEM [PBP-1], NAF [PBP 1-4; non-selective], CRO [PBP-2], CEC [PBP-3], and FOX [PBP-4]. The free average unbound concentration (*f*Cavg) of 3.9 mg/L of DAP was utilized (220), while the β-lactam antibiotics were dosed at *f*Cavg concentrations when below the β-lactam MIC or at ½ the MIC (**Supplementary Table 5.1**).

Time-kill experiments. A standard initial inoculum of ~ 1 x 10^6 colony forming units (CFU)/mL was used to approximate bacterial densities in infective endocarditis (51). DAP-R strains were cultured in 1 mL CAMHB media and time points were taken at 0-, 2-, 4-, 8-, 12-, and 24-hours post antibiotic exposure. Samples were plated on CAMHA plates and read after 24 hours of growth at 37˚C. At least three experimental runs were performed for each condition.

Whole genome sequencing (WGS). Genomic DNA was extracted with the Promega Wizard Genomic DNA kit per manufacturer's guidelines. Genomic DNA libraries were prepared then sequenced on a NovaSeq (Illumina) with 2x150 bp chemistry. Short read sequence data for isolates were mapped to reference *S. aureus* Mu50 (RefSeq accession GCF_000009665.1); and either USA300 (GCF_000568455.1),

N315 (GCF_000009645.1), or MRSA252 (GCF_000011505.1) for CC8, CC5, or CC30 isolates respectively using Snippy v4.6.x. Predicted protein consequences of variants were identified using snpEff v5.0, with custom databases constructed from the above listed RefSeq genomes. SnpEff was run on snippy outputs to retrieve unique genes between isogenic parent and daughter pairs.

5.3 Results

Time-kill activity. Time-kill experiments for all six DAP combinations with β-lactams were performed on the nine DAP-R study strains (**Figure 5.3.1**). Change in bacterial growth 24 hours post-treatment, presented in **Figure 5.3.2**, shows that all combinations were bactericidal after 24 hours in 5 of the DAP-R strains (CB 185, 5080, 1634, 5059, and 5016). In the DAP-R strains CB 5082 and CB 1664, only the CRO+DAP and NAF+DAP combinations were ineffective respectively. The DAP-R strain CB 5089 was killed by NAF+DAP and MEM+DAP combinations but had some growth with the other β-lactam combinations. Finally, all DAP + β-lactam combinations were ineffective in killing the strain CB 5063.

SNP annotation. Following WGS, DAP-R strains were aligned to their respective DAP-S parent strains to annotate the SNPs acquired during development of DAP resistance (**Supplementary Table 5.2**). Mutations previously associated with decreased susceptibility to DAP, including those in *mprF*, *walk*, *rpoB*, and *cls2*, were common in DAP-R isolates (**Table 5.3.1**). These SNPs agree with previously annotated mutations in *mprF* (104).

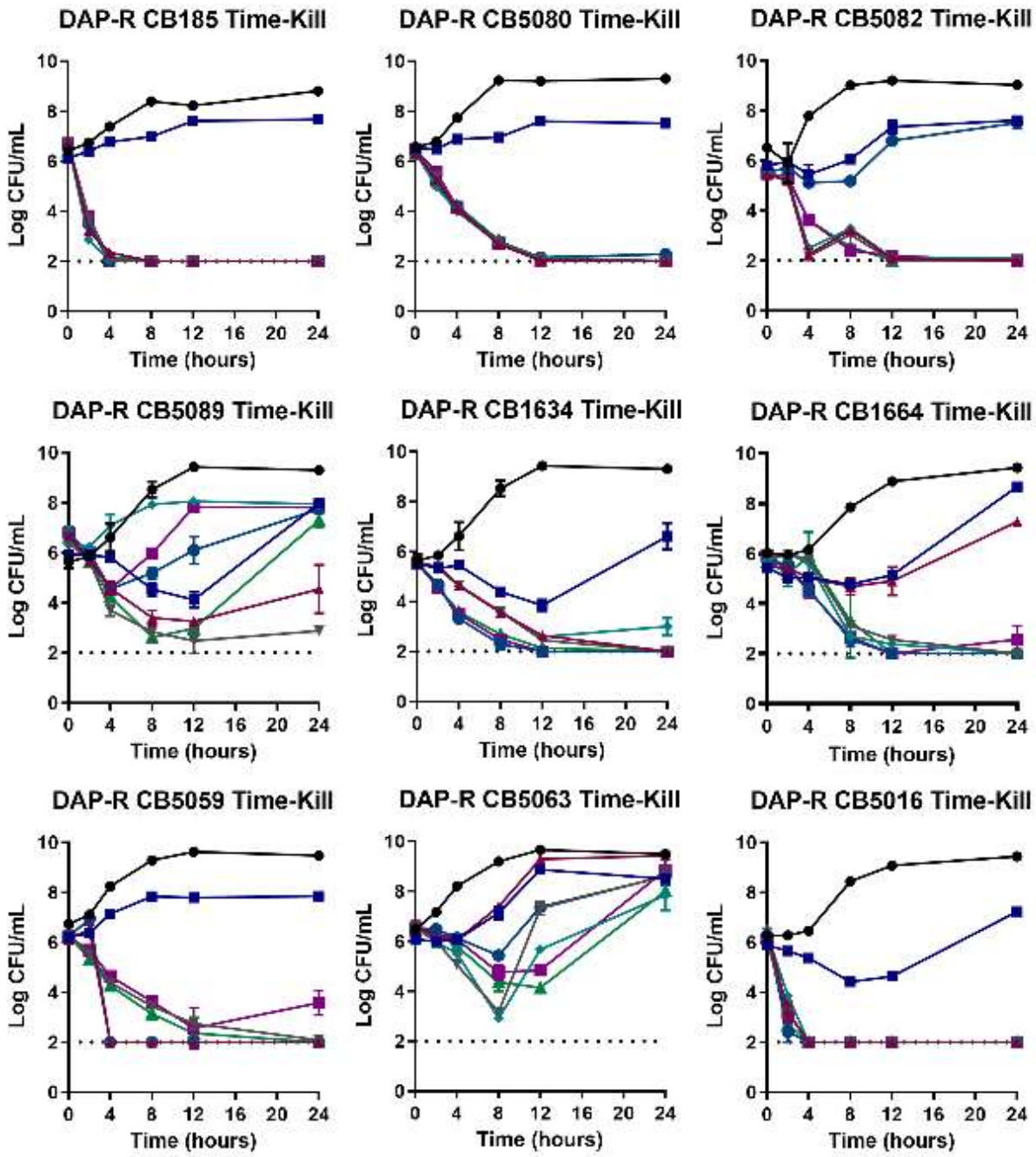

Figure 5.3.1 Time-kill activity of DAP in combination with six different β-lactams in DAP-R clinical isolates.

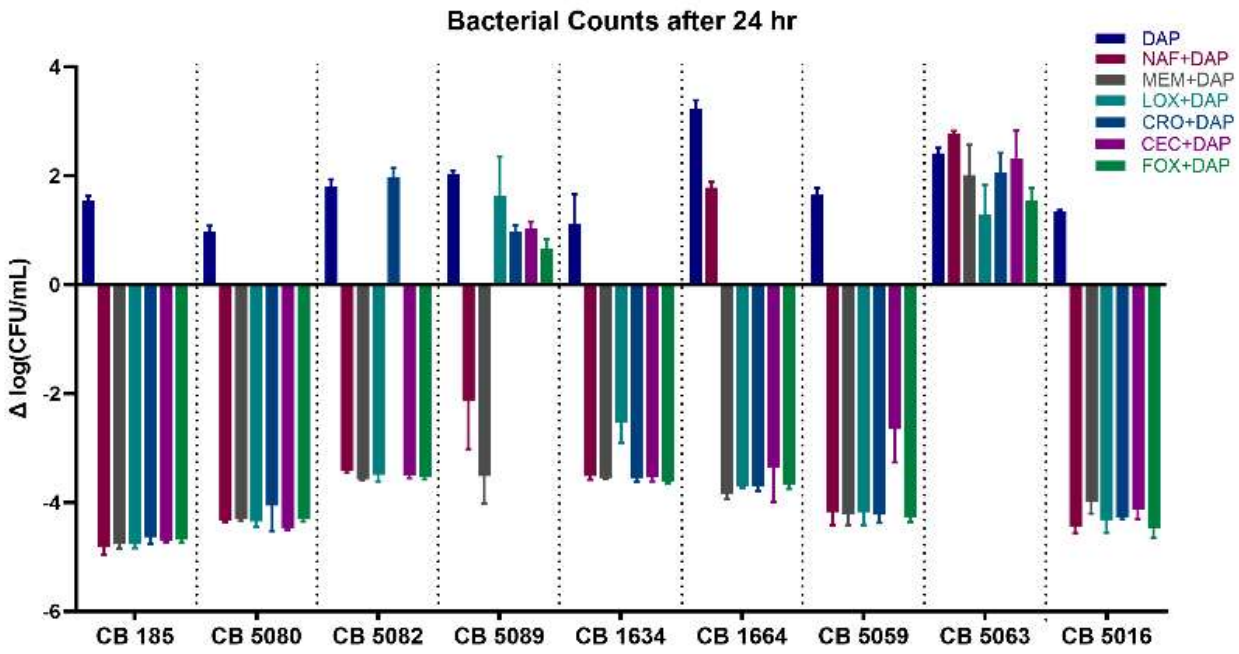

Figure 5.3.2 Quantification of bacterial killing of DAP in combination with six different β-lactams in DAP-R clinical isolates after 24 hours.

In addition, SNPs in innate immune evasion genes (*sbi*, *sdrD*, and *sdrC*) were identified in multiple strains (**Table 5.3.2**). Second immunoglobulin-binding protein (Sbi*)* is a multifunctional immune evasion factor that binds the Fc region of IgG to prevent host recognition. The serine-aspartate repeat-containing proteins (SdrD and SdrC) are important for adherence in MRSA biofilm formation. SdrD promotes *S. aureus* adherence to host cells and inhibits neutrophil-mediated bacterial death. SdrC is an important molecular determinant for cell-to-cell adhesion in biofilm formation.

In addition to these SNPs, there were several distinct mutations identified in each individual strain (**Table 5.3.3**). Of note, the single unique mutation in the strain CB 1664 was a frameshift in serine-threonine phosphatase *stp1*. Stp1 is the cognate phosphatase to Stk1, a serine-threonine kinase involved in regulation of cellular processes.

Table 5.3.1 SNPs previously associated with evolution of DAP-R in MRSA.

DAP-R strains	SNPs			
	mprF	***walK***	***rpoB***	***cls2***
CB185	L826F			L52F
CB5080	L826F		S464P	
CB5082	L341S		G489E	
CB5089	S295L			
CB1634	L826F	K158fs[a]		
CB1664	L826F	R86H	R484H	
CB5059	I420N	T474I	K468Q S486L	Q329R
CB5063	L341S			
CB5016	Disruptive in frame deletion L42del	N584S		

[a]frameshift

Table 5.3.2 SNPs in host innate immune evasion genes.

DAP-R strains	SNPs		
	sbi	***sdrD***	***sdrC***
CB185			
CB5080	Disruptive in frame insertion E285_S286ins*		
CB5082		D1171Q	
CB5089		D370N	
CB1634			
CB1664	Disruptive in frame insertion E285_S286ins*		Disruptive in frame insertion D485_S486del
CB5059		D370N	Conserved in frame deletion S786S_D787del
CB5063	T334K	V521fs[a] S227R	D865Q
CB5016	Disruptive in frame insertion E285_S286ins*		

*insertion sequence GAATCACCAAAAGTTGAAGTCCCTCAAATCC

[a]frameshift

Table 5.3.3. Genes with high or medium impact SNPs present unique to one strain. * Indicates truncated gene. Bold indicates high impact SNP (variant assumed to have a disruptive impact on the protein).

DAP-R strains	Strain specific SNPs
CB185	*airS*
CB5080	*esaG, fmtB, secY, set6, set8, mapW*, SA2370*
CB5082	*hlb, sak, scn, SAS058*
CB5089	*aroB, fur*
CB1634	*dppb**
CB1664	***stp1***
CB5059	*bioF, purA, ssl11, tetM, **treP**, radC*, vraT*
CB5063	*copA, crtN, cysJ, **dat**, fnb, **fruA**, **gntK**, htsA, mnhA2, mqo, mrp, nifZ, norA, pta, **queA**, rex, rsp, scc, ssl12, tnp, **vraG**, **ychF**, SA0139, SA0839, SA0840, SA1035, SA1158, SA1559, SA2081, SA2231, SA2369*
CB5016	*ami, rplC, tst*

5.4 Discussion

While the synergistic activity of DAP combinations with β-lactams has been thoroughly detailed, there remains discrepancy in the effectiveness of this treatment in specific isolates. Within our strain set, five of the nine strains exhibited consistent bacterial killing with all DAP combinations with β-lactams. The other four stains did not respond to one or more of the β-lactam combinations, illustrating the diversity in activity of this regimen, particularly in DAP-R MRSA strains.

The strain set utilized in this study was previously characterized by Mishra et al. including clonal complex (CC) typing. Most of the strains were either CC5 or CC8, two of the most common clinical MRSA lineages (256, 257). However, the strain set CB5062/ CB5063 are CC30 isolates. Interestingly, this strain pair was also unresponsive to any DAP + β-lactam combinations. Strains from the CC30 lineage are distinguished by their ability to form persister cells, initiate hematogenous complications, and increase the risk of mortality (258-260). The ability of CC30 strains to evade host innate immunity is partially based on increased expression of staphylococcal protein A (Spa) and enhanced resistance to innate host defense peptides such as hNP-1 (261). Our finding that this strain is unresponsive to combination therapy

highlights the threat of CC30 isolates. However, as our study focuses on a small and narrowly defined strain set, further investigation into the prevalence of this phenotype in specific lineages, primarily isolates from the CC30 lineage, is required.

Four of the six DAP combinations with β-lactams did not result in bacterial killing in CB5089. While only one combination was inactive and in CB5082 and CB1664, DAP+CRO and DAP+NAF respectively. These three DAP-R strains also all grew with the small colony variant (SCV) phenotype. Staphylococcal isolates that present as SCVs arise from prolonged environmental stress and typically have decreased virulence along with an enhanced ability to persist within host cells (262-264). SCVs have reduced susceptibility to aminoglycosides due to decreased antibiotic uptake, a result of reduced membrane electron gradient (265, 266). Further, the slow growth of SCVs reduces the effectiveness of cell wall active antibiotics, including β-lactams (264). A 2009 study by Begic and colleagues showed that DAP is less effective in SCVs at early time points, but after 24 hours there is no difference in activity (compared to non-SCV strains) (267). To our knowledge, there have been no studies into the activity of DAP combinations with β-lactams specifically in SCV isolates. Based on the data collected here and the documented difficulty in the treatment of SCV isolates, it is understandable that they would be less susceptible to antibiotic therapies. However, as with the CC30 hypothesis, a more comprehensive study comparing the activity in isolates with or without the SCV phenotype is necessary.

The WGS results of this strain collection provided novel insights that are worth further investigation. First, identification of SNPs in innate immune evasion genes in multiple independent isolates suggests a link between the development of DAP-R and these proteins. Historically, DAP-R MRSA strains are reported to be less susceptible to host-derived immune defenses, likely in part due to cross-resistance of DAP with antimicrobial HDPs (LL-37) (79, 268, 269). Evasion of this response is one of the characteristics of DAP-R MRSA infections that make them particularly difficult to eradicate.

Sbi is a multifunctional immune evasion protein that contains two IgG-binding domains, similar to those of staphylococcal protein A (Spa), and two domains that bind to complement factor C3 (270). The C-terminal domain (CTD), where all our SNPs were located, is responsible for anchoring the protein to the cell envelope (271). Sbi with a truncated CTD loses its IgG-binding functionality but the C3 binding was retained (271); thus, it is likely the Sbi remains primarily unbound in our isolates as well. If the identified SNPs in Sbi in fact hinder anchoring, it is possible that DAP-R isolates have an increased abundance of Spa sufficient to block IgG binding independently and therefore Sbi sequestered entirely to perform its C3 binding functionality. This hypothesis is supported by the proteomic data presented in **Chapter 3** and suggests a potential mechanism by which DAP-R strains would be less susceptible to the immune system.

Serine-aspartate repeat containing (Sdr) proteins are members of the MSCRAMM (Microbial Surface Components Recognizing Adhesive Matrix Molecules) family of surface proteins. The Sdr proteins contain an N-terminal signal peptide followed by a ligand binding domain (containing N1, N2, and N3 subdomains), two to five B repeats, an R domain that contains the Ser-Asp (SD) repeats, a cell wall anchoring motif, and a cytoplasmic C terminal end (272).

SdrC plays a role in bacterial adherence to surfaces and biofilm formation through homophilic cell to cell interactions (273). The SD repeat region self-associates to promote cellular and surface attachment, however it is specifically not required for either (274). The SNPs annotated in SdrC were exclusively in this region in the protein, perhaps hindering the ability of the cells to aggregate. If the cells were less prone to aggregate, it is possible the bacterial cells would be more widely distributed increasing the likelihood of bacteremia, consistent with the increased prevalence in DAP-R MRSA strains.

SdrD is important for adhesion to host cells via binding to desmoglein 1 (Dsg1) (275). The D370N missense mutations, along with the frameshift at V251, are both within the N2/N3 ligand-binding domain of the protein, suggesting a potential inference in host cell adhesion in isolated harboring these SNPs. The

missense mutation D1117Q is in the SD repeat region, whose function remains largely undefined in this protein. Finally, the S227R SNP occurs in the N terminal signal sequence of the protein. Given the location of the identified SNPs, these isolates are less likely to colonize and internalize on host cells, implying a greater likelihood of bacteremic infection. Although we can hypothesize the impacts of these SNPs on protein function, validation of these predicted phenotypes required additional investigation.

Further, sequencing identified several SNPs previously unassociated with development of DAP-R. Of particular interest, in the strain CB1664 wherein the DAP+NAF combination was inactive, the only strain unique SNP was a frameshift in *stp*1. This is the first reported incidence of any SNP in *stp1* coinciding with development of DAP-R, however previous studies have reported a link between *stp1* and reduced vancomycin susceptibility (276-278). Stp1 is the cognate phosphatase to Stk1, a penicillin-binding and serine/threonine kinase associated (PASTA) kinase involved in regulation of cell wall biosynthesis, antibiotic susceptibility, and virulence (279-281). Importantly, deletion of *stk1* has been shown to enhance susceptibility to β-lactam antibiotics (282-284). The identified frameshift in Stp1 would likely hinder most or all of the protein's activity. Based on the association between Stp1 and Stk1, this would likely lead to disruption of cell wall homeostasis that would alter both DAP and β-lactam activity.

One drawback to the current study is the focus on only six β-lactam antibiotics. Although the panel of β-lactams utilized represents diverse classes and PBP-binding profiles, certain β-lactams that are of clinical importance, such as ceftaroline (CPT), were not included. CPT was left out of the study because of its potent anti-MRSA activity alone, as well as antimicrobial stewardship guidance that entail selection of narrower spectrum antibiotics targeted to gram-positive organisms for initial treatment (29, 285). However, combinations of DAP with ceftaroline (CPT) have shown immense promise against DAP-R MRSA and deserve further investigation, particularly in cases where combinations with more common β-lactams are ineffective (145, 146, 148, 168).

The data presented here outline several pathways moving forward to better understand the disparity in activity of DAP combinations with β-lactams. Two main phenotypes, CC30 lineage and SCV growth, were observed in strains with less combination activity. Further, we reported the occurrence of SNPs in innate immune evasion genes alongside development of DAP-R. Determination of whether these SNPs are a result of the chronicity of infection or specifically resistance to DAP will required additional investigation. Finally, we identified a number of previously unreported SNPs coinciding with the development of DAP-R. Although investigation of a more extensive strain collection is necessary to validate the preliminary findings here, we have identified several novel characteristics that could help predict the activity of DAP combinations with β-lactams.

Chapter 6. Conclusions and Future Work

6.1 Concluding Remarks

Infections caused by MRSA are becoming increasingly severe and resistant to virtually all antibiotics, including the lipopeptide DAP. Furthermore, in recent years there has been a concerning uptick in the prevalence of DAP-R in clinical *S. aureus* isolates (286). In these instances, combinations of DAP + a β-lactam antibiotic are recommended for treatment (126, 145). In this dissertation, the mechanisms underlying DAP + β-lactam combinations were investigated to optimize their bactericidal effect in DAP-R MRSA.

As discussed in **Chapter 1**, treatment with DAP + β-lactams has been shown to hinder and even prevent the development of DAP-R, mediated by prevention of characteristic SNPs in multi-peptide resistance factor *mprF* (124). Based on the ability of β-lactams to hinder DAP-R development, we wondered what impact β-lactams have on strains that are already DAP-R. To that end, we passaged 3 DAP-R MRSA strains in different β-lactams. The results detailed in **Chapter 2** revealed the potential of β-lactams to restore these strains to a DAP-S phenotype. Reversion of DAP susceptibility was dependent on additional SNPs in *mprF* with retention of the initial gain-of-function mutations. Susceptibility to DAP in both the passage strains and strains with the double *mprF* mutation knocked-in (DM) was similar to, or even greater than, that of the initial DAP-S parent strains by MIC. Both the passage and DM strains reverted characteristic DAP-R cell envelope phenotypes.

Based on the profound impact of β-lactams on DAP susceptibility, **Chapter 3** investigated the application of DAP + β-lactam combinations to optimize synergy. Pre-treatment with β-lactams followed by subsequent DAP treatment enhanced bacterial killing compared to standard simultaneous dosing. To further investigate the effect of β-lactam conditioning on the cells, proteomic analysis was performed

either with or without β-lactam pre-conditioning. These analyses revealed that strains pre-conditioned with β-lactams had a decreased abundance of riboflavin biosynthesis proteins and key *S. aureus* autolysins. Comparison of β-lactam-induced responses showed variation depending on specific β-lactams.

Development of DAP-R involves alteration of several cell envelope phenotypes, including surface charge, membrane fluidity, and phospholipid content (56, 97). Based on the discrepancies in β-lactam response reported in the proteomic data, we investigated the individual impacts of β-lactams on DAP-R associated cell envelope phenotypes in **Chapter 4**. All six study β-lactams presented phenotypes that would revert at least one DAP-R mediated alteration. MEM and LOX conditioning decreased surface charge, membrane fluidity, and increased CL content compared to untreated. Decreased surface charge and membrane fluidity was also found CRO and FOX conditions. NAF samples had decreased surface charge and CEC samples had increased DAP binding, compared to respective untreated isolates. Collectively these data show that β-lactams alter phenotypes important for DAP-R, albeit via unique mechanisms.

As the impact of β-lactams on DAP-R phenotypes differs, we asked whether these differences would correlate with the extent of synergistic activity, and further whether the differences in synergy were universal or strain specific. In **Chapter 5**, we assessed the activity of six DAP + β-lactam combinations in a set of nine diverse MRSA clinical bloodstream isolates. Collectively, there was no significant change in activity between β-lactam combinations, but in four strains at least one combination was inactive. The CRO combination and the NAF combination were inactive in CB5082 and CB1664 respectively. In CB5089, only two of the six combinations led to bacterial killing, and in CB5063 all combination were inactive. To identify differences between strains, WGS and SNP calling was performed for all strain pairs. In addition to genes frequently associated with DAP-R (*mprF*, *walk*, *cls2*, and *rpoB*), SNPs in innate immune evasion factors *sbi*, *sdrC*, and *sdrC* were found in multiple isolates. In addition, several strain specific SNPs were identified among our study set. Of note, CB5063 was the only CC30 lineage strain tested in our study.

In conclusion, the work presented here enhances our understanding of DAP + β-lactam combinations, and specifically the role of β-lactams in DAP-R MRSA. **Chapter 2** uncovered the ability of β-lactams to revert DAP-R MRSA strains to a DAP-S phenotype. The data in **Chapter 3** shows β-lactam pretreatment followed by DAP improves bacterial killing compared to simultaneous dosing and that the impact of pretreatment varies between distinct β-lactams. **Chapter 4** describes β-lactam specific alterations of the cell envelope that are favorable for DAP activity, and **Chapter 5** illustrates the diversity in strain response to DAP + β-lactam combinations. The results presented here provide valuable information about DAP + β-lactam combinations and how combination treatment can be better utilized in the future.

6.2 Future Work

While DAP + β-lactam combinations are the recommended treatment for DAP-R MRSA, the underlying mechanism of activity remains undefined. To effectively utilize these combinations in treatment we need to understand the distinct impact and binding of β-lactams, the precise process by which β-lactams improve DAP activity, and how to identify which strains will respond to specific treatments.

6.2.1 Distinct Impacts of Individual β-Lactams

Despite widespread resistance to β-lactam antibiotics, they remain the gold standard of treatment for bacterial infections and have drawn substantial interest as a supplement to antibiotics from other classes (287). To understand the full potential of β-lactams in the context of MRSA, a more thorough understanding of their binding profiles and off target effects is required.

Results presented in **Chapter 3** and **Chapter 4** show that in addition to inhibiting PBP-mediated cross-linking, β-lactams also have distinct secondary effects on the cell. Also as detailed in **Chapter 5**, specific β-lactams synergize differently in certain strains. To delineate β-lactam responses requires a more detailed understanding of the specific impacts of individual β-lactams. For example, while PCA analysis of the proteomics data showed similarities in response to NAF, LOX, and CRO, a more thorough analysis of the data would determine whether the differences between β-lactams are a result of the variation in concentrations or if different proteins are actually targeted. To relate these proteomic changes to activity, a similar study utilizing a strain where contrasting activity is seen with different combinations (such as CB5089) would be useful.

6.2.2 Mechanism Behind DAP + β-Lactam Interactions

The data presented in **Chapters 2**, **3**, and **4** detailing the impact of β-lactams on DAP-R MRSA suggests that synergy of DAP + β-lactam combinations is based on β-lactam priming the cell for DAP activity. The recent finding of the initial DAP, PGN, and UDP-coupled intermediate complex provides the basis for a potential mechanism of synergy (45). Inhibition of PBPs by β-lactam binding leads to a buildup of cell wall precursors, as the cell is unable to perform cross-linking. An increased amount of these cell wall precursors thereby increases the number of sites for DAP to insert into the cell, thus increasing its activity. This hypothesis also explains why β-lactam pre-conditioning would improve activity compared to simultaneous treatment because the pre-conditioning allows the cell to buildup precursors prior to DAP addition. This hypothesis could be tested by increasing the amount of CW precursors in the membrane (either biologically or synthetically) without inhibiting the PBPs and testing the susceptibility of these isolates to DAP.

Another implication of the tripartite complex is DAP sequestration of lipid II, which would lead to delocalization or decreased activity of different proteins. A recent paper identified lipid II as a molecular

signal for the PASTA kinase/phosphatase pair Stk1/Stp1 (290). As Stk1 plays a role in β-lactam sensitivity, DAP complexing with lipid II could hypersensitize isolates to β-lactams (i.e. the see-saw effect). To test this hypothesis would require determination of whether DAP sequesters lipid II and if this impacts Stk1/Stp1 localization. The DAP-lipid II interaction and its impact on Stk1/Stp1 could be visualized through imaging techniques using click chemistry for the former and fluorescent tagging for the latter.

The chaperone PrsA, which is under the control of the two-component regulator VraSR, is reported to play an important role in the see-saw effect (137). As VraSR is a known target of Stk1, it is likely that identified SNPs would play a role in the see-saw effect (291). In addition, frameshift mutations in Stp1 have been reported in VISA and DAP-R isolates [**Chapter 5**] (292, 293) implying a role for these proteins in glycopeptide and/or lipopeptide resistance. To evaluate the potential role of Stp1 in the see-saw effect, *stp1* knockout strains should be constructed and tested for their susceptibility to DAP and β-lactams compared to the parent strain. Alternatively, wild-type Stp1 could be cloned back into the study strains (with the frameshift SNPs) and susceptibility screening performed.

6.2.3 Optimization of Treatment Strategies

Although treatment with DAP + β-lactam combinations are recommended for cases of persistent MRSA bacteremia, their efficacy is not consistent in all *S. aureus* isolates (294). Our investigation in **Chapter 5** revealed key phenotypic and genotypic correlates that act as a starting point to better understand these differences. The one strain in our study that none of the combinations were effective against was also the only strain of the CC30 lineage. CC30 MRSA isolates tend to cause complicated, persistent, and/or severe infection in patients, likely through production of an phenol soluble modulin (PSM) toxin (259, 261, 295). Identification of CC linage as a mechanism to discern whether to utilize DAP + β-lactam treatment would be important, however a larger scale study with additional CC30 isolates is needed to determine whether this phenotype is consistent.

Another potential indicator of unresponsive strains is the small colony variant (SCV) phenotype. The three other strains in **Chapter 5** where at least one combination was inactive presented with the SCV phenotype. SCV isolates often occur in persistent infections following prolonged antibiotic exposure and present with slow growth, reduced membrane electron gradient, and an ability to survive in host cells (261, 264). Treatment with β-lactams alone is less effective in these isolates due to the reduced growth rate, however DAP retains its bactericidal activity (267). Whether or not this phenotype is directly related to DAP + β-lactam synergy will require additional studies, ideally with DAP-R SCV genetic mutants. These mutants could be generated by passaging SCV isolates in DAP or by genetic mutation of DAP-R isolates. Time-kill activity assays of different DAP-β-lactam combinations would be run in the resulting mutants alongside their respective parent strains to determine whether there is any discrepancy.

Further complicating the hypothesis of SCV phenotype playing a role in synergy is the lack of reliable methods to detect SCV isolates. In culture, wild-type bacteria will often overgrow SCV colonies, and some will even revert to their initial phenotype (264). A reliable detection method, such as culturing of isolates in conditions activating the stringent response, could be implemented to more accurately identify these SCV strains.

In addition to the previous phenotypes, several of the SNPs identified in **Chapter 5** warrant further investigation, particularly the mutations identified in innate immune evasion genes *sbi*, *sdrD*, and *sdrC*. SNPs in these genes have not been studied in relation to DAP-R and evaluating the outcomes of these mutations would provide important insight into possible treatment strategies. Deactivation or repression of these proteins would suggest treatment strategies known to stimulate innate immunity in the host. Alternatively, activation or increased expression of these proteins would enhance our understanding of why these infections are difficult to eradicate.

Finally, improvement of diagnostic antimicrobial testing procedures is important for proper management and treatment of MRSA. Cross-resistance between DAP and HDPs has been widely reported and highlights the importance of taking into consideration the host environment when studying DAP (60, 71, 104). In fact, the presence of certain innate immune HDPs, such as LL-37, have been shown to provide more accurate MIC values that better correlate with clinical outcomes (296). Furthermore, the presence of other media components including bicarbonate are important for measuring accurate susceptibility profiles (164, 297-299). Reliable susceptibility testing of isolates is imperative for efficient and effective treatment of patients, and therefore reconsideration of testing standards, particularly in relation to the test media/matrix, is warranted.

In conclusion, the work presented here provides insight into the role of β-lactams in DAP-R MRSA, however further investigation of DAP-β-lactam combinations will allow us to continue improving treatment outcomes. The preliminary results presented here provide a starting point for important future studies in the field.

Appendix

Supplementary Data for Chapter 2

Supplemental Methods

Construction of mprF-mutants by allelic exchange

The introduction of a secondary *mprF* mutation into the three DAP-R backgrounds (which contain a single *mprF* mutation) was conducted using the allelic exchange protocol developed by Monk and Stinear with modification [199] (outlined below).

Oligonucleotides tailed with sequence complementary to pIMAY-Z were designed to amplify a ≈1.2kb region surrounding the secondary *mprF* mutation (table S2), the LOX passaged DAP-resensitized strains serving as a donor for the sequence. Amplicons were gel extracted and three separate Seamless Ligation Cloning Extracts (SLiCE) were performed into the linearized pIMAY-Z backbone [200]. Each 10 µL SLiCE reaction contained 1 µL of 10 × ligation buffer (NEB), 1 µL pIMAY-Z (50–100 ng/µL), 3 µL of gel extracted insert (20–30 ng/µL), 4 µL of dH2O, and 1 µL of SLiCE, incubated at 37 °C for 30 min.

The generation of competent cells (for E. coli): an overnight culture of E. coli strain IM08B [201] grown in Luria–Bertani broth (LB) was diluted 1:200 and incubated at 37 °C with agitation (200 rpm) to an optical density at 600 nm (OD600) of 0.5–0.7. Culture were moved to ice (minimum 15 min) to arrest growth, with all subsequent steps performed at 4°C. Cells were collected by centrifugation (5,000 x g, 20 min), washed twice with an equal volume of autoclaved ice-cold dH 2O, then washed twice with an equal volume of ice-cold 10 % (v/v) glycerol in dH 20, and lastly resuspended 1:1000 in the original culture volume of ice-cold 10 % (v/v) glycerol in dH20. Aliquots of 40 µL were frozen at – 80 °C.

Before the transformation of IM08B, the SLiCE reaction was dialyzed for 10 min on a mixed cellulose ester membrane filter (0.025 µM, MF-Millipore). Electrocompetent IM08B cells were thawed on ice and 5 µL of SLiCE reaction was added to the cells; then, they were gently flicked to mix. Cells were transferred to a 1 mm electroporation cuvette (Bio-Rad) and electroporated at 1800 V, 200 Ω and 25 µF. Cells were immediately resuspended in 1 mL of LB broth and incubated at 37 °C for 1 hour. IM08B transformants were selected in LB supplemented with 10 µg/mL chloramphenicol, incubated overnight at 37 °C with agitation (200 rpm).

The FavorPrep Plasmid Extraction Mini Kit (Favorgen) was used to isolate pIMAY-Z, following the manufacturer's guidelines with the following exceptions: 25 mL of culture was run through each column, and 2.5 x volume of buffers FAPD1, FAPD2 and FAPD3 were used. Plasmids were concentrated using the Novagen Pellet Paint Co-Precipitant precipitation protocol. To create the electrocompetent S. aureus cells, once the cells were diluted to an OD600 of 0.5 (Cell Density Meter, Biowave), they were incubated for ≈1.5 hours to an OD600 of ≈1.0. Concentrated pIMAY-Z was electroporated into the respective DAP-R strains (J03, D712 and C25) according to the published protocol [199].

Allelic exchange was performed following the "Slow (2015) Integration" approach [199]. At the final stage, white colonies (potential *mprF*-double mutants (DM)) were screened on MH agar supplemented with 4 µg/mL daptomycin in parallel grown on BHI agar.

Suspected *mprF* DM colonies and cultures of the parent DAP-R strains used for allelic exchange underwent whole-genome sequencing 2 (WGS) to confirm their genotype, performed as previously described [41]. Briefly, gDNA was extracted from a single colony (Chemagic DNA/RNA kit, Perkin Elmer), WGS libraries prepared (Nextera XT DNA preparation kit, Illumina), and sequencing conducted on a NextSeq (Illumina) with 2 x 150 bp chemistry. The short-read sequence data were mapped to complete reference genomes J01 (CC8, RefSeq accession NZ_CP040619.1) or D592 (CC5, NZ_CP040665.1), and mutations were identified using Snippy v4.6.0 (https://github.com/tseemann/snippy). Both the primary (from the DAP-R parent) and secondary (introduced) *mprF* mutations were confirmed in all three backgrounds. Only one off-target missense mutations was identified: a A308V amino acid change in predicted gene FFX42_RS09315 in the D712 *mprF* DM (reference D592, CC5 background).

Supplementary Table 2.1 Oligonucleotides used in allelic exchange protocol.

OLIGONUCLEOTIDE NAME	5’ TO 3’ SEQUENCE
PIMAY-Z_C25_F	CCTCACTAAAGGGAACAAAAGCTGGGTACCTGGTGCTTATAATGTTGGGC
PIMAY-Z_C25_R	CGACTCACTATAGGGCGAATTGGAGCTCGACGTAACATCTTTAGCAGG
PIMAY-Z_J03_F	CCTCACTAAAGGGAACAAAAGCTGGGTACCCGTTAGGTGATGAAAATGCC
PIMAY-Z_J03_R	CGACTCACTATAGGGCGAATTGGAGCTCGACCCATTAGATACAGGTGG
PIMAY-Z_D712_F	CCTCACTAAAGGGAACAAAAGCTGGGTACCAAGAAGCACTCATAATCGGC
PIMAY-Z_D712_R	CGACTCACTATAGGGCGAATTGGAGCTCCGTAAGTGAAGAATGTCGCC

Supplementary Table 2.2 Isolate characteristics including previously identified *mprF* SNPs (112, 125, 168, 202) and antibiotic susceptibilities in DAP-S and DAP-NS Isolates. Results include broth dilution and

ISOLATE	*mprF* SNP	DAP MIC	NAF MIC	MEM MIC	LOX MIC	CRO MIC	FOX MIC
J01	---	0.5	32	8	16	128	64
J03	T345I	2	16	4	2	128	64
D592	---	0.5	256	512	512	256	256
D712	L341S	2	128	512	512	256	256
JKD 6004	---	0.5	256	512	512	512	512
JKD 6005	---	2	128	512	512	512	512
C1	---	0.19*	16	32	32	4	32
C2	L826F	2	16	16	2	16	32
C3	---	0.5	32	32	64	128	32
C4	P314L	4	32	16	2	16	128
C5	---	0.25	32	32	2	128	32
C6	T345A	3*	32	16	0.125	32	32
C7	---	0.5	64	32	16	64	64
C8	---	3*	64	32	2	8	32
C9	---	0.5	32	16	1	32	32
C10	L826F	3*	16	8	0.063	4	32
C13	---	0.75*	4	16	4	16	64
C14	T472K	4	0.25	2	0.125	4	32
C15	---	0.75*	64	32	256	32	64
C16	M347R	4	32	16	32	16	128
C17	---	0.5	64	32	128	64	32
C18	L341S	4	64	32	64	64	64
C19	---	0.38*	128	32	64	64	64
C21	L826F	4	32	8	0.5	16	32
C22	---	0.5	8	4	0.125	8	64
C23	---	4	64	32	64	128	128
C24	---	0.5	4	8	4	64	32
C25	S295L	3*	0.25	4	0.25	16	32
C26	---	0.38*	128	128	256	512	64
C27	T345K	2	128	128	512	512	128
C30	---	0.25	32	8	8	16	32
C31	L826F	2	32	4	2	4	32
C32	---	0.5	4	4	2	32	32
C33	S337L	2	4	4	4	16	16
C34	---	0.38*	64	8	32	32	64
C35	---	4	64	8	2	32	32
C36	---	0.5	128	128	512	128	64
C37	V351E	3*	1	8	0.25	16	32
C38	---	0.75*	32	8	16	16	64
C39	L826F	3*	32	8	16	8	64
C40	---	0.25	16	8	0.5	4	32
C41	M347R	3*	2	16	0.25	16	32
C42	---	0.75*	16	8	4	64	64
C43	S337L	3*	8	8	2	16	64
C46	---	0.38*	32	16	8	32	16
C47	L826F	3*	128	32	8	32	64
C48	---	0.5	16	8	0.25	4	32
C49	T345I	2	16	32	0.25	16	64
C50	---	0.5	64	128	512	256	128
C51	T345I	2	64	128	128	128	64

Etest method confirmation.

Supplementary Table 2.3 Mutations following β-lactam passage after 28 days.

GENE	J03					D712					C25				
	MEDIA	NAF	LOX	CRO	FOX	MEDIA	NAF	LOX	CRO	FOX	MEDIA	NAF	LOX	CRO	FOX
mprF	+	-	+	+	-	-	+	+	+	+	+	+	+	-	+
div1B	-	-	+	-	-	-	-	-	-	-	-	-	+	-	-
rpoB	-	-	-	-	-	-	-	-	+	-	-	-	-	-	-
rpoC	-	-	-	-	-	-	+	+	+	-	-	-	-	-	-
prs	-	-	-	-	+	-	-	-	-	-	-	-	-	-	-
lysS	-	-	-	+	-	-	-	-	-	-	-	-	-	-	-
ftsX	-	-	-	-	+	-	-	-	-	-	-	-	-	-	-
rpsB	-	-	-	-	+	-	-	-	-	-	-	-	-	-	-
FF957_RS08465	-	-	-	+	-	-	-	-	-	-	-	-	-	-	-
dtd	-	-	-	-	+	-	-	-	-	-	-	-	-	-	-
manA	-	-	-	-	+	-	-	-	-	-	-	-	-	-	-
FF957_RS13855	+	-	-	-	-	-	-	-	-	-	-	-	-	-	-
oatA	-	-	-	-	+	-	-	-	-	-	-	-	-	-	-
citM	+	-	-	-	-	-	-	-	-	-	-	-	-	-	-
apt	-	-	-	-	-	-	-	-	-	-	-	+	-	-	-
BPH2313_01859	-	-	-	-	-	-	-	-	-	-	+	+	+	+	+
BPH2313_01770	-	-	-	-	-	-	-	-	-	-	-	+	+	+	+
BPH2313_01902	-	-	-	-	-	-	-	-	-	-	-	+	+	-	-
BPH2313_01982	-	-	-	-	-	-	-	-	-	-	+	-	+	+	-
BPH2313_02517	-	-	-	-	-	-	-	-	-	-	+	+	+	+	+
BPH2313_02526	-	-	-	-	-	-	-	-	-	-	+	-	-	-	-

Supplementary Data for Chapter 3

Supplementary Table 3.1 MIC values and test concentrations utilized in the study.

ANTIBIOTIC	DAP-S D592 MIC [MG/L]	DAP-R D712 MIC [MG/L]	TEST CONCENTRATION [MG/L]
Daptomycin (DAP)	0.5	3	
Nafcillin (NAF)	128	128	2.6
Meropenem (MEM)	64	64	24
Cloxacillin (LOX)	1024	512	1.35
Ceftriaxone (CRO)	2048	1024	19
Cefaclor (CEC)	256	128	3.25
Cefoxitin (FOX)	256	256	22

Supplementary Figure 3.1 D712 growth curve over the 4 hr time window with β-lactams only.

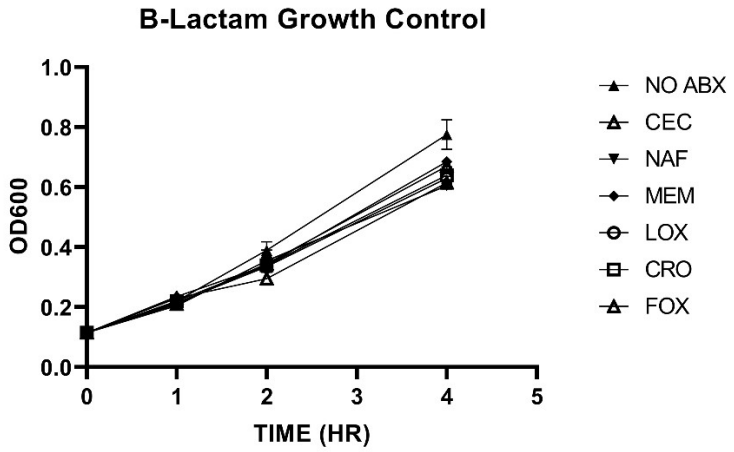

Supplementary Table 3.2 Proteins with significantly altered ratios in DAP-S D592 verses DAP-R D712 samples. Bold proteins are decreased in the DAP-R sample.

PROTEIN ACCESSION (NO ABX)	PROTEIN ACCESSION (NAF)	PROTEIN ACCESSION (MEM)	PROTEIN ACCESSION (LOX)	PROTEIN ACCESSION (CRO)	PROTEIN ACCESSION (CEC)	PROTEIN ACCESSION (FOX)
A0A0H3JPD9	Q2FF31	Q2FF31	Q2FF31	Q2FF31	A0A0H2XKF9	Q2FF31
P60684	A0A0H2XEL4	Q2FI09	A0A0H2XJ08	A0A0H2XHC5	Q2FF31	A0A0H2XEL4
A0A0H3JY03	A0A0H2XH11	A0A0H2XK44	A0A0H2XFF6	A0A0H2XI50	A0A0H2XGH6	A0A0H2XFW1
A0A0H3JUY9	A0A0H2XI78	A0A0H2XG24	A0A0H2XJD3	Q2FFM1	Q2FK44	A0A0H2XF98
A0A0H3JSS2	Q2FF32	Q2FI07	A0A0H2XH77	A0A0H2XIN0	A0A0H2XHT0	A0A0H2XH14
Q99SF0	Q2FFQ5	A0A0H2XI72	Q2FFX3	A0A0H2XFP5	A0A0H2XI29	A0A0H2XI50
Q932I8	A0A0H2XGX4	A0A0H2XKD0	A0A0H2XDI1	A0A0H2XGI8	A0A0H2XIN7	Q2FIS2
Q99V38	A0A0H2XI72	Q2FII7	A0A0H2XJ60	A0A0H2XIA2	Q2FKC6	A0A0H2XIN0
A0A0H3JQ59	Q2FGA1	Q2FI12	A0A0H2XI50	Q2FFQ5	Q2FFQ5	Q2FF54
A0A0H3JVR2	A0A0H2XGL0	A0A0H2XJC3	A0A0H2XIN0	Q2FIV6	A0A0H2XF08	A0A0H2XIK0
P66152	Q2FHH9	A0A0H2XEX9	Q2FFQ5	A0A0H2XFF6	A0A0H2XI01	A0A0H2XHC5
A0A0H3JWY7	A0A0H2XIN0	Q2FJM8	A0A0H2XH66	A0A0H2XGV4	A0A0H2XIB7	A0A0H2XH55
A0A0H3JTT5	A0A0H2XJK1	Q2FI05	A0A0H2XFV7	A0A0H2XHX8	A0A0H2XJC3	A0A0H2XIR6
A0A0H3JTV4	A0A0H2XDI1	A0A0H2XHT0	A0A0H2XGI5	A0A0H2XGF4	A0A0H2XJG5	A0A0H2XG09
A0A0H3JPH0	A0A0H2XI62	A0A0H2XFS4	A0A0H2XIY7	A0A0H2XIY7	A0A0H2XIN0	A0A0H2XDI1
A0A0H3JSP8	A0A0H2XI50	A0A0H2XIN0	Q2FFM1	Q2FEK3	A0A0H2XFP5	A0A0H2XGD5
Q932F7	A0A0H2XGI9	Q2FFQ5	**A0A0H2XHK2**	A0A0H2XGK0	A0A0H2XI50	A0A0H2XGL0
P60747	Q2FDQ4	Q2FDT8	**A0A0H2XIJ2**	A0A0H2XHQ7	A0A0H2XHC8	A0A0H2XGI8
A0A0H3JSF2	A0A0H2XJ60	Q2FIS2	**A0A0H2XI99**	A0A0H2XDI1	**A0A0H2XHM3**	A0A0H2XI62
A0A0H3K4Z7	Q2FJ77	Q2FE79	**A0A0H2XG66**	Q2FIS2	**A0A0H2XJB2**	A0A0H2XFP5
P66298	A0A0H2XDE4	A0A0H2XGV4	**Q2FJH7**	Q2FIP5	**A0A0H2XGP6**	A0A0H2XFV7
Q99SG2	Q2FK94	**A0A0H2XIF0**	**A0A0H2XJH7**	A0A0H2XH34	**A0A0H2XHP9**	A0A0H2XHM0
A0A0H3JTU6	A0A0H2XFV7	**A0A0H2XHH4**	**A0A0H2XIK9**	A0A0H2XHQ5	**A0A0H2XDT0**	A0A0H2XF08
P60448	A0A0H2XGI5	**Q2FF00**	**A0A0H2XII8**	A0A0H2XIB2	**Q2FJJ8**	A0A0H2XGB6
A0A0H3JPM4	A0A0H2XF42	**Q2FDH2**	**Q2FH87**	Q2FJK2	**A0A0H2XFP1**	A0A0H2XG96
Q99WV0	Q2FJP8	**A0A0H2XH77**	**A0A0H2XES0**	A0A0H2XGC9	**A0A0H2XIJ2**	A0A0H2XH34
A0A0H3JT27	A0A0H2XGC9	**Q2FGD8**	**A0A0H2XER0**	A0A0H2XH45	**Q2FEK3**	Q2FEK3
Q99UX4	A0A0H2XH34	**A0A0H2XDZ4**	**A0A0H2XIN4**	Q2FIJ2	**A0A0H2XI99**	A0A0H2XHI8
P0A001	A0A0H2XG88	**Q2FHG5**	**Q2FF18**	A0A0H2XFL7	**A0A0H2XI48**	A0A0H2XIY7
Q99UX8	Q2FE79	**A0A0H2XJ08**	**A0A0H2XGK8**	A0A0H2XDY2	**A0A0H2XIU9**	Q2FIF3
A0A0H3JT69	A0A0H2XGV4	**Q2FK29**	**A0A0H2XI38**	A0A0H2XJ17	**A0A0H2XI72**	Q2FEC8
A0A0H3JXD5	A0A0H2XIC4			A0A0H2XGL0	**A0A0H2XIV9**	A0A0H2XIS0
Q7A2Q0	Q2FIG2			A0A0H2XFV7	**A0A0H2XGK8**	Q2FJ77
A0A0H3JSY9	A0A0H2XH45			Q2FE79	**A0A0H2XIH9**	Q2FHT6
Q99VG5	A0A0H2XHJ1			A0A0H2XJD2	**A0A0H2XH00**	A0A0H2XGP1
A0A0H3JRM3	A0A0H2XIL8			A0A0H2XFR9		A0A0H2XI48
Q99TR3	A0A0H2XF08			A0A0H2XHG7		A0A0H2XGV4
A0A0H3K0F3	**Q2FEB2**			A0A0H2XIR9		A0A0H2XJ48
A0A0H3JSS0	**A0A0H2XJ47**			Q2FGY5		A0A0H2XF07
Q99S37	**A0A0H2XIJ2**			Q2FDT8		Q2FFQ5
Q99S30	**A0A0H2XHY4**			A0A0H2XIR6		Q2FJQ9
A0A0H3JU21	**A0A0H2XGR6**			A0A0H2XIG4		**A0A0H2XK99**
A0A0H3JPE2	**A0A0H2XFY7**			A0A0H2XH87		**A0A0H2XI37**
A0A0H3JXR3	**A0A0H2XHH4**			A0A0H2XJG5		**Q2FFR1**
A0A0H3JSH8	**A0A0H2XHF5**			A0A0H2XGX4		**A0A0H2XHA2**
A0A0H3JX59	**A0A0H2XG24**			A0A0H2XGW5		**Q2FF08**
A0A0H3JU24	**Q2FF28**			A0A0H2XFT6		**A0A0H2XIP6**
A0A0H3JXQ3	**A0A0H2XI99**			A0A0H2XHQ0		**A0A0H2XIN1**
A0A0H3JXH5	**A0A0H2XIA8**			A0A0H2XK79		**Q2FJP6**
P65201	**Q2FHN8**			A0A0H2XIC0		**Q2FHD6**
P0C000	**A0A0H2XH75**			A0A0H2XIW1		**Q2FHN5**
A0A0H3JT20	**A0A0H2XIN1**			A0A0H2XEN6		**Q2FHN8**
Q99X26	**Q2FHN5**			A0A0H2XEA7		**Q2FIR2**
A0A0H3JTI6	**Q2FHN4**			**Q2FEP6**		**Q2FDM1**
Q932K5	**A0A0H2XGK8**			**Q2FJA3**		**A0A0H2XJB2**

Q7A2R7	A0A0H2XJH7	A0A0H2XDX3	A0A0H2XJ71
A0A0H3JRV0		A0A0H2XJ47	A0A0H2XDZ4
A0A0H3JTJ1		Q2FGE8	Q2FE79
A0A0H3JQI2		A0A0H2XG66	Q2FDE7
A0A0H3JSY4		Q2FH87	A0A0H2XH75
A0A0H3JTC7		Q2FEB2	Q2FK29
A0A0H3K181		A0A0H2XHV3	Q2FJ78
A0A0H3JRZ4		Q2FJ95	A0A0H2XIH9
P60223		Q2FEQ5	A0A0H2XJH7
A0A0H3JR05		A0A0H2XHY4	A0A0H2XJ17
A0A0H3JQB2		Q2FHL4	A0A0H2XJ08
Q99W47		Q2FES9	Q2FFX3
A0A0H3JPG4		A0A0H2XIJ2	A0A0H2XH77
A0A0H3JU33		A0A0H2XEA4	A0A0H2XHA4
A0A0H3JUX1		A0A0H2XI99	
A0A0H3JTU7		A0A0H2XFJ8	
P0A015		A0A0H2XGK8	
P68799		A0A0H2XJH7	
		Q2FJ15	
		Q2FEQ2	
		Q2FK58	

Supplementary Table 3.3 Proteins with significantly altered ratios in ABX verses NO ABX conditions in DAP-R D712. Bold proteins are increased in β-lactam treated sample.

Protein Accession (NAF)	Protein Accession (MEM)	Protein Accession (LOX)	Protein Accession (CRO)	Protein Accession (CEC)	Protein Accession (FOX)
A0A0H2XEV3	Q2FHV3	Q2FF18	Q2FF18	Q2FHV3	Q2FHV3
A0A0H2XDU2	Q2FER2	A0A0H2XJ08	A0A0H2XJK1	Q2FER2	Q2FF31
Q2FGE5	A0A0H2XH59	A0A0H2XHA4	A0A0H2XIA2	A0A0H2XJ55	A0A0H2XHA4
A0A0H2XH11	A0A0H2XDT0	A0A0H2XG19	A0A0H2XG53	A0A0H2XII2	A0A0H2XJ55
Q2FF18	Q2FF31	A0A0H2XEV3	A0A0H2XIB2	A0A0H2XJY0	A0A0H2XH59
Q2FF31	Q2FK29	Q2FFX3	A0A0H2XJD9	A0A0H2XJB2	A0A0H2XII2
A0A0H2XGZ2	A0A0H2XJ55	A0A0H2XHX1	Q2FHG5	A0A0H2XHN9	Q2FER2
Q2FJ15	Q2FI09	A0A0H2XG89	A0A0H2XG31	A0A0H2XH59	Q2FFX3
A0A0H2XI57	A0A0H2XKH9	Q2FHG5	A0A0H2XJU8	A0A0H2XGI6	A0A0H2XJ08
A0A0H2XG53	A0A0H2XGI6	A0A0H2XIA2	Q2FHZ0	Q2FF08	A0A0H2XJ17
Q2FG64	Q2FF19	A0A0H2XJD9	A0A0H2XH59	A0A0H2XFV0	A0A0H2XE66
A0A0H2XIB2	Q2FF18	A0A0H2XIB2	A0A0H2XIA9	Q2FII7	A0A0H2XHV2
A0A0H2XDX7	Q2FH87	A0A0H2XGD6	A0A0H2XED9	Q2FHL4	A0A0H2XG04
A0A0H2XH59	A0A0H2XJ17	A0A0H2XH77	Q2FEQ2	Q2FJ74	Q2FDT8
A0A0H2XJH7	Q2FDT8	A0A0H2XIX5	Q2FGE8	Q2FDM1	Q2FK47
A0A0H2XGV3	Q2FJH7	A0A0H2XIK9	A0A0H2XEN6	Q2FH99	Q2FDM1
A0A0H2XI83	Q2FGH2	A0A0H2XED9	Q2FEG1	Q2FHJ7	Q2FE79
Q2FGX5	Q2FE72	A0A0H2XH78	Q2FIV6	A0A0H2XK83	Q2FH87
Q2FIC1	A0A0H2XFV0	A0A0H2XGP0	Q2FEZ8	A0A0H2XIR6	Q2FIV6
A0A0H2XIT5	Q2FF08	A0A0H2XI83	Q2FF25	A0A0H2XJD9	A0A0H2XIF1
Q2FIV6	Q2FHG5	Q2FHZ0	Q2FJA0	A0A0H2XFF1	A0A0H2XJD9
A0A0H2XH78	Q2FHL4	Q2FIC3	A0A0H2XGI9	Q2FEQ5	Q2FIR2
Q2FDT8	A0A0H2XFP1	Q2FES9	A0A0H2XHQ5	A0A0H2XHV2	A0A0H2XGI6
A0A0H2XH66	A0A0H2XHA4	Q2FEG1	Q2FHL4	Q2FEP9	Q2FF18
A0A0H2XIH9	Q2FHJ7	A0A0H2XII0	**Q2FHV3**	**Q2FJ80**	Q2FF08
Q2FJD9	A0A0H2XE66	A0A0H2XGV3	**Q2FER1**	**Q2FJG3**	Q2FGB0
A0A0H2XHY4	A0A0H2XFS9	A0A0H2XJU8	**A0A0H2XGC9**	**A0A0H2XG15**	A0A0H2XEL7
	Q2FG58	**Q2FEK3**	**A0A0H2XH28**	**A0A0H2XHM1**	A0A0H2XIR9
	A0A0H2XIF1	**A0A0H2XIL8**	**A0A0H2XIY2**	**A0A0H2XIH4**	Q2FJK2
	A0A0H2XJ08	**A0A0H2XDU2**	**Q2FJD9**	**Q2FJN3**	Q2FJM8
	A0A0H2XEN6	**A0A0H2XHY4**	**A0A0H2XIH9**	**Q2FER1**	A0A0H2XEN6
	Q2FJ94		**A0A0H2XHY4**	**Q2FEL8**	A0A0H2XH77
	A0A0H2XEL7			**A0A0H2XIF0**	A0A0H2XIJ3
	Q2FH99			**A0A0H2XH15**	A0A0H2XFF1
	A0A0H2XF32			**A0A0H2XFM8**	Q2FI18
	Q2FIV6			**Q2FG51**	A0A0H2XK03
	A0A0H2XHD0			**Q2FER8**	Q2FER6
	A0A0H2XIJ2			**A0A0H2XG12**	Q2FHJ7
	A0A0H2XIJ3			**A0A0H2XFV3**	**A0A0H2XHM1**
	A0A0H2XJD9			**A0A0H2XIB7**	**Q2FER1**
	A0A0H2XJU8			**A0A0H2XHY4**	**A0A0H2XI48**
	A0A0H2XDZ4			**A0A0H2XG53**	**Q2FGK9**
	A0A0H2XHN9			**A0A0H2XI29**	**A0A0H2XFM8**
	A0A0H2XHT5			**A0A0H2XHT7**	**A0A0H2XG15**
	Q2FEQ6				**A0A0H2XGK8**
	A0A0H2XHM0				**Q2FJN3**
	Q2FEP9				**Q2FEK3**
	Q2FJ74				**A0A0H2XEF4**
	Q2FEQ5				**A0A0H2XJC7**
	Q2FDM1				**A0A0H2XHQ7**
	Q2FER3				**A0A0H2XGW9**
	Q2FF25				**A0A0H2XGK0**
	Q2FEP1				**Q2FG51**
	A0A0H2XDE4				**Q2FEL8**
	Q2FG57				**Q2FJK1**

A0A0H2XGN0
A0A0H2XG15
A0A0H2XIF0
Q2FJ80
A0A0H2XFR7
A0A0H2XFM8
Q2FJN3
Q2FER1
Q2FG51
A0A0H2XG53
Q2FEL8
Q2FFM1
Q2FFI9
A0A0H2XJC3
A0A0H2XHP9
A0A0H2XF98
A0A0H2XHT7
A0A0H2XHY4
A0A0H2XI29

Q2FFI9
Q2FJ78
A0A0H2XG12
A0A0H2XHP9
A0A0H2XFW1
A0A0H2XG01
A0A0H2XG53
A0A0H2XHY4
A0A0H2XHT7

Supplementary Table 3.4 Proteins with significantly altered ratios in ABX verses NO ABX conditions in DAP-S D592. Bold proteins are increased in β-lactam treated sample.

PROTEIN ACCESSION (NAF)	PROTEIN ACCESSION (MEM)	PROTEIN ACCESSION (LOX)	PROTEIN ACCESSION (CRO)	PROTEIN ACCESSION (CEC)	PROTEIN ACCESSION (FOX)
A0A0H2XI38	A0A0H2XH59	A0A0H2XJ08	Q2FF18	Q2FHV3	Q2FHV3
Q2FF31	A0A0H2XKH9	Q2FF18	A0A0H2XIA2	A0A0H2XII2	A0A0H2XDZ9
A0A0H2XEV3	A0A0H2XJ55	A0A0H2XH77	A0A0H2XJK1	A0A0H2XJ55	A0A0H2XH59
A0A0H2XDU2	Q2FHV3	Q2FFX3	Q2FH24	A0A0H2XGP4	A0A0H2XJ55
Q2FGE5	Q2FDT8	A0A0H2XIA2	A0A0H2XIB2	A0A0H2XKF9	Q2FF18
Q2FF18	A0A0H2XES0	A0A0H2XHA4	A0A0H2XH00	A0A0H2XDZ9	Q2FGB0
A0A0H2XFT0	A0A0H2XIQ3	Q2FGE5	A0A0H2XEV3	A0A0H2XH59	Q2FDT8
A0A0H2XID1	Q2FF18	A0A0H2XHX1	Q2FIV6	Q2FER2	A0A0H2XE66
A0A0H2XGV3	Q2FGB0	A0A0H2XH00	Q2FHZ0	A0A0H2XI01	A0A0H2XII2
A0A0H2XJK1	A0A0H2XHY0	A0A0H2XEV3	Q2FH23	A0A0H2XJB2	A0A0H2XG24
A0A0H2XGZ2	A0A0H2XHG8	A0A0H2XIB0	A0A0H2XGD6	Q2FF31	A0A0H2XER0
A0A0H2XIA2	A0A0H2XG24	Q2FGX5	A0A0H2XIB0	A0A0H2XG24	A0A0H2XIN4
A0A0H2XI27	A0A0H2XDT0	A0A0H2XGV3	A0A0H2XID1	A0A0H2XIC5	A0A0H2XG31
A0A0H2XH59	A0A0H2XE66	A0A0H2XG89	A0A0H2XER0	A0A0H2XIN7	Q2FER2
Q2FIV6	Q2FER2	A0A0H2XGD6	Q2FIC3	A0A0H2XGI6	Q2FK47
A0A0H2XIB2	Q2FF19	A0A0H2XED9	Q2FF31	A0A0H2XES0	A0A0H2XH00
A0A0H2XK60	Q2FJH7	A0A0H2XI83	A0A0H2XIN4	Q2FII7	A0A0H2XIR9
A0A0H2XH77	A0A0H2XK19	Q2FF31	**Q2FHV3**	A0A0H2XIQ3	Q2FDM1
A0A0H2XJ08	A0A0H2XE84	A0A0H2XG19	**A0A0H2XH39**	**A0A0H2XIX5**	A0A0H2XHA4
Q2FHZ0	Q2FDM1	Q2FIC3	**Q2FHI6**	**Q2FER1**	A0A0H2XEN8
Q2FDT8	A0A0H2XG31	A0A0H2XGP0	**Q2FJD9**	**A0A0H2XFM8**	A0A0H2XGK5
A0A0H2XEN6	A0A0H2XIR9	A0A0H2XGZ2	**A0A0H2XHY4**	**A0A0H2XH15**	A0A0H2XHT5
A0A0H2XED9	A0A0H2XFP1	A0A0H2XHT0	**A0A0H2XF37**	**A0A0H2XIP4**	A0A0H2XJD9
A0A0H2XI83	A0A0H2XIJ3	A0A0H2XIX5		**Q2FG51**	Q2FF94
Q2FH04	A0A0H2XIN4	Q2FKC6		**A0A0H2XF98**	Q2FJH7
Q2FEG1	A0A0H2XJ17	Q2FES9		**Q2FJN3**	A0A0H2XIJ3
A0A0H2XGI9	A0A0H2XEN8	Q2FHZ0		**Q2FJK1**	A0A0H2XGI6
Q2FFX3	**A0A0H2XIB7**	A0A0H2XIH4		**A0A0H2XI29**	Q2FFK2
Q2FGH0	**A0A0H2XF96**	A0A0H2XIB2		**A0A0H2XG12**	A0A0H2XHV2
A0A0H2XIN9	**Q2FJK2**	A0A0H2XH59		**A0A0H2XG53**	A0A0H2XEV3
A0A0H2XHA4	**Q2FFI9**	A0A0H2XGN6		**A0A0H2XHT7**	A0A0H2XEL7
A0A0H2XHU9	**Q2FG51**	A0A0H2XGN2		**A0A0H2XHY4**	A0A0H2XDU9
A0A0H2XIJ2	**A0A0H2XG12**	A0A0H2XGI9			A0A0H2XIB2
Q2FHV3	**A0A0H2XHP9**	A0A0H2XJD9			A0A0H2XEN6
Q2FGD8	**Q2FJN3**	Q2FFI4			Q2FI18
Q2FEN9	**A0A0H2XIF0**	A0A0H2XIA9			Q2FHZ0
Q2FEQ5	**A0A0H2XHT7**	A0A0H2XIH9			A0A0H2XJW7
A0A0H2XH28	**A0A0H2XHY4**	A0A0H2XK60			A0A0H2XJV8
Q2FEQ0	**A0A0H2XG53**	A0A0H2XKA8			A0A0H2XG38
A0A0H2XH39	**A0A0H2XF98**	A0A0H2XE39			**Q2FEQ0**
A0A0H2XG58	**A0A0H2XI29**	A0A0H2XFE1			**A0A0H2XFQ3**
A0A0H2XHY4		Q2FHG5			**A0A0H2XGI0**
Q2FJD9		**Q2FHV3**			**Q2FGJ3**
		Q2FGE4			**A0A0H2XGB2**
		A0A0H2XIY2			**A0A0H2XG58**
		Q2FFJ4			**A0A0H2XG15**
		Q2FJ77			**A0A0H2XFM8**
		Q2FEK3			**Q2FGK9**
		A0A0H2XFQ6			**A0A0H2XJC7**
		Q2FJD9			**Q2FEL8**
		A0A0H2XHY4			**Q2FF00**
		A0A0H2XF37			**A0A0H2XGK0**
					A0A0H2XHT7
					Q2FJK1
					A0A0H2XHT2

A0A0H2XH39
A0A0H2XEF4
Q2FHK6
Q2FJN3
A0A0H2XG12
A0A0H2XG53
A0A0H2XHY4

Supplementary Data for Chapter 4

Supplementary Table 4.1 Bacteriostatic concentrations of β-lactam antibiotics (mg/L) for test strains.

STRAIN	NAF	LOX	MEM	CRO	CEC	FOX
CB1483	128	16	7	512	128	64
CB185	32	0.5	1.1	512	128	128
CB5079	16	16	7.5	4	128	64
CB5080	8	2	2.5	16	64	48
CB5083	64	1	12	128	64	32
CB5082	64	1	24	16	64	128
CB5088	8	6	3.75	128	64	48
CB5089	8	4	2.5	16	32	32
CB1631	12	2	0.6	128	64	64
CB1634	4	0.5	0.15	8	128	32
CB1663	8	4	15	128	64	64
CB1664	4	0.5	2.5	32	32	64
CB5057	16	2.5	2.5	32	32	72
CB5059	64	10	10	32	64	128
CB5062	256	512	512	512	128	64
CB5063	256	512	512	512	128	128
CB5015	128	128	8	32	16	64
CB5016	256	256	1	256	128	128

Supplementary Figure 4.1 Fluorescence quantification (**A**) and confocal images (**B**) of N315 knockouts of either *S. aureus* cardiolipin synthase gene. *indicates p<0.05 vs N315.

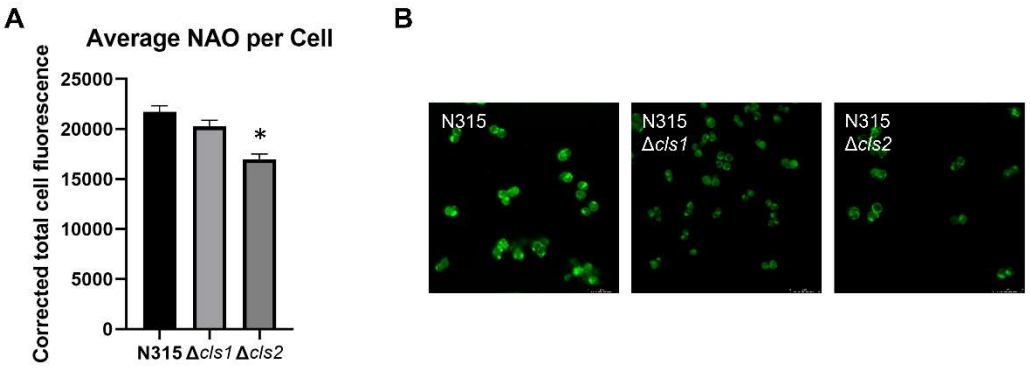

Supplementary Data for Chapter 5

Supplementary Table 5.1 Test concentrations of β-lactam antibiotics (mg/L) for test strains.

STRAIN	NAF	LOX	MEM	CRO	CEC	FOX
CB1483	2.6	1.35	24	19	3.25	22
CB185	2.6	1.35	8	19	3.25	22
CB5079	2.6	1.35	4	2	3.25	22
CB5080	2.6	0.125	2	8	3.25	22
CB5083	2.6	1.35	8	19	3.25	22
CB5082	2.6	0.5	24	8	3.25	22
CB5088	2.6	1.35	2	19	3.25	22
CB5089	2.6	0.25	2	8	3.25	22
CB1631	2.6	0.5	8	19	3.25	22
CB1634	0.25	0.075	1	4	3.25	22
CB1663	2.6	0.5	4	19	3.25	22
CB1664	1	0.25	1	19	3.25	22
CB5057	2.6	0.5	1	19	3.25	8
CB5059	2.6	0.25	0.5	19	3.25	22
CB5062	2.6	1.35	24	19	3.25	22
CB5063	2.6	1.35	24	19	3.25	22
CB5015	2.6	0.5	4	19	3.25	22
CB5016	2.6	0.5	24	19	3.25	22

Supplementary Table 5.2 Genes with high or medium impact SNPs. *Indicates truncated gene. Bold indicates high impact SNP (variant assumed to have a disruptive impact on the protein).

DAP-R strains	Strain specific SNPs
CB185	*airS, cls2, mprF,* ***rectT***
CB5080	*clfB, coa, esaG, fmtB, mapW*, mprF, rpoB, sasK, secY, set6, set8, ssb,* ***yabJ****, SA0087, SA0394, SA2370*
CB5082	*hlb, int,* ***lytA****, metE, mprF, rpoB, sak, scn, sdrD, sep, SAS058*
CB5089	*agrC, aroB, fur, mprF, sdrD, SA0087, SA1559*
CB1634	*dppb*, lytA*, mprF,* ***saeR****,* ***walK***
CB1664	*mprF,* ***recT****, rpoB, sbi, sdrC,* ***stp1****, walK*
CB5059	*agrC, bioF, ebhA, fnbB, mprF, purA, radC*, sasK, sdrC, ssl11, tetM,* ***treP****, vraT, walk, SA0087, SA0394, SA1559*
CB5063	*cls2, coa, copA, crtN, cysJ,* ***dat****,* ***ebhA****, fnb,* ***fruA****,* ***gntK****, htsA,* ***metE****, mnhA2, mprF, mqo, mrp, nifZ, norA, pta,* ***queA****, rex, rsp, sbi, scc, sdrC,* ***sdrD****, ssl12, tnp,* ***vraG****,* ***ychF****, SA0139, SA0839, SA0840, SA1035, SA1158, SA1559, SA2081, SA2231, SA2369*
CB5016	*ami, clfB, int, mprF, rplC, sbi, sep, ssb, tst, walk, SA1805*

References

1. Rice LB. 2008. Federal Funding for the Study of Antimicrobial Resistance in Nosocomial Pathogens: No ESKAPE. J Infect Dis 197:1079–1081.
2. Nelson RE, Hatfield KM, Wolford H, Samore MH, Scott RD, Reddy SC, Olubajo B, Paul P, Jernigan JA, Baggs J. 2021. National Estimates of Healthcare Costs Associated With Multidrug-Resistant Bacterial Infections Among Hospitalized Patients in the United States. Clin Infect Dis 72:S17-S26.
3. Muhlen S, Dersch P. 2016. Anti-virulence Strategies to Target Bacterial Infections. Curr Top Microbiol Immunol 398:147-183.
4. Khatib R, Johnson LB, Sharma M, Fakih MG, Ganga R, Riederer K. 2009. Persistent *Staphylococcus aureus* bacteremia: incidence and outcome trends over time. Scand J Infect Dis 41:4-9.
5. van Hal SJ, Jensen SO, Vaska VL, Espedido BA, Paterson DL, Gosbell IB. 2012. Predictors of mortality in Staphylococcus aureus Bacteremia. Clin Microbiol Rev 25:362-86.
6. Gerber JS, Coffin SE, Smathers SA, Zaoutis TE. 2009. Trends in the incidence of methicillin-resistant Staphylococcus aureus infection in children's hospitals in the United States. Clin Infect Dis 49:65-71.
7. Services USDoHaH. 2019. Antibiotic Resistance Threats in the United States. CDC, CDC, Atlanta, GA.
8. Vestergaard M, Frees D, Ingmer H. 2019. Antibiotic Resistance and the MRSA Problem. Microbiol Spectr 7.
9. Walsh TR, Howe RA. 2002. The prevalence and mechanisms of vancomycin resistance in *Staphylococcus aureus*. Annu Rev Microbiol 56:657-75.
10. Yocum RR, Waxman DJ, Rasmussen JR, Strominger JL. 1979. Mechanism of penicillin action: penicillin and substrate bind covalently to the same active site serine in two bacterial D-alanine carboxypeptidases. Proc Natl Acad Sci U S A 76:2730-4.
11. Waxman DJ, Strominger JL. 1983. Penicillin-binding proteins and the mechanism of action of β-lactam antibiotics. Annu Rev Biochem 52:825-69.
12. Sauvage E, Kerff F, Terrak M, Ayala JA, Charlier P. 2008. The penicillin-binding proteins: structure and role in peptidoglycan biosynthesis. FEMS Microbiol Rev 32:234-58.
13. Tipper DJ, Strominger JL. 1965. Mechanism of action of penicillins: a proposal based on their structural similarity to acyl-D-alanyl-D-alanine. Proc Natl Acad Sci U S A 54:1133-1141.

14. Goffin C, Ghuysen JM. 1998. Multimodular penicillin-binding proteins: an enigmatic family of orthologs and paralogs. Microbiol Mol Biol Rev 62:1079-93.
15. Wyke AW, Ward JB, Hayes MV, Curtis NA. 1981. A role *in vivo* for penicillin-binding protein-4 of *Staphylococcus aureus*. Eur J Biochem 119:389-93.
16. Pinho MG, de Lencastre H, Tomasz A. 2000. Cloning, characterization, and inactivation of the gene *pbpC*, encoding penicillin-binding protein 3 of *Staphylococcus aureus*. J Bacteriol 182:1074-9.
17. Wada A, Watanabe H. 1998. Penicillin-binding protein 1 of *Staphylococcus aureus* is essential for growth. J Bacteriol 180:2759-65.
18. Pinho MG, de Lencastre H, Tomasz A. 2001. An acquired and a native penicillin-binding protein cooperate in building the cell wall of drug-resistant staphylococci. Proc Natl Acad Sci U S A 98:10886-91.
19. Kozarich JW, Strominger JL. 1978. A membrane enzyme from *Staphylococcus aureus* which catalyzes transpeptidase, carboxypeptidase, and penicillinase activities. J Biol Chem 253:1272-8.
20. Qiao Y, Lebar MD, Schirner K, Schaefer K, Tsukamoto H, Kahne D, Walker S. 2014. Detection of lipid-linked peptidoglycan precursors by exploiting an unexpected transpeptidase reaction. J Am Chem Soc 136:14678-81.
21. Sauvage E, Kerff F, Terrak M, Ayala JA, Charlier P. 2008. The penicillin-binding proteins: structure and role in peptidoglycan biosynthesis. FEMS Microbiol Rev 32:234-258.
22. Reed P, Atilano ML, Alves R, Hoiczyk E, Sher X, Reichmann NT, Pereira PM, Roemer T, Filipe SR, Pereira-Leal JB, Ligoxygakis P, Pinho MG. 2015. *Staphylococcus aureus* Survives with a Minimal Peptidoglycan Synthesis Machine but Sacrifices Virulence and Antibiotic Resistance. PLoS Pathog 11:e1004891.
23. Katayama Y, Ito T, Hiramatsu K. 2000. A new class of genetic element, staphylococcus cassette chromosome *mec*, encodes methicillin resistance in *Staphylococcus aureus*. Antimicrob Agents Chemother 44:1549-55.
24. Antignac A, Tomasz A. 2009. Reconstruction of the phenotypes of methicillin-resistant *Staphylococcus aureus* by replacement of the staphylococcal cassette chromosome mec with a plasmid-borne copy of *Staphylococcus sciuri pbpD* gene. Antimicrob Agents Chemother 53:435-41.
25. Hartman BJ, Tomasz A. 1984. Low-affinity penicillin-binding protein associated with β-lactam resistance in *Staphylococcus aureus*. J Bacteriol 158:513-516.

26. Pinho MG, Filipe SR, de Lencastre H, Tomasz A. 2001. Complementation of the essential peptidoglycan transpeptidase function of penicillin-binding protein 2 (PBP2) by the drug resistance protein PBP2A in *Staphylococcus aureus*. J Bacteriol 183:6525-31.

27. Otero LH, Rojas-Altuve A, Llarrull LI, Carrasco-Lopez C, Kumarasiri M, Lastochkin E, Fishovitz J, Dawley M, Hesek D, Lee M, Johnson JW, Fisher JF, Chang M, Mobashery S, Hermoso JA. 2013. How allosteric control of *Staphylococcus aureus* penicillin binding protein 2a enables methicillin resistance and physiological function. Proc Natl Acad Sci U S A 110:16808-13.

28. Fishovitz J, Hermoso JA, Chang M, Mobashery S. 2014. Penicillin-binding protein 2a of methicillin-resistant *Staphylococcus aureus*. IUBMB Life 66:572-7.

29. Fernandez R, Paz LI, Rosato RR, Rosato AE. 2014. Ceftaroline is active against heteroresistant methicillin-resistant *Staphylococcus aureus* clinical strains despite associated mutational mechanisms and intermediate levels of resistance. Antimicrob Agents Chemother 58:5736-46.

30. Long SW, Olsen RJ, Mehta SC, Palzkill T, Cernoch PL, Perez KK, Musick WL, Rosato AE, Musser JM. 2014. PBP2a mutations causing high-level Ceftaroline resistance in clinical methicillin-resistant *Staphylococcus aureus* isolates. Antimicrob Agents Chemother 58:6668-74.

31. Chan LC, Basuino L, Diep B, Hamilton S, Chatterjee SS, Chambers HF. 2015. Ceftobiprole- and ceftaroline-resistant methicillin-resistant *Staphylococcus aureus*. Antimicrob Agents Chemother 59:2960-3.

32. Liu C, Bayer A, Cosgrove SE, Daum RS, Fridkin SK, Gorwitz RJ, Kaplan SL, Karchmer AW, Levine DP, Murray BE, M JR, Talan DA, Chambers HF. 2011. Clinical practice guidelines by the infectious diseases society of america for the treatment of methicillin-resistant *Staphylococcus aureus* infections in adults and children: executive summary. Clin Infect Dis 52:285-92.

33. Dhand A, Sakoulas G. 2012. Reduced vancomycin susceptibility among clinical *Staphylococcus aureus* isolates ('the MIC Creep'): implications for therapy. F1000 Med Rep 4:4.

34. van Hal SJ, Lodise TP, Paterson DL. 2012. The clinical significance of vancomycin minimum inhibitory concentration in *Staphylococcus aureus* infections: a systematic review and meta-analysis. Clin Infect Dis 54:755-71.

35. Kehrmann J, Kaase M, Szabados F, Gatermann SG, Buer J, Rath PM, Steinmann J. 2011. Vancomycin MIC creep in MRSA blood culture isolates from Germany: a regional problem? Eur J Clin Microbiol Infect Dis 30:677-83.

36. Robbel L, Marahiel MA. 2010. Daptomycin, a bacterial lipopeptide synthesized by a nonribosomal machinery. J Biol Chem 285:27501-8.

37. Debono M, Abbott BJ, Molloy RM, Fukuda DS, Hunt AH, Daupert VM, Counter FT, Ott JL, Carrell CB, Howard LC, et al. 1988. Enzymatic and chemical modifications of lipopeptide antibiotic A21978C: the synthesis and evaluation of daptomycin (LY146032). J Antibiot (Tokyo) 41:1093-105.

38. Moore CL, Osaki-Kiyan P, Haque NZ, Perri MB, Donabedian S, Zervos MJ. 2012. Daptomycin versus vancomycin for bloodstream infections due to methicillin-resistant *Staphylococcus aureus* with a high vancomycin minimum inhibitory concentration: a case-control study. Clin Infect Dis 54:51-8.

39. Murray KP, Zhao JJ, Davis SL, Kullar R, Kaye KS, Lephart P, Rybak MJ. 2013. Early use of daptomycin versus vancomycin for methicillin-resistant *Staphylococcus aureus* bacteremia with vancomycin minimum inhibitory concentration >1 mg/L: a matched cohort study. Clin Infect Dis 56:1562-9.

40. Fowler VG, Jr., Boucher HW, Corey GR, Abrutyn E, Karchmer AW, Rupp ME, Levine DP, Chambers HF, Tally FP, Vigliani GA, Cabell CH, Link AS, DeMeyer I, Filler SG, Zervos M, Cook P, Parsonnet J, Bernstein JM, Price CS, Forrest GN, Fätkenheuer G, Gareca M, Rehm SJ, Brodt HR, Tice A, Cosgrove SE. 2006. Daptomycin versus standard therapy for bacteremia and endocarditis caused by *Staphylococcus aureus*. N Engl J Med 355:653-65.

41. Claeys KC, Zasowski EJ, Casapao AM, Lagnf AM, Nagel JL, Nguyen CT, Hallesy JA, Compton MT, Kaye KS, Levine DP, Davis SL, Rybak MJ. 2016. Daptomycin Improves Outcomes Regardless of Vancomycin MIC in a Propensity-Matched Analysis of Methicillin-Resistant Staphylococcus aureus Bloodstream Infections. Antimicrob Agents Chemother 60:5841-8.

42. Ho SW, Jung D, Calhoun JR, Lear JD, Okon M, Scott WR, Hancock RE, Straus SK. 2008. Effect of divalent cations on the structure of the antibiotic daptomycin. Eur Biophys J 37:421-33.

43. Zhang T, Muraih JK, Mintzer E, Tishbi N, Desert C, Silverman J, Taylor S, Palmer M. 2013. Mutual inhibition through hybrid oligomer formation of daptomycin and the semisynthetic lipopeptide antibiotic CB-182,462. Biochim Biophys Acta 1828:302-8.

44. Jung D, Rozek A, Okon M, Hancock RE. 2004. Structural transitions as determinants of the action of the calcium-dependent antibiotic daptomycin. Chem Biol 11:949-57.

45. Grein F, Muller A, Scherer KM, Liu X, Ludwig KC, Klockner A, Strach M, Sahl HG, Kubitscheck U, Schneider T. 2020. Ca(2+)-Daptomycin targets cell wall biosynthesis by forming a tripartite complex with undecaprenyl-coupled intermediates and membrane lipids. Nat Commun 11:1455.

46. Pogliano J, Pogliano N, Silverman JA. 2012. Daptomycin-Mediated Reorganization of Membrane Architecture Causes Mislocalization of Essential Cell Division Proteins. J Bacteriol 194:4494-4504.

47. Taylor SD, Palmer M. 2016. The action mechanism of daptomycin. Bioorg Med Chem 24:6253-6268.

48. Silverman JA, Perlmutter NG, Shapiro HM. 2003. Correlation of daptomycin bactericidal activity and membrane depolarization in *Staphylococcus aureus*. Antimicrob Agents Chemother 47:2538-44.

49. Allen NE, Alborn WE, Jr., Hobbs JN, Jr. 1991. Inhibition of membrane potential-dependent amino acid transport by daptomycin. Antimicrob Agents Chemother 35:2639-42.

50. Alborn WE, Jr., Allen NE, Preston DA. 1991. Daptomycin disrupts membrane potential in growing *Staphylococcus aureus*. Antimicrob Agents Chemother 35:2282-7.

51. Clinical and Laboratory Standards Institute. 2021. Performance Standards for Antimicrobial Susceptibility Testing; CLSI supplement M100 31st ed. ed. Clinical and Laboratory Standards Institute, USA.

52. Moise PA, North D, Steenbergen JN, Sakoulas G. 2009. Susceptibility relationship between vancomycin and daptomycin in *Staphylococcus aureus*: facts and assumptions. Lancet Infect Dis 9:617-24.

53. Mariani PG, Sader HS, Jones RN. 2006. Development of decreased susceptibility to daptomycin and vancomycin in a *Staphylococcus aureus* strain during prolonged therapy. J Antimicrob Chemother 58:481-3.

54. Sharma M, Riederer K, Chase P, Khatib R. 2008. High rate of decreasing daptomycin susceptibility during the treatment of persistent *Staphylococcus aureus* bacteremia. Eur J Clin Microbiol Infect Dis 27:433-7.

55. Levy DT, Steed ME, Rybak MJ, Guo Y, Gialanella P, Hanau L, Muggia V, Ostrowsky B. 2012. Successful treatment of a left ventricular assist device infection with daptomycin non-susceptible methicillin-resistant *Staphylococcus aureus*: case report and review of the literature. Transpl Infect Dis 14:E89-96.

56. Bayer AS, Schneider T, Sahl HG. 2013. Mechanisms of daptomycin resistance in *Staphylococcus aureus*: role of the cell membrane and cell wall. Ann N Y Acad Sci 1277:139-58.

57. Friedman L, Alder JD, Silverman JA. 2006. Genetic changes that correlate with reduced susceptibility to daptomycin in *Staphylococcus aureus*. Antimicrob Agents Chemother 50:2137-45.

58. Yang SJ, Xiong YQ, Dunman PM, Schrenzel J, Francois P, Peschel A, Bayer AS. 2009. Regulation of *mprF* in daptomycin-nonsusceptible *Staphylococcus aureus* strains. Antimicrob Agents Chemother 53:2636-7.

59. Jones T, Yeaman MR, Sakoulas G, Yang SJ, Proctor RA, Sahl HG, Schrenzel J, Xiong YQ, Bayer AS. 2008. Failures in clinical treatment of *Staphylococcus aureus* Infection with daptomycin are associated with alterations in surface charge, membrane phospholipid asymmetry, and drug binding. Antimicrob Agents Chemother 52:269-78.

60. Bayer AS, Mishra NN, Sakoulas G, Nonejuie P, Nast CC, Pogliano J, Chen KT, Ellison SN, Yeaman MR, Yang SJ. 2014. Heterogeneity of *mprF* sequences in methicillin-resistant *Staphylococcus aureus* clinical isolates: role in cross-resistance between daptomycin and host defense antimicrobial peptides. Antimicrob Agents Chemother 58:7462-7.

61. Ernst CM, Peschel A. 2011. Broad-spectrum antimicrobial peptide resistance by MprF-mediated aminoacylation and flipping of phospholipids. Mol Microbiol 80:290-9.

62. Ernst CM, Kuhn S, Slavetinsky CJ, Krismer B, Heilbronner S, Gekeler C, Kraus D, Wagner S, Peschel A. 2015. The lipid-modifying multiple peptide resistance factor is an oligomer consisting of distinct interacting synthase and flippase subunits. mBio 6.

63. Song D, Jiao H, Liu Z. 2021. Phospholipid translocation captured in a bifunctional membrane protein MprF. Nat Commun 12:2927.

64. Ernst CM, Slavetinsky CJ, Kuhn S, Hauser JN, Nega M, Mishra NN, Gekeler C, Bayer AS, Peschel A. 2018. Gain-of-Function Mutations in the Phospholipid Flippase MprF Confer Specific Daptomycin Resistance. mBio 9.

65. Roy H, Ibba M. 2009. Broad range amino acid specificity of RNA-dependent lipid remodeling by multiple peptide resistance factors. J Biol Chem 284:29677-83.

66. Peschel A, Jack RW, Otto M, Collins LV, Staubitz P, Nicholson G, Kalbacher H, Nieuwenhuizen WF, Jung G, Tarkowski A, van Kessel KP, van Strijp JA. 2001. *Staphylococcus aureus* resistance to human defensins and evasion of neutrophil killing via the novel virulence factor MprF is based on modification of membrane lipids with l-lysine. J Exp Med 193:1067-76.

67. Ernst CM, Staubitz P, Mishra NN, Yang SJ, Hornig G, Kalbacher H, Bayer AS, Kraus D, Peschel A. 2009. The bacterial defensin resistance protein MprF consists of separable domains for lipid lysinylation and antimicrobial peptide repulsion. PLoS Pathog 5:e1000660.

68. Mishra NN, Yang SJ, Chen L, Muller C, Saleh-Mghir A, Kuhn S, Peschel A, Yeaman MR, Nast CC, Kreiswirth BN, Crémieux AC, Bayer AS. 2013. Emergence of daptomycin resistance in daptomycin-naïve rabbits with methicillin-resistant *Staphylococcus aureus* prosthetic joint infection is associated with resistance to host defense cationic peptides and *mprF* polymorphisms. PLoS One 8:e71151.

69. Mishra NN, Yang SJ, Sawa A, Rubio A, Nast CC, Yeaman MR, Bayer AS. 2009. Analysis of cell membrane characteristics of *in vitro*-selected daptomycin-resistant strains of methicillin-resistant *Staphylococcus aureus*. Antimicrob Agents Chemother 53:2312-8.

70. Yang SJ, Mishra NN, Rubio A, Bayer AS. 2013. Causal role of single nucleotide polymorphisms within the *mprF* gene of *Staphylococcus aureus* in daptomycin resistance. Antimicrob Agents Chemother 57:5658-64.

71. Bayer AS, Mishra NN, Chen L, Kreiswirth BN, Rubio A, Yang SJ. 2015. Frequency and Distribution of Single-Nucleotide Polymorphisms within mprF in Methicillin-Resistant *Staphylococcus aureus* Clinical Isolates and Their Role in Cross-Resistance to Daptomycin and Host Defense Antimicrobial Peptides. Antimicrob Agents Chemother 59:4930-4937.

72. Mehta S, Cuirolo AX, Plata KB, Riosa S, Silverman JA, Rubio A, Rosato RR, Rosato AE. 2012. VraSR two-component regulatory system contributes to *mprF*-mediated decreased susceptibility to daptomycin in *in vivo*-selected clinical strains of methicillin-resistant *Staphylococcus aureus*. Antimicrob Agents Chemother 56:92-102.

73. Mishra NN, Bayer AS. 2013. Correlation of Cell Membrane Lipid Profiles with Daptomycin Resistance in Methicillin-Resistant *Staphylococcus aureus*. Antimicrob Agents Chemother 57:1082-85.

74. Oku Y, Kurokawa K, Ichihashi N, Sekimizu K. 2004. Characterization of the Staphylococcus aureus mprF gene, involved in lysinylation of phosphatidylglycerol. Microbiology (Reading) 150:45-51.

75. Peleg AY, Miyakis S, Ward DV, Earl AM, Rubio A, Cameron DR, Pillai S, Moellering RC, Jr., Eliopoulos GM. 2012. Whole genome characterization of the mechanisms of daptomycin resistance in clinical and laboratory derived isolates of *Staphylococcus aureus*. PLoS One 7:e28316.

76. Hines KM, Waalkes A, Penewit K, Holmes EA, Salipante SJ, Werth BJ, Xu L. 2017. Characterization of the Mechanisms of Daptomycin Resistance among Gram-Positive Bacterial Pathogens by Multidimensional Lipidomics. mSphere 2.

77. Arias CA, Panesso D, McGrath DM, Qin X, Mojica MF, Miller C, Diaz L, Tran TT, Rincon S, Barbu EM, Reyes J, Roh JH, Lobos E, Sodergren E, Pasqualini R, Arap W, Quinn JP, Shamoo Y, Murray BE, Weinstock GM. 2011. Genetic basis for *in vivo* daptomycin resistance in enterococci. N Engl J Med 365:892-900.

78. Müller A, Wenzel M, Strahl H, Grein F, Saaki TNV, Kohl B, Siersma T, Bandow JE, Sahl H-G, Schneider T, Hamoen LW. 2016. Daptomycin inhibits cell envelope synthesis by interfering with fluid membrane microdomains. Proc Natl Acad Sci U S A 113:E7077-86.

79. Jiang J-H, Bhuiyan MS, Shen H-H, Cameron DR, Rupasinghe TWT, Wu C-M, Le Brun AP, Kostoulias X, Domene C, Fulcher AJ, McConville MJ, Howden BP, Lieschke GJ, Peleg AY. 2019. Antibiotic resistance and host immune evasion in *Staphylococcus aureus* mediated by a metabolic adaptation. Proc Natl Acad Sci U S A 116:3722-3727.

80. Zhang T, Muraih JK, Tishbi N, Herskowitz J, Victor RL, Silverman J, Uwumarenogie S, Taylor SD, Palmer M, Mintzer E. 2014. Cardiolipin prevents membrane translocation and permeabilization by daptomycin. J Biol Chem 289:11584-11591.

81. Koprivnjak T, Zhang D, Ernst CM, Peschel A, Nauseef WM, Weiss JP. 2011. Characterization of *Staphylococcus aureus* cardiolipin synthases 1 and 2 and their contribution to accumulation of cardiolipin in stationary phase and within phagocytes. J Bacteriol 193:4134-42.

82. Martin PK, Li T, Sun D, Biek DP, Schmid MB. 1999. Role in cell permeability of an essential two-component system in *Staphylococcus aureus*. J Bacteriol 181:3666-73.

83. Kuhn S, Slavetinsky CJ, Peschel A. 2015. Synthesis and function of phospholipids in *Staphylococcus aureus*. Int J Med Microbiol 305:196-202.

84. Pader V, Hakim S, Painter KL, Wigneshweraraj S, Clarke TB, Edwards AM. 2016. *Staphylococcus aureus* inactivates daptomycin by releasing membrane phospholipids. Nat Microbiol 2:16194.

85. Shen T, Hines KM, Ashford NK, Werth BJ, Xu L. 2021. Varied Contribution of Phospholipid Shedding From Membrane to Daptomycin Tolerance in *Staphylococcus aureus*. Front Mol Biosci 8:679949.

86. Kumar K, Chen J, Drlica K, Shopsin B. 2017. Tuning of the Lethal Response to Multiple Stressors with a Single-Site Mutation during Clinical Infection by *Staphylococcus aureus*. mBio 8.

87. Fowler VG, Jr., Sakoulas G, McIntyre LM, Meka VG, Arbeit RD, Cabell CH, Stryjewski ME, Eliopoulos GM, Reller LB, Corey GR, Jones T, Lucindo N, Yeaman MR, Bayer AS. 2004. Persistent bacteremia due to methicillin-resistant *Staphylococcus aureus* infection is associated with agr dysfunction and low-level in vitro resistance to thrombin-induced platelet microbicidal protein. J Infect Dis 190:1140-9.

88. Schweizer ML, Furuno JP, Sakoulas G, Johnson JK, Harris AD, Shardell MD, McGregor JC, Thom KA, Perencevich EN. 2011. Increased mortality with accessory gene regulator (*agr*) dysfunction in *Staphylococcus aureus* among bacteremic patients. Antimicrob Agents Chemother 55:1082-7.

89. Mwangi MM, Wu SW, Zhou Y, Sieradzki K, de Lencastre H, Richardson P, Bruce D, Rubin E, Myers E, Siggia ED, Tomasz A. 2007. Tracking the *in vivo* evolution of multidrug resistance in *Staphylococcus aureus* by whole-genome sequencing. Proc Natl Acad Sci U S A 104:9451-6.

90. Iwata Y, Satou K, Tsuzuku H, Furuichi K, Senda Y, Sakai-Takemori Y, Wada T, Fujita S, Miyake T, Yasuda H, Sakai N, Kitajima S, Toyama T, Shinozaki Y, Sagara A, Miyagawa T, Hara A, Shimizu M, Kamikawa Y, Kaneko S, Wada T. 2017. Down-regulation of the two-component system and cell-wall biosynthesis-related genes was associated with the reversion to daptomycin susceptibility in daptomycin non-susceptible methicillin-resistant *Staphylococcus aureus*. Eur J Clin Microbiol Infect Dis 36:1839-1845.

91. Haag AF, Bagnoli F. 2017. The Role of Two-Component Signal Transduction Systems in *Staphylococcus aureus* Virulence Regulation. Curr Top Microbiol Immunol 409:145-198.

92. Falord M, Mader U, Hiron A, Debarbouille M, Msadek T. 2011. Investigation of the *Staphylococcus aureus* GraSR regulon reveals novel links to virulence, stress response and cell wall signal transduction pathways. PLoS One 6:e21323.

93. Falord M, Karimova G, Hiron A, Msadek T. 2012. GraXSR proteins interact with the VraFG ABC transporter to form a five-component system required for cationic antimicrobial peptide sensing and resistance in *Staphylococcus aureus*. Antimicrob Agents Chemother 56:1047-58.

94. Meehl M, Herbert S, Gotz F, Cheung A. 2007. Interaction of the GraRS two-component system with the VraFG ABC transporter to support vancomycin-intermediate resistance in *Staphylococcus aureus*. Antimicrob Agents Chemother 51:2679-89.

95. Peschel A, Otto M, Jack RW, Kalbacher H, Jung G, Gotz F. 1999. Inactivation of the *dlt* operon in *Staphylococcus aureus* confers sensitivity to defensins, protegrins, and other antimicrobial peptides. J Biol Chem 274:8405-10.

96. Yang SJ, Kreiswirth BN, Sakoulas G, Yeaman MR, Xiong YQ, Sawa A, Bayer AS. 2009. Enhanced expression of *dltABCD* is associated with the development of daptomycin nonsusceptibility in a clinical endocarditis isolate of *Staphylococcus aureus*. J Infect Dis 200:1916-20.

97. Mishra NN, Bayer AS, Weidenmaier C, Grau T, Wanner S, Stefani S, Cafiso V, Bertuccio T, Yeaman MR, Nast CC, Yang SJ. 2014. Phenotypic and genotypic characterization of daptomycin-resistant methicillin-resistant *Staphylococcus aureus* strains: relative roles of *mprF* and *dlt* operons. PLoS One 9:e107426.

98. Bertsche U, Weidenmaier C, Kuehner D, Yang SJ, Baur S, Wanner S, Francois P, Schrenzel J, Yeaman MR, Bayer AS. 2011. Correlation of daptomycin resistance in a clinical *Staphylococcus aureus* strain with increased cell wall teichoic acid production and D-alanylation. Antimicrob Agents Chemother 55:3922-8.

99. Cafiso V, Bertuccio T, Purrello S, Campanile F, Mammina C, Sartor A, Raglio A, Stefani S. 2014. *dltA* overexpression: A strain-independent keystone of daptomycin resistance in methicillin-resistant *Staphylococcus aureus*. Int J Antimicrob Agents 43:26-31.

100. Howden BP, McEvoy CR, Allen DL, Chua K, Gao W, Harrison PF, Bell J, Coombs G, Bennett-Wood V, Porter JL, Robins-Browne R, Davies JK, Seemann T, Stinear TP. 2011. Evolution of multidrug resistance during *Staphylococcus aureus* infection involves mutation of the essential two component regulator *WalKR*. PLoS Pathog 7:e1002359.

101. Jiang JH, Dexter C, Cameron DR, Monk IR, Baines SL, Abbott IJ, Spelman DW, Kostoulias X, Nethercott C, Howden BP, Peleg AY. 2019. Evolution of Daptomycin Resistance in Coagulase-Negative Staphylococci Involves Mutations of the Essential Two-Component Regulator WalKR. Antimicrob Agents Chemother 63.

102. Delaune A, Dubrac S, Blanchet C, Poupel O, Mader U, Hiron A, Leduc A, Fitting C, Nicolas P, Cavaillon JM, Adib-Conquy M, Msadek T. 2012. The WalKR system controls major staphylococcal virulence genes and is involved in triggering the host inflammatory response. Infect Immun 80:3438-53.

103. Song Y, Rubio A, Jayaswal RK, Silverman JA, Wilkinson BJ. 2013. Additional routes to *Staphylococcus aureus* daptomycin resistance as revealed by comparative genome sequencing, transcriptional profiling, and phenotypic studies. PLoS One 8:e58469.

104. Mishra NN, McKinnell J, Yeaman MR, Rubio A, Nast CC, Chen L, Kreiswirth BN, Bayer AS. 2011. *In vitro* cross-resistance to daptomycin and host defense cationic antimicrobial peptides in clinical methicillin-resistant *Staphylococcus aureus* isolates. Antimicrob Agents Chemother 55:4012-8.

105. Patel D, Husain M, Vidaillac C, Steed ME, Rybak MJ, Seo SM, Kaatz GW. 2011. Mechanisms of *in-vitro*-selected daptomycin-non-susceptibility in *Staphylococcus aureus*. Int J Antimicrob Agents 38:442-6.

106. Cafiso V, Bertuccio T, Spina D, Purrello S, Campanile F, Di Pietro C, Purrello M, Stefani S. 2012. Modulating activity of vancomycin and daptomycin on the expression of autolysis cell-wall turnover and membrane charge genes in hVISA and VISA strains. PLoS One 7:e29573.

107. Belcheva A, Golemi-Kotra D. 2008. A close-up view of the VraSR two-component system. A mediator of *Staphylococcus aureus* response to cell wall damage. J Biol Chem 283:12354-64.

108. Kuroda M, Kuroda H, Oshima T, Takeuchi F, Mori H, Hiramatsu K. 2003. Two-component system VraSR positively modulates the regulation of cell-wall biosynthesis pathway in *Staphylococcus aureus*. Mol Microbiol 49:807-21.

109. Gardete S, Wu SW, Gill S, Tomasz A. 2006. Role of VraSR in antibiotic resistance and antibiotic-induced stress response in *Staphylococcus aureus*. Antimicrob Agents Chemother 50:3424-34.

110. Taglialegna A, Varela MC, Rosato RR, Rosato AE. 2019. VraSR and Virulence Trait Modulation during Daptomycin Resistance in Methicillin-Resistant *Staphylococcus aureus* Infection. mSphere 4.

111. Boyle-Vavra S, Yin S, Jo DS, Montgomery CP, Daum RS. 2013. VraT/YvqF is required for methicillin resistance and activation of the VraSR regulon in *Staphylococcus aureus*. Antimicrob Agents Chemother 57:83-95.

112. Du W, Brown JR, Sylvester DR, Huang J, Chalker AF, So CY, Holmes DJ, Payne DJ, Wallis NG. 2000. Two active forms of UDP-N-acetylglucosamine enolpyruvyl transferase in gram-positive bacteria. J Bacteriol 182:4146-52.

113. Kuroda M, Ohta T, Uchiyama I, Baba T, Yuzawa H, Kobayashi I, Cui L, Oguchi A, Aoki K, Nagai Y, Lian J, Ito T, Kanamori M, Matsumaru H, Maruyama A, Murakami H, Hosoyama A, Mizutani-Ui Y, Takahashi NK, Sawano T, Inoue R, Kaito C, Sekimizu K, Hirakawa H, Kuhara S, Goto S, Yabuzaki J, Kanehisa M, Yamashita A, Oshima K, Furuya K, Yoshino C, Shiba T, Hattori M, Ogasawara N, Hayashi H, Hiramatsu K. 2001. Whole genome sequencing of meticillin-resistant *Staphylococcus aureus*. Lancet 357:1225-40.

114. Blake KL, O'Neill AJ, Mengin-Lecreulx D, Henderson PJ, Bostock JM, Dunsmore CJ, Simmons KJ, Fishwick CW, Leeds JA, Chopra I. 2009. The nature of *Staphylococcus aureus* MurA and MurZ and approaches for detection of peptidoglycan biosynthesis inhibitors. Mol Microbiol 72:335-43.

115. Reed P, Veiga H, Jorge AM, Terrak M, Pinho MG. 2011. Monofunctional transglycosylases are not essential for *Staphylococcus aureus* cell wall synthesis. J Bacteriol 193:2549-56.

116. Capone A, Cafiso V, Campanile F, Parisi G, Mariani B, Petrosillo N, Stefani S. 2016. In vivo development of daptomycin resistance in vancomycin-susceptible methicillin-resistant Staphylococcus aureus severe infections previously treated with glycopeptides. Eur J Clin Microbiol Infect Dis 35:625-31.

117. Berti AD, Baines SL, Howden BP, Sakoulas G, Nizet V, Proctor RA, Rose WE. 2015. Heterogeneity of genetic pathways toward daptomycin nonsusceptibility in *Staphylococcus aureus* determined by adjunctive antibiotics. Antimicrob Agents Chemother 59:2799-806.

118. Cui L, Isii T, Fukuda M, Ochiai T, Neoh HM, Camargo IL, Watanabe Y, Shoji M, Hishinuma T, Hiramatsu K. 2010. An RpoB mutation confers dual heteroresistance to daptomycin and vancomycin in *Staphylococcus aureus*. Antimicrob Agents Chemother 54:5222-33.

119. Baek KT, Thogersen L, Mogenssen RG, Mellergaard M, Thomsen LE, Petersen A, Skov S, Cameron DR, Peleg AY, Frees D. 2015. Stepwise decrease in daptomycin susceptibility in clinical *Staphylococcus aureus* isolates associated with an initial mutation in *rpoB* and a compensatory inactivation of the *clpX* gene. Antimicrob Agents Chemother 59:6983-91.

120. Gao W, Cameron DR, Davies JK, Kostoulias X, Stepnell J, Tuck KL, Yeaman MR, Peleg AY, Stinear TP, Howden BP. 2013. The RpoB H(4)(8)(1)Y rifampicin resistance mutation and an active stringent response reduce virulence and increase resistance to innate immune responses in *Staphylococcus aureus*. J Infect Dis 207:929-39.

121. Guo Y, Wang B, Rao L, Wang X, Zhao H, Li M, Yu F. 2021. Molecular Characteristics of Rifampin-Sensitive and -Resistant Isolates and Characteristics of *rpoB* Gene Mutations in Methicillin-Resistant *Staphylococcus aureus*. Infect Drug Resist 14:4591-4600.

122. Steed ME, Vidaillac C, Rybak MJ. 2010. Novel daptomycin combinations against daptomycin-nonsusceptible methicillin-resistant *Staphylococcus aureus* in an *in vitro* model of simulated endocardial vegetations. Antimicrob Agents Chemother 54:5187-92.

123. Dhand A, Sakoulas G. 2014. Daptomycin in combination with other antibiotics for the treatment of complicated methicillin-resistant *Staphylococcus aureus* bacteremia. Clin Ther 36:1303-16.

124. Berti AD, Wergin JE, Girdaukas GG, Hetzel SJ, Sakoulas G, Rose WE. 2012. Altering the Proclivity towards Daptomycin Resistance in Methicillin-Resistant *Staphylococcus aureus* Using Combination with Other Antibiotics. Antimicrob Agents Chemother 56:5046-5053.

125. Mehta S, Singh C, Plata KB, Chanda PK, Paul A, Riosa S, Rosato RR, Rosato AE. 2012. β- Lactams Increase the Antibacterial Activity of Daptomycin against Clinical Methicillin-Resistant *Staphylococcus aureus* Strains and Prevent Selection of Daptomycin- Resistant Derivatives. Antimicrob Agents Chemother 56:6192-6200.

126. Jorgensen SCJ, Zasowski EJ, Trinh TD, Lagnf AM, Bhatia S, Sabagha N, Abdul-Mutakabbir JC, Alosaimy S, Mynatt RP, Davis SL, Rybak MJ. 2020. Daptomycin Plus β-Lactam Combination Therapy for Methicillin-resistant *Staphylococcus aureus* Bloodstream Infections: A Retrospective, Comparative Cohort Study. Clin Infect Dis 71:1-10.

127. Rand KH, Houck HJ. 2004. Synergy of daptomycin with oxacillin and other β-lactams against methicillin-resistant *Staphylococcus aureus*. Antimicrob Agents Chemother 48:2871-5.

128. Rose WE, Schulz LT, Andes D, Striker R, Berti AD, Hutson PR, Shukla SK. 2012. Addition of Ceftaroline to Daptomycin after Emergence of Daptomycin-Nonsusceptible *Staphylococcus aureus* during Therapy Improves Antibacterial Activity. Antimicrob Agents Chemother 56:5296-5302.

129. Shafiq I, Bulman ZP, Spitznogle SL, Osorio JE, Reilly IS, Lesse AJ, Parameswaran GI, Mergenhagen KA, Tsuji BT. 2017. A combination of ceftaroline and daptomycin has synergistic and bactericidal activity in vitro against daptomycin nonsusceptible methicillin-resistant *Staphylococcus aureus* (MRSA). Infect Dis (Lond) 49:410-416.

130. Lee YC, Chen PY, Wang JT, Chang SC. 2019. A study on combination of daptomycin with selected antimicrobial agents: in vitro synergistic effect of MIC value of 1 mg/L against MRSA strains. BMC Pharmacol Toxicol 20:25.

131. Eliazar J, Johnson T, Chbib C. 2021. Pre-clinical Impact of the Synergistic Mechanism of Daptomycin and Ceftaroline on Patients with Methicillin-resistant *Staphylococcus aureus* Bacteremia Infections. Curr Rev Clin Exp Pharmacol 16:296-299.

132. Yang SJ, Xiong YQ, Boyle-Vavra S, Daum R, Jones T, Bayer AS. 2010. Daptomycin-oxacillin combinations in treatment of experimental endocarditis caused by daptomycin-nonsusceptible strains of methicillin-resistant *Staphylococcus aureus* with evolving oxacillin susceptibility (the "seesaw effect"). Antimicrob Agents Chemother 54:3161-9.

133. Renzoni A, Kelley WL, Rosato RR, Martinez MP, Roch M, Fatouraei M, Haeusser DP, Margolin W, Fenn S, Turner RD, Foster SJ, Rosato AE. 2017. Molecular Bases Determining Daptomycin Resistance-Mediated Resensitization to β-Lactams (Seesaw Effect) in Methicillin-Resistant *Staphylococcus aureus*. Antimicrob Agents Chemother 61:e01634-16.

134. Jiang S, Zhuang H, Zhu F, Wei X, Zhang J, Sun L, Ji S, Wang H, Wu D, Zhao F, Yan R, Yu Y, Chen Y. 2022. The Role of *mprF* Mutations in Seesaw Effect of Daptomycin-Resistant Methicillin-Resistant *Staphylococcus aureus* Isolates. Antimicrob Agents Chemother 66:e0129521.

135. Jousselin A, Manzano C, Biette A, Reed P, Pinho MG, Rosato AE, Kelley WL, Renzoni A. 2015. The *Staphylococcus aureus* Chaperone PrsA Is a New Auxiliary Factor of Oxacillin Resistance Affecting Penicillin-Binding Protein 2A. Antimicrob Agents Chemother 60:1656-66.

136. Roch M, Lelong E, Panasenko OO, Sierra R, Renzoni A, Kelley WL. 2019. Thermosensitive PBP2a requires extracellular folding factors PrsA and HtrA1 for *Staphylococcus aureus* MRSA β-lactam resistance. Commun Biol 2:417.

137. de Carvalho C, Taglialegna A, Rosato AE. 2021. Impact of PrsA on membrane lipid composition during daptomycin-resistance-mediated β-lactam sensitization in clinical MRSA strains. J Antimicrob Chemother 77:135-147.

138. Jousselin A, Renzoni A, Andrey DO, Monod A, Lew DP, Kelley WL. 2012. The posttranslocational chaperone lipoprotein PrsA is involved in both glycopeptide and oxacillin resistance in *Staphylococcus aureus*. Antimicrob Agents Chemother 56:3629-40.

139. Drummelsmith J, Winstall E, Bergeron MG, Poirier GG, Ouellette M. 2007. Comparative proteomics analyses reveal a potential biomarker for the detection of vancomycin-intermediate *Staphylococcus aureus* strains. J Proteome Res 6:4690-702.

140. Kuroda M, Kuwahara-Arai K, Hiramatsu K. 2000. Identification of the up- and down-regulated genes in vancomycin-resistant *Staphylococcus aureus* strains Mu3 and Mu50 by cDNA differential hybridization method. Biochem Biophys Res Commun 269:485-90.

141. McCallum N, Spehar G, Bischoff M, Berger-Bachi B. 2006. Strain dependence of the cell wall-damage induced stimulon in *Staphylococcus aureus*. Biochim Biophys Acta 1760:1475-81.

142. Sankaran K, Wu HC. 1994. Lipid modification of bacterial prolipoprotein. Transfer of diacylglyceryl moiety from phosphatidylglycerol. J Biol Chem 269:19701-6.

143. Stoll H, Dengjel J, Nerz C, Gotz F. 2005. *Staphylococcus aureus* deficient in lipidation of prelipoproteins is attenuated in growth and immune activation. Infect Immun 73:2411-23.

144. Sievers S, Ernst CM, Geiger T, Hecker M, Wolz C, Becher D, Peschel A. 2010. Changing the phospholipid composition of *Staphylococcus aureus* causes distinct changes in membrane proteome and membrane-sensory regulators. Proteomics 10:1685-93.

145. McCreary EK, Kullar R, Geriak M, Zasowski EJ, Rizvi K, Schulz LT, Ouellette K, Vasina L, Haddad F, Rybak MJ, Zervos MJ, Sakoulas G, Rose WE. 2020. Multicenter Cohort of Patients With

Methicillin-Resistant S*taphylococcus aureus* Bacteremia Receiving Daptomycin Plus Ceftaroline Compared With Other MRSA Treatments. Open Forum Infect Dis 7:ofz538.

146. Hornak JP, Anjum S, Reynoso D. 2019. Adjunctive ceftaroline in combination with daptomycin or vancomycin for complicated methicillin-resistant *Staphylococcus aureus* bacteremia after monotherapy failure. Ther Adv Infect Dis 6:2049936119886504.
147. Alosaimy S, Sabagha NL, Lagnf AM, Zasowski EJ, Morrisette T, Jorgensen SCJ, Trinh TD, Mynatt RP, Rybak MJ. 2020. Monotherapy with Vancomycin or Daptomycin versus Combination Therapy with β-Lactams in the Treatment of Methicillin-Resistant *Staphylococcus aureus* Bloodstream Infections: A Retrospective Cohort Analysis. Infect Dis Ther 9:325-339.
148. Geriak M, Haddad F, Rizvi K, Rose W, Kullar R, LaPlante K, Yu M, Vasina L, Ouellette K, Zervos M, Nizet V, Sakoulas G. 2019. Clinical Data on Daptomycin plus Ceftaroline versus Standard of Care Monotherapy in the Treatment of Methicillin-Resistant *Staphylococcus aureus* Bacteremia. Antimicrob Agents Chemother 63.
149. Credito K, Lin G, Appelbaum PC. 2007. Activity of daptomycin alone and in combination with rifampin and gentamicin against *Staphylococcus aureus* assessed by time-kill methodology. Antimicrob Agents Chemother 51:1504-7.
150. Snydman DR, McDermott LA, Jacobus NV. 2005. Evaluation of in vitro interaction of daptomycin with gentamicin or β-lactam antibiotics against *Staphylococcus aureus* and Enterococci by FIC index and timed-kill curves. J Chemother 17:614-21.
151. Nadrah K, Strle F. 2011. Antibiotic Combinations with Daptomycin for Treatment of *Staphylococcus aureus* Infections. Chemother Res Pract 2011:619321.
152. Dhand A, Bayer AS, Pogliano J, Yang SJ, Bolaris M, Nizet V, Wang G, Sakoulas G. 2011. Use of antistaphylococcal β-lactams to increase daptomycin activity in eradicating persistent bacteremia due to methicillin-resistant *Staphylococcus aureus*: role of enhanced daptomycin binding. Clin Infect Dis 53:158-63.
153. Werth BJ, Sakoulas G, Rose WE, Pogliano J, Tewhey R, Rybak MJ. 2013. Ceftaroline increases membrane binding and enhances the activity of daptomycin against daptomycin-nonsusceptible vancomycin-intermediate *Staphylococcus aureus* in a pharmacokinetic/pharmacodynamic model. Antimicrob Agents Chemother 57:66-73.
154. Berti AD, Theisen E, Sauer J-D, Nonejuie P, Olson J, Pogliano J, Sakoulas G, Nizet V, Proctor RA, Rose WE. 2015. Penicillin Binding Protein 1 Is Important in the Compensatory Response of

Staphylococcus aureus to Daptomycin-Induced Membrane Damage and Is a Potential Target for β-Lactam-Daptomycin Synergy. Antimicrob Agents Chemother 60:451-458.

155. Ono D, Yamaguchi T, Hamada M, Sonoda S, Sato A, Aoki K, Kajiwara C, Kimura S, Fujisaki M, Tojo H, Sasaki M, Murakami H, Kato K, Ishii Y, Tateda K. 2019. Analysis of synergy between β-lactams and anti-methicillin-resistant *Staphylococcus aureus* agents from the standpoint of strain characteristics and binding action. J Infect Chemother 25:273-280.
156. Kale-Pradhan PB, Giuliano C, Jongekrijg A, Rybak MJ. 2020. Combination of Vancomycin or Daptomycin and β-lactam Antibiotics: A Meta-analysis. Pharmacotherapy 40:648-658.
157. Kocaoglu O, Carlson EE. 2015. Profiling of β-lactam selectivity for penicillin-binding proteins in *Escherichia coli* strain DC2. Antimicrob Agents Chemother 59:2785-90.
158. Curtis NA, Orr D, Ross GW, Boulton MG. 1979. Affinities of penicillins and cephalosporins for the penicillin-binding proteins of *Escherichia coli* K-12 and their antibacterial activity. Antimicrob Agents Chemother 16:533-9.
159. Williamson R, Hakenbeck R, Tomasz A. 1980. *In vivo* interaction of β-lactam antibiotics with the penicillin-binding proteins of *Streptococcus pneumoniae*. Antimicrob Agents Chemother 18:629-37.
160. Tonin E, Tomasz A. 1986. β-lactam-specific resistant mutants of *Staphylococcus aureus*. Antimicrob Agents Chemother 30:577-83.
161. Berti AD, Sakoulas G, Nizet V, Tewhey R, Rose WE. 2013. β-Lactam antibiotics targeting PBP1 selectively enhance daptomycin activity against methicillin-resistant *Staphylococcus aureus*. Antimicrob Agents Chemother 57:5005-12.
162. Sakoulas G, Okumura CY, Thienphrapa W, Olson J, Nonejuie P, Dam Q, Dhand A, Pogliano J, Yeaman MR, Hensler ME, Bayer AS, Nizet V. 2014. Nafcillin enhances innate immune-mediated killing of methicillin-resistant *Staphylococcus aureus*. J Mol Med (Berl) 92:139-49.
163. Le J, Dam Q, Schweizer M, Thienphrapa W, Nizet V, Sakoulas G. 2016. Effects of vancomycin versus nafcillin in enhancing killing of methicillin-susceptible *Staphylococcus aureus* causing bacteremia by human cathelicidin LL-37. Eur J Clin Microbiol Infect Dis 35:1441-7.
164. Ersoy SC, Abdelhady W, Li L, Chambers HF, Xiong YQ, Bayer AS. 2019. Bicarbonate Resensitization of Methicillin-Resistant *Staphylococcus aureus* to β-Lactam Antibiotics. Antimicrob Agents Chemother 63.

165. Simonetti O, Cirioni O, Goteri G, Lucarini G, Kamysz E, Kamysz W, Orlando F, Rizzetto G, Molinelli E, Morroni G, Ghiselli R, Provinciali M, Giacometti A, Offidani A. 2021. Efficacy of Cathelicidin LL-37 in an MRSA Wound Infection Mouse Model. Antibiotics (Basel) 10.

166. Hou M, Zhang N, Yang J, Meng X, Yang R, Li J, Sun T. 2013. Antimicrobial peptide LL-37 and IDR-1 ameliorate MRSA pneumonia in vivo. Cell Physiol Biochem 32:614-23.

167. Ciandrini E, Morroni G, Arzeni D, Kamysz W, Neubauer D, Kamysz E, Cirioni O, Brescini L, Baffone W, Campana R. 2018. Antimicrobial Activity of Different Antimicrobial Peptides (AMPs) Against Clinical Methicillin-resistant *Staphylococcus aureu*s (MRSA). Curr Top Med Chem 18:2116-2126.

168. Barber KE, Werth BJ, Rybak MJ. 2015. The combination of ceftaroline plus daptomycin allows for therapeutic de-escalation and daptomycin sparing against MRSA. J Antimicrob Chemother 70:505-9.

169. Entenza JM, Giddey M, Vouillamoz J, Moreillon P. 2010. *In vitro* prevention of the emergence of daptomycin resistance in *Staphylococcus aureus* and enterococci following combination with amoxicillin/clavulanic acid or ampicillin. Int J Antimicrob Agents 35:451-6.

170. Gould IM, Miro JM, Rybak MJ. 2013. Daptomycin: the role of high-dose and combination therapy for Gram-positive infections. Int J Antimicrob Agents 42:202-10.

171. Johnson TM, Molina KC, Miller MA, Kiser TH, Huang M, Mueller SW. 2021. Combination ceftaroline and daptomycin salvage therapy for complicated methicillin-resistant *Staphylococcus aureus* bacteraemia compared with standard of care. Int J Antimicrob Agents 57:106310.

172. Wang C, Ye C, Liao L, Wang Z, Hu Y, Deng C, Liu L. 2020. Adjuvant β-Lactam Therapy Combined with Vancomycin or Daptomycin for Methicillin-Resistant *Staphylococcus aureus* Bacteremia: a Systematic Review and Meta-analysis. Antimicrob Agents Chemother 64.

173. Bartash R, Nori P. 2017. β-lactam combination therapy for the treatment of *Staphylococcus aureus* and *Enterococcus* species bacteremia: A summary and appraisal of the evidence. Int J Infect Dis 63:7-12.

174. Foster TJ. 2019. Can beta-Lactam Antibiotics Be Resurrected to Combat MRSA? Trends Microbiol 27:26-38.

175. Liu C, Bayer A, Cosgrove SE, Daum RS, Fridkin SK, Gorwitz RJ, Kaplan SL, Karchmer AW, Levine DP, Murray BE, M JR, Talan DA, Chambers HF, Infectious Diseases Society of A. 2011. Clinical practice guidelines by the infectious diseases society of america for the treatment of methicillin-resistant Staphylococcus aureus infections in adults and children. Clin Infect Dis 52:e18-55.

176. Rodvold KA, McConeghy KW. 2014. Methicillin-resistant Staphylococcus aureus therapy: past, present, and future. Clin Infect Dis 58 Suppl 1:S20-7.

177. Chan LC, Basuino L, Dip EC, Chambers HF. 2015. Comparative efficacies of tedizolid phosphate, vancomycin, and daptomycin in a rabbit model of methicillin-resistant *Staphylococcus aureus* endocarditis. Antimicrob Agents Chemother 59:3252-6.

178. Roberts KD, Sulaiman RM, Rybak MJ. 2015. Dalbavancin and Oritavancin: An Innovative Approach to the Treatment of Gram-Positive Infections. Pharmacotherapy 35:935-48.

179. Guskey MT, Tsuji BT. 2010. A comparative review of the lipoglycopeptides: oritavancin, dalbavancin, and telavancin. Pharmacotherapy 30:80-94.

180. Bayer AS, Mishra NN, Cheung AL, Rubio A, Yang SJ. 2016. Dysregulation of mprF and dltABCD expression among daptomycin-non-susceptible MRSA clinical isolates. J Antimicrob Chemother 71:2100-4.

181. Yang SJ, Mishra NN, Kang KM, Lee GY, Park JH, Bayer AS. 2018. Impact of Multiple Single-Nucleotide Polymorphisms Within *mprF* on Daptomycin Resistance in *Staphylococcus aureus*. Microb Drug Resist 24:1075-1081.

182. Mishra NN, Liu GY, Yeaman MR, Nast CC, Proctor RA, McKinnell J, Bayer AS. 2011. Carotenoid-related alteration of cell membrane fluidity impacts *Staphylococcus aureus* susceptibility to host defense peptides. Antimicrob Agents Chemother 55:526-31.

183. Mishra NN, Rubio A, Nast CC, Bayer AS. 2012. Differential Adaptations of Methicillin-Resistant *Staphylococcus aureus* to Serial *In Vitro* Passage in Daptomycin: Evolution of Daptomycin Resistance and Role of Membrane Carotenoid Content and Fluidity. Int J Microbiol 2012:683450.

184. Vignaroli C, Rinaldi C, Varaldo PE. 2011. Striking "seesaw effect" between daptomycin nonsusceptibility and beta-lactam susceptibility in Staphylococcus haemolyticus. Antimicrob Agents Chemother 55:2495-6; author reply 296-7.

185. Ortwine JK, Werth BJ, Sakoulas G, Rybak MJ. 2013. Reduced glycopeptide and lipopeptide susceptibility in *Staphylococcus aureus* and the "seesaw effect": Taking advantage of the back door left open? Drug Resist Updat 16:73-9.

186. Patel JB, Jevitt LA, Hageman J, McDonald LC, Tenover FC. 2006. An association between reduced susceptibility to daptomycin and reduced susceptibility to vancomycin in *Staphylococcus aureus*. Clin Infect Dis 42:1652-3.

187. Fischer A, Yang SJ, Bayer AS, Vaezzadeh AR, Herzig S, Stenz L, Girard M, Sakoulas G, Scherl A, Yeaman MR, Proctor RA, Schrenzel J, Francois P. 2011. Daptomycin resistance mechanisms in

clinically derived *Staphylococcus aureus* strains assessed by a combined transcriptomics and proteomics approach. J Antimicrob Chemother 66:1696-711.

188. Renzoni A, Kelley WL, Rosato RR, Martinez MP, Roch M, Fatouraei M, Haeusser DP, Margolin W, Fenn S, Turner RD, Foster SJ, Rosato AE. 2017. Molecular Bases Determining Daptomycin Resistance-Mediated Resensitization to β-Lactams (Seesaw Effect) in Methicillin-Resistant *Staphylococcus aureus*. Antimicrob Agents Chemother 61.
189. Jenson RE, Baines SL, Howden BP, Mishra NN, Farah S, Lew C, Berti AD, Shukla SK, Bayer AS, Rose WE. 2020. Prolonged Exposure to β-Lactam Antibiotics Reestablishes Susceptibility of Daptomycin-Nonsusceptible *Staphylococcus aureus* to Daptomycin. Antimicrob Agents Chemother 64:e00890-20.
190. Pereira SF, Henriques AO, Pinho MG, de Lencastre H, Tomasz A. 2009. Evidence for a dual role of PBP1 in the cell division and cell separation of Staphylococcus aureus. Mol Microbiol 72:895-904.
191. Cingolani P, Platts A, Wang le L, Coon M, Nguyen T, Wang L, Land SJ, Lu X, Ruden DM. 2012. A program for annotating and predicting the effects of single nucleotide polymorphisms, SnpEff: SNPs in the genome of Drosophila melanogaster strain w1118; iso-2; iso-3. Fly (Austin) 6:80-92.
192. Monk IR, Stinear TP. 2021. From cloning to mutant in 5 days: rapid allelic exchange in *Staphylococcus aureus*. Access Microbiol 3:000193.
193. Zhang Y, Werling U, Edelmann W. 2012. SLiCE: a novel bacterial cell extract-based DNA cloning method. Nucleic Acids Res 40:e55.
194. Monk IR, Tree JJ, Howden BP, Stinear TP, Foster TJ. 2015. Complete Bypass of Restriction Systems for Major *Staphylococcus aureus* Lineages. mBio 6:e00308-15.
195. Mishra NN, Bayer AS, Moise PA, Yeaman MR, Sakoulas G. 2012. Reduced susceptibility to host-defense cationic peptides and daptomycin coemerge in methicillin-resistant *Staphylococcus aureus* from daptomycin-naive bacteremic patients. J Infect Dis 206:1160-7.
196. Mishra NN, Bayer AS. 2013. Correlation of cell membrane lipid profiles with daptomycin resistance in methicillin-resistant *Staphylococcus aureus*. Antimicrob Agents Chemother 57:1082-5.
197. Kim S-H, Kim K-H, Kim H-B, Kim N-J, Kim E-C, Oh M-d, Choe K-W. 2008. Outcome of Vancomycin Treatment in Patients with Methicillin-Susceptible *Staphylococcus aureus* Bacteremia. Antimicrob Agents Chemother 52:192.

198. Zheng X, Berti AD, McCrone S, Roch M, Rosato AE, Rose WE, Chen B. 2018. Combination Antibiotic Exposure Selectively Alters the Development of Vancomycin Intermediate Resistance in *Staphylococcus aureus*. Antimicrob Agents Chemother 62.

199. Berti AD, Wergin JE, Girdaukas GG, Hetzel SJ, Sakoulas G, Rose WE. 2012. Altering the proclivity towards daptomycin resistance in methicillin-resistant *Staphylococcus aureus* using combinations with other antibiotics. Antimicrob Agents Chemother 56:5046-53.

200. Mehta S, Singh C, Plata KB, Chanda PK, Paul A, Riosa S, Rosato RR, Rosato AE. 2012. β-Lactams increase the antibacterial activity of daptomycin against clinical methicillin-resistant *Staphylococcus aureus* strains and prevent selection of daptomycin-resistant derivatives. Antimicrob Agents Chemother 56:6192-200.

201. Kosowska-Shick K, McGhee PL, Appelbaum PC. 2010. Affinity of ceftaroline and other β-lactams for penicillin-binding proteins from *Staphylococcus aureus* and *Streptococcus pneumoniae*. Antimicrob Agents Chemother 54:1670-7.

202. Howden BP, Johnson PD, Ward PB, Stinear TP, Davies JK. 2006. Isolates with low-level vancomycin resistance associated with persistent methicillin-resistant Staphylococcus aureus bacteremia. Antimicrob Agents Chemother 50:3039-47.

203. Cui L, Ma X, Sato K, Okuma K, Tenover FC, Mamizuka EM, Gemmell CG, Kim MN, Ploy MC, El-Solh N, Ferraz V, Hiramatsu K. 2003. Cell wall thickening is a common feature of vancomycin resistance in Staphylococcus aureus. J Clin Microbiol 41:5-14.

204. Cui L, Neoh HM, Shoji M, Hiramatsu K. 2009. Contribution of vraSR and graSR point mutations to vancomycin resistance in vancomycin-intermediate Staphylococcus aureus. Antimicrob Agents Chemother 53:1231-4.

205. Cui L, Tominaga E, Neoh HM, Hiramatsu K. 2006. Correlation between Reduced Daptomycin Susceptibility and Vancomycin Resistance in Vancomycin-Intermediate Staphylococcus aureus. Antimicrob Agents Chemother 50:1079-82.

206. Rose WE, Schulz LT, Andes D, Striker R, Berti AD, Hutson PR, Shukla SK. 2012. Addition of ceftaroline to daptomycin after emergence of daptomycin-nonsusceptible *Staphylococcus aureus* during therapy improves antibacterial activity. Antimicrob Agents Chemother 56:5296-302.

207. Gaupp R, Lei S, Reed JM, Peisker H, Boyle-Vavra S, Bayer AS, Bischoff M, Herrmann M, Daum RS, Powers R, Somerville GA. 2015. *Staphylococcus aureus* metabolic adaptations during the

transition from a daptomycin susceptibility phenotype to a daptomycin nonsusceptibility phenotype. Antimicrob Agents Chemother 59:4226-38.

208. Turner NA, Sharma-Kuinkel BK, Maskarinec SA, Eichenberger EM, Shah PP, Carugati M, Holland TL, Fowler VG, Jr. 2019. Methicillin-resistant *Staphylococcus aureus*: an overview of basic and clinical research. Nat Rev Microbiol 17:203-218.
209. Miller WR, Bayer AS, Arias CA. 2016. Mechanism of Action and Resistance to Daptomycin in *Staphylococcus aureus* and Enterococci. Cold Spring Harb Perspect Med 6:a026997.
210. Heidary M, Khosravi AD, Khoshnood S, Nasiri MJ, Soleimani S, Goudarzi M. 2018. Daptomycin. J Antimicrob Chemother 73:1-11.
211. Straus SK, Hancock RE. 2006. Mode of action of the new antibiotic for Gram-positive pathogens daptomycin: comparison with cationic antimicrobial peptides and lipopeptides. Biochim Biophys Acta 1758:1215-23.
212. Scott WR, Baek SB, Jung D, Hancock RE, Straus SK. 2007. NMR structural studies of the antibiotic lipopeptide daptomycin in DHPC micelles. Biochim Biophys Acta 1768:3116-26.
213. Muraih JK, Pearson A, Silverman J, Palmer M. 2011. Oligomerization of daptomycin on membranes. Biochim Biophys Acta Biomembr 1808:1154-1160.
214. Muthaiyan A, Silverman JA, Jayaswal RK, Wilkinson BJ. 2008. Transcriptional profiling reveals that daptomycin induces the *Staphylococcus aureus* cell wall stress stimulon and genes responsive to membrane depolarization. Antimicrob Agents Chemother 52:980-90.
215. Tsai M, Ohniwa RL, Kato Y, Takeshita SL, Ohta T, Saito S, Hayashi H, Morikawa K. 2011. *Staphylococcus aureus* requires cardiolipin for survival under conditions of high salinity. BMC Microbiol 11.
216. Schlame M. 2008. Cardiolipin synthesis for the assembly of bacterial and mitochondrial membranes. J Lipid Res 49:1607-20.
217. Horvath SE, Daum G. 2013. Lipids of mitochondria. Prog Lipid Res 52:590-614.
218. Rand KH, Houck HJ. 2004. Synergy of Daptomycin with Oxacillin and Other β-Lactams against Methicillin-Resistant *Staphylococcus aureus*. Antimicrob Agents Chemother 48:2871-2875.
219. Berti A, Rose W, Nizet V, Sakoulas G. 2020. Antibiotics and Innate Immunity: A Cooperative Effort Toward the Successful Treatment of Infections. Open Forum Infect Dis 7:ofaa302.
220. Dvorchik BH, Brazier D, DeBruin MF, Arbeit RD. 2003. Daptomycin pharmacokinetics and safety following administration of escalating doses once daily to healthy subjects. Antimicrob Agents Chemother 47:1318-23.

221. Rose WE, Knier RM, Hutson PR. 2010. Pharmacodynamic effect of clinical vancomycin exposures on cell wall thickness in heterogeneous vancomycin-intermediate *Staphylococcus aureus*. J Antimicrob Chemother 65:2149-54.

222. Szklarczyk D, Gable AL, Nastou KC, Lyon D, Kirsch R, Pyysalo S, Doncheva NT, Legeay M, Fang T, Bork P, Jensen LJ, von Mering C. 2021. The STRING database in 2021: customizable protein-protein networks, and functional characterization of user-uploaded gene/measurement sets. Nucleic Acids Res 49:D605-D612.

223. Ernst CM, Peschel A. 2019. MprF-mediated daptomycin resistance. Int J Med Microbiol 309:359-363.

224. Lu D, Wormann ME, Zhang X, Schneewind O, Grundling A, Freemont PS. 2009. Structure-based mechanism of lipoteichoic acid synthesis by *Staphylococcus aureus* LtaS. Proc Natl Acad Sci U S A 106:1584-9.

225. Xia G, Kohler T, Peschel A. 2010. The wall teichoic acid and lipoteichoic acid polymers of *Staphylococcus aureus*. Int J Med Microbiol 300:148-54.

226. Koprivnjak T, Mlakar V, Swanson L, Fournier B, Peschel A, Weiss JP. 2006. Cation-induced transcriptional regulation of the *dlt* operon of *Staphylococcus aureus*. J Bacteriol 188:3622-30.

227. Gao J, Stewart GC. 2004. Regulatory elements of the *Staphylococcus aureus* protein A (Spa) promoter. J Bacteriol 186:3738-48.

228. Bischoff M, Dunman P, Kormanec J, Macapagal D, Murphy E, Mounts W, Berger-Bachi B, Projan S. 2004. Microarray-based analysis of the *Staphylococcus aureus* sigmaB regulon. J Bacteriol 186:4085-99.

229. Vestergaard M, Leng B, Haaber J, Bojer MS, Vegge CS, Ingmer H. 2016. Genome-Wide Identification of Antimicrobial Intrinsic Resistance Determinants in *Staphylococcus aureus*. Front Microbiol 7:2018.

230. Vestergaard M, Nohr-Meldgaard K, Bojer MS, Krogsgard Nielsen C, Meyer RL, Slavetinsky C, Peschel A, Ingmer H. 2017. Inhibition of the ATP Synthase Eliminates the Intrinsic Resistance of *Staphylococcus aureus* towards Polymyxins. mBio 8.

231. Akhova AV, Tkachenko AG. 2014. ATP/ADP alteration as a sign of the oxidative stress development in *Escherichia coli* cells under antibiotic treatment. FEMS Microbiol Lett 353:69-76.

232. Dubrac S, Bisicchia P, Devine KM, Msadek T. 2008. A matter of life and death: cell wall homeostasis and the WalKR (YycGF) essential signal transduction pathway. Mol Microbiol 70:1307-22.

233. Gajdiss M, Monk IR, Bertsche U, Kienemund J, Funk T, Dietrich A, Hort M, Sib E, Stinear TP, Bierbaum G. 2020. YycH and YycI Regulate Expression of *Staphylococcus aureus* Autolysins by Activation of WalRK Phosphorylation. Microorganisms 8.

234. Alves FCB, Albano M, Andrade B, Chechi JL, Pereira AFM, Furlanetto A, Rall VLM, Fernandes AAH, Dos Santos LD, Barbosa LN, Fernandes Junior A. 2020. Comparative Proteomics of Methicillin-Resistant *Staphylococcus aureus* Subjected to Synergistic Effects of the Lantibiotic Nisin and Oxacillin. Microb Drug Resist 26:179-189.

235. Fischer M, Bacher A. 2005. Biosynthesis of flavocoenzymes. Nat Prod Rep 22:324-50.

236. Blake KL, O'Neill AJ. 2013. Transposon library screening for identification of genetic loci participating in intrinsic susceptibility and acquired resistance to antistaphylococcal agents. J Antimicrob Chemother 68:12-6.

237. Foster SJ. 1995. Molecular characterization and functional analysis of the major autolysin of *Staphylococcus aureus* 8325/4. J Bacteriol 177:5723-5.

238. Trotonda MP, Xiong YQ, Memmi G, Bayer AS, Cheung AL. 2009. Role of mgrA and sarA in methicillin-resistant Staphylococcus aureus autolysis and resistance to cell wall-active antibiotics. J Infect Dis 199:209-18.

239. Singh VK, Carlos MR, Singh K. 2010. Physiological significance of the peptidoglycan hydrolase, LytM, in *Staphylococcus aureus*. FEMS Microbiol Lett 311:167-75.

240. Ramadurai L, Jayaswal RK. 1997. Molecular cloning, sequencing, and expression of *lytM*, a unique autolytic gene of *Staphylococcus aureus*. J Bacteriol 179:3625-31.

241. Allen NE, Hobbs JN, Alborn WE, Jr. 1987. Inhibition of peptidoglycan biosynthesis in gram-positive bacteria by LY146032. Antimicrob Agents Chemother 31:1093-9.

242. Utaida S, Dunman PM, Macapagal D, Murphy E, Projan SJ, Singh VK, Jayaswal RK, Wilkinson BJ. 2003. Genome-wide transcriptional profiling of the response of *Staphylococcus aureus* to cell-wall-active antibiotics reveals a cell-wall-stress stimulon. Microbiology (Reading) 149:2719-2732.

243. Sakoulas G, Moise PA, Casapao AM, Nonejuie P, Olson J, Okumura CY, Rybak MJ, Kullar R, Dhand A, Rose WE, Goff DA, Bressler AM, Lee Y, Pogliano J, Johns S, Kaatz GW, Ebright JR, Nizet V. 2014. Antimicrobial salvage therapy for persistent staphylococcal bacteremia using daptomycin plus ceftaroline. Clin Ther 36:1317-33.

244. Rose WE, Fallon M, Moran JJM, Vanderloo JP. 2012. Vancomycin Tolerance in Methicillin-Resistant *Staphylococcus aureus* Influence of Vancomycin, Daptomycin, and Telavancin on Differential Resistance Gene Expression. Antimicrob Agents Chemother 56:4422-27.

245. Tran TT, Panesso D, Mishra NN, Mileykovskaya E, Guan Z, Munita JM, Reyes J, Diaz L, Weinstock GM, Murray BE, Shamoo Y, Dowhan W, Bayer AS, Arias CA. 2013. Daptomycin-resistant Enterococcus faecalis diverts the antibiotic molecule from the division septum and remodels cell membrane phospholipids. mBio 4:e00281-13.

246. Pillai SK, Gold HS, Sakoulas G, Wennersten C, Moellering RC, Jr., Eliopoulos GM. 2007. Daptomycin nonsusceptibility in *Staphylococcus aureus* with reduced vancomycin susceptibility is independent of alterations in MprF. Antimicrob Agents Chemother 51:2223-5.

247. Boudjemaa R, Cabriel C, Dubois-Brissonnet F, Bourg N, Dupuis G, Gruss A, Leveque-Fort S, Briandet R, Fontaine-Aupart MP, Steenkeste K. 2018. Impact of Bacterial Membrane Fatty Acid Composition on the Failure of Daptomycin To Kill *Staphylococcus aureus*. Antimicrob Agents Chemother 62.

248. Jiang JH, Bhuiyan MS, Shen HH, Cameron DR, Rupasinghe TWT, Wu CM, Le Brun AP, Kostoulias X, Domene C, Fulcher AJ, McConville MJ, Howden BP, Lieschke GJ, Peleg AY. 2019. Antibiotic resistance and host immune evasion in *Staphylococcus aureus* mediated by a metabolic adaptation. Proc Natl Acad Sci U S A 116:3722-3727.

249. Muraih JK, Harris J, Taylor SD, Palmer M. 2012. Characterization of daptomycin oligomerization with perylene excimer fluorescence: stoichiometric binding of phosphatidylglycerol triggers oligomer formation. Biochim Biophys Acta 1818:673-8.

250. Tsai M, Ohniwa RL, Kato Y, Takeshita SL, Ohta T, Saito S, Hayashi H, Morikawa K. 2011. *Staphylococcus aureus* requires cardiolipin for survival under conditions of high salinity. BMC Microbiol 11:13.

251. van Hal SJ, Paterson DL, Gosbell IB. 2011. Emergence of daptomycin resistance following vancomycin-unresponsive *Staphylococcus aureus* bacteraemia in a daptomycin-naive patient--a review of the literature. Eur J Clin Microbiol Infect Dis 30:603-10.

252. Abdul-Mutakabbir JC, Kebriaei R, Stamper KC, Sheikh Z, Maassen PT, Lev KL, Rybak MJ. 2020. Dalbavancin, Vancomycin and Daptomycin Alone and in Combination with Cefazolin against Resistant Phenotypes of *Staphylococcus aureus* in a Pharmacokinetic/Pharmacodynamic Model. Antibiotics (Basel) 9.

253. Millar BC, Prendergast BD, Moore JE. 2008. Community-associated MRSA (CA-MRSA): an emerging pathogen in infective endocarditis. J Antimicrob Chemother 61:1-7.

254. Molina KC, Morrisette T, Miller MA, Huang V, Fish DN. 2020. The Emerging Role of β-Lactams in the Treatment of Methicillin-Resistant *Staphylococcus aureus* Bloodstream Infections. Antimicrob Agents Chemother 64.

255. Tong SYC, Lye DC, Yahav D, Sud A, Robinson JO, Nelson J, Archuleta S, Roberts MA, Cass A, Paterson DL, Foo H, Paul M, Guy SD, Tramontana AR, Walls GB, McBride S, Bak N, Ghosh N, Rogers BA, Ralph AP, Davies J, Ferguson PE, Dotel R, McKew GL, Gray TJ, Holmes NE, Smith S, Warner MS, Kalimuddin S, Young BE, Runnegar N, Andresen DN, Anagnostou NA, Johnson SA, Chatfield MD, Cheng AC, Fowler VG, Jr., Howden BP, Meagher N, Price DJ, van Hal SJ, O'Sullivan MVN, Davis JS, Australasian Society for Infectious Diseases Clinical Research N. 2020. Effect of Vancomycin or Daptomycin With vs Without an Antistaphylococcal β-Lactam on Mortality, Bacteremia, Relapse, or Treatment Failure in Patients With MRSA Bacteremia: A Randomized Clinical Trial. JAMA 323:527-537.

256. Rasmussen G, Monecke S, Ehricht R, Soderquist B. 2013. Prevalence of clonal complexes and virulence genes among commensal and invasive S*taphylococcus aureus* isolates in Sweden. PLoS One 8:e77477.

257. Perovic O, Iyaloo S, Kularatne R, Lowman W, Bosman N, Wadula J, Seetharam S, Duse A, Mbelle N, Bamford C, Dawood H, Mahabeer Y, Bhola P, Abrahams S, Singh-Moodley A. 2015. Prevalence and Trends of *Staphylococcus aureus* Bacteraemia in Hospitalized Patients in South Africa, 2010 to 2012: Laboratory-Based Surveillance Mapping of Antimicrobial Resistance and Molecular Epidemiology. PLoS One 10:e0145429.

258. Liu L, Wang Y, Bojer MS, Andersen PS, Ingmer H. 2020. High persister cell formation by clinical *Staphylococcus aureus* strains belonging to clonal complex 30. Microbiology (Reading) 166:654-658.

259. Fowler VG, Jr., Nelson CL, McIntyre LM, Kreiswirth BN, Monk A, Archer GL, Federspiel J, Naidich S, Remortel B, Rude T, Brown P, Reller LB, Corey GR, Gill SR. 2007. Potential associations between hematogenous complications and bacterial genotype in *Staphylococcus aureus* infection. J Infect Dis 196:738-47.

260. Blomfeldt A, Eskesen AN, Aamot HV, Leegaard TM, Bjornholt JV. 2016. Population-based epidemiology of *Staphylococcus aureus* bloodstream infection: clonal complex 30 genotype is associated with mortality. Eur J Clin Microbiol Infect Dis 35:803-13.

261. Cheung GY, Kretschmer D, Duong AC, Yeh AJ, Ho TV, Chen Y, Joo HS, Kreiswirth BN, Peschel A, Otto M. 2014. Production of an attenuated phenol-soluble modulin variant unique to the MRSA clonal complex 30 increases severity of bloodstream infection. PLoS Pathog 10:e1004298.

262. Proctor RA, van Langevelde P, Kristjansson M, Maslow JN, Arbeit RD. 1995. Persistent and relapsing infections associated with small-colony variants of *Staphylococcus aureus*. Clin Infect Dis 20:95-102.

263. Kahl BC. 2014. Small colony variants (SCVs) of *Staphylococcus aureus*--a bacterial survival strategy. Infect Genet Evol 21:515-22.

264. Melter O, Radojevic B. 2010. Small colony variants of *Staphylococcus aureus*--review. Folia Microbiol (Praha) 55:548-58.

265. McNamara PJ, Proctor RA. 2000. *Staphylococcus aureus* small colony variants, electron transport and persistent infections. Int J Antimicrob Agents 14:117-22.

266. Schaaff F, Bierbaum G, Baumert N, Bartmann P, Sahl HG. 2003. Mutations are involved in emergence of aminoglycoside-induced small colony variants of *Staphylococcus aureus*. Int J Med Microbiol 293:427-35.

267. Begic D, von Eiff C, Tsuji BT. 2009. Daptomycin pharmacodynamics against *Staphylococcus aureus hemB* mutants displaying the small colony variant phenotype. J Antimicrob Chemother 63:977-81.

268. Bhuiyan MS, Jiang JH, Kostoulias X, Theegala R, Lieschke GJ, Peleg AY. 2021. The Resistance to Host Antimicrobial Peptides in Infections Caused by Daptomycin-Resistant *Staphylococcus aureus*. Antibiotics (Basel) 10.

269. Patton T, Jiang JH, Lundie RJ, Bafit M, Gao W, Peleg AY, O'Keeffe M. 2020. Daptomycin-resistant *Staphylococcus aureus* clinical isolates are poorly sensed by dendritic cells. Immunol Cell Biol 98:42-53.

270. Smith EJ, Corrigan RM, van der Sluis T, Grundling A, Speziale P, Geoghegan JA, Foster TJ. 2012. The immune evasion protein Sbi of *Staphylococcus aureus* occurs both extracellularly and anchored to the cell envelope by binding lipoteichoic acid. Mol Microbiol 83:789-804.

271. Smith EJ, Visai L, Kerrigan SW, Speziale P, Foster TJ. 2011. The Sbi protein is a multifunctional immune evasion factor of *Staphylococcus aureus*. Infect Immun 79:3801-9.

272. Wang X, Ge J, Liu B, Hu Y, Yang M. 2013. Structures of SdrD from *Staphylococcus aureus* reveal the molecular mechanism of how the cell surface receptors recognize their ligands. Protein Cell 4:277-85.

273. Feuillie C, Formosa-Dague C, Hays LM, Vervaeck O, Derclaye S, Brennan MP, Foster TJ, Geoghegan JA, Dufrene YF. 2017. Molecular interactions and inhibition of the staphylococcal biofilm-forming protein SdrC. Proc Natl Acad Sci U S A 114:3738-3743.

274. Barbu EM, Mackenzie C, Foster TJ, Hook M. 2014. SdrC induces staphylococcal biofilm formation through a homophilic interaction. Mol Microbiol 94:172-85.

275. Askarian F, Ajayi C, Hanssen AM, van Sorge NM, Pettersen I, Diep DB, Sollid JU, Johannessen M. 2016. The interaction between *Staphylococcus aureus* SdrD and desmoglein 1 is important for adhesion to host cells. Sci Rep 6:22134.

276. Cameron DR, Ward DV, Kostoulias X, Howden BP, Moellering RC, Jr., Eliopoulos GM, Peleg AY. 2012. Serine/threonine phosphatase Stp1 contributes to reduced susceptibility to vancomycin and virulence in *Staphylococcus aureus*. J Infect Dis 205:1677-87.

277. Cheung A, Duclos B. 2012. Stp1 and Stk1: the Yin and Yang of vancomycin sensitivity and virulence in vancomycin-intermediate *Staphylococcus aureus* strains. J Infect Dis 205:1625-7.

278. Hu Q, Peng H, Rao X. 2016. Molecular Events for Promotion of Vancomycin Resistance in Vancomycin Intermediate *Staphylococcus aureus*. Front Microbiol 7:1601.

279. Tamber S, Schwartzman J, Cheung AL. 2010. Role of PknB kinase in antibiotic resistance and virulence in community-acquired methicillin-resistant *Staphylococcus aureus* strain USA300. Infect Immun 78:3637-46.

280. Kant S, Asthana S, Missiakas D, Pancholi V. 2017. A novel STK1-targeted small-molecule as an "antibiotic resistance breaker" against multidrug-resistant *Staphylococcus aureus*. Sci Rep 7:5067.

281. Huemer M, Shambat SM, Pereira S, Gestel LV, Bergada-Pijuan J, Gómez-Mejia A, Chang C-C, Vulin C, Bär J, Dworkin J, Zinkernagel AS. 2021. Ser/Thr phospho-regulation by PknB and Stp mediates bacterial quiescence and antibiotic persistence in *Staphylococcus aureus*. bioRxiv doi:10.1101/2021.05.06.442895.

282. Ohlsen K, Donat S. 2010. The impact of serine/threonine phosphorylation in *Staphylococcus aureus*. Int J Med Microbiol 300:137-41.

283. Vornhagen J, Burnside K, Whidbey C, Berry J, Qin X, Rajagopal L. 2015. Kinase Inhibitors that Increase the Sensitivity of Methicillin Resistant *Staphylococcus aureus* to β-Lactam Antibiotics. Pathogens 4:708-21.

284. Chatterjee A, Poon R, Chatterjee SS. 2020. Stp1 Loss of Function Promotes β-Lactam Resistance in *Staphylococcus aureus* That Is Independent of Classical Genes. Antimicrob Agents Chemother 64.

285. Yim J, Molloy LM, Newland JG. 2017. Use of Ceftaroline Fosamil in Children: Review of Current Knowledge and its Application. Infect Dis Ther 6:57-67.

286. Kaur DC, Chate SS. 2015. Study of Antibiotic Resistance Pattern in Methicillin-Resistant *Staphylococcus aureus* with Special Reference to Newer Antibiotics. J Glob Infect Dis 7:78-84.

287. Pandey N, Cascella M. 2022. β-Lactam Antibiotics, StatPearls, Treasure Island (FL).

288. Kocaoglu O, Tsui HC, Winkler ME, Carlson EE. 2015. Profiling of β-lactam selectivity for penicillin-binding proteins in *Streptococcus pneumoniae* D39. Antimicrob Agents Chemother 59:3548-55.

289. Moya B, Beceiro A, Cabot G, Juan C, Zamorano L, Alberti S, Oliver A. 2012. Pan-β-lactam resistance development in *Pseudomonas aeruginosa* clinical strains: molecular mechanisms, penicillin-binding protein profiles, and binding affinities. Antimicrob Agents Chemother 56:4771-8.

290. Hardt P, Engels I, Rausch M, Gajdiss M, Ulm H, Sass P, Ohlsen K, Sahl HG, Bierbaum G, Schneider T, Grein F. 2017. The cell wall precursor lipid II acts as a molecular signal for the Ser/Thr kinase PknB of *Staphylococcus aureus*. Int J Med Microbiol 307:1-10.

291. Donat S, Streker K, Schirmeister T, Rakette S, Stehle T, Liebeke M, Lalk M, Ohlsen K. 2009. Transcriptome and functional analysis of the eukaryotic-type serine/threonine kinase PknB in *Staphylococcus aureus*. J Bacteriol 191:4056-69.

292. Machado H, Seif Y, Sakoulas G, Olson CA, Hefner Y, Anand A, Jones YZ, Szubin R, Palsson BO, Nizet V, Feist AM. 2021. Environmental conditions dictate differential evolution of vancomycin resistance in *Staphylococcus aureus*. Commun Biol 4:793.

293. Deresinski S. 2013. The multiple paths to heteroresistance and intermediate resistance to vancomycin in *Staphylococcus aureus*. J Infect Dis 208:7-9.

294. Cortes-Penfield N, Oliver NT, Hunter A, Rodriguez-Barradas M. 2018. Daptomycin and combination daptomycin-ceftaroline as salvage therapy for persistent methicillin-resistant *Staphylococcus aureus* bacteremia. Infect Dis (Lond) 50:643-647.

295. McAdam PR, Templeton KE, Edwards GF, Holden MT, Feil EJ, Aanensen DM, Bargawi HJ, Spratt BG, Bentley SD, Parkhill J, Enright MC, Holmes A, Girvan EK, Godfrey PA, Feldgarden M, Kearns AM, Rambaut A, Robinson DA, Fitzgerald JR. 2012. Molecular tracing of the emergence,

adaptation, and transmission of hospital-associated methicillin-resistant *Staphylococcus aureus*. Proc Natl Acad Sci U S A 109:9107-12.

296. Ledger EVK, Mesnage S, Edwards AM. 2021. Human serum triggers antibiotic tolerance in *Staphtlococcus aureus*. bioRxiv doi:10.1101/2021.11.11.468061.

297. Ersoy SC, Chambers HF, Proctor RA, Rosato AE, Mishra NN, Xiong YQ, Bayer AS. 2021. Impact of Bicarbonate on PBP2a Production, Maturation, and Functionality in Methicillin-Resistant *Staphylococcus aureus* (MRSA). Antimicrob Agents Chemother doi:10.1128/AAC.02621-20.

298. Ersoy SC, Hanson BM, Proctor RA, Arias CA, Tran TT, Chambers HF, Bayer AS. 2021. Impact of Bicarbonate-β-Lactam Exposures on Methicillin-Resistant *Staphylococcus aureus* (MRSA) Gene Expression in Bicarbonate-β-Lactam-Responsive vs. Non-Responsive Strains. Genes (Basel) 12.

299. Ersoy SC, Rose WE, Patel R, Proctor RA, Chambers HF, Harrison EM, Pak Y, Bayer AS. 2021. A Combined Phenotypic-Genotypic Predictive Algorithm for *In Vitro* Detection of Bicarbonate: β-Lactam Sensitization among Methicillin-Resistant *Staphylococcus aureus* (MRSA). Antibiotics (Basel) 10.

300. Falagas ME, Athanasaki F, Voulgaris GL, Triarides NA, Vardakas KZ. 2019. Resistance to Fosfomycin: Mechanisms, Frequency and Clinical Consequences. Int J Antimicrob Agents 53:22-28.

301. Lee YC, Chen PY, Wang JT, Chang SC. 2020. Prevalence of fosfomycin resistance and gene mutations in clinical isolates of methicillin-resistant *Staphylococcus aureus*. Antimicrob Resist Infect Control 9:135.

302. Dinh A, Salomon J, Bru JP, Bernard L. 2012. Fosfomycin: efficacy against infections caused by multidrug-resistant bacteria. Scand J Infect Dis 44:182-9.

303. Florent A, Chichmanian RM, Cua E, Pulcini C. 2011. Adverse events associated with intravenous fosfomycin. Int J Antimicrob Agents 37:82-3.

304. Fu Z, Ma Y, Chen C, Guo Y, Hu F, Liu Y, Xu X, Wang M. 2015. Prevalence of Fosfomycin Resistance and Mutations in *murA*, *glpT*, and *uhpT* in Methicillin-Resistant *Staphylococcus aureus* Strains Isolated from Blood and Cerebrospinal Fluid Samples. Front Microbiol 6:1544.

305. Pujol M, Miro JM, Shaw E, Aguado JM, San-Juan R, Puig-Asensio M, Pigrau C, Calbo E, Montejo M, Rodriguez-Alvarez R, Garcia-Pais MJ, Pintado V, Escudero-Sanchez R, Lopez-Contreras J, Morata L, Montero M, Andres M, Pasquau J, Arenas MD, Padilla B, Murillas J, Jover-Saenz A, Lopez-Cortes LE, Garcia-Pardo G, Gasch O, Videla S, Hereu P, Tebe C, Pallares N, Sanllorente M, Dominguez MA, Camara J, Ferrer A, Padulles A, Cuervo G, Carratala J, Investigators MBT. 2021.

Daptomycin Plus Fosfomycin Versus Daptomycin Alone for Methicillin-resistant *Staphylococcus aureus* Bacteremia and Endocarditis: A Randomized Clinical Trial. Clin Infect Dis 72:1517-1525.

306. Mishra NN, Lew C, Abdelhady W, Lapitan CK, Proctor RA, Rose WE, Bayer AS. 2022. Synergy Mechanisms of Daptomycin-Fosfomycin Combinations in Daptomycin-Susceptible and -Resistant Methicillin-Resistant *Staphylococcus aureus*: *In Vitro*, *Ex Vivo*, and *In Vivo* Metrics. Antimicrob Agents Chemother 66:e0164921.